`

ABSTRACT

ABERG, CHRISTOPHER MARK. Modification of Polymer Membranes: A Study of Cross-linking and In-Situ Growth of Palladium-Containing Nanoparticles in Polymer Matrices. (Under the direction of Richard J. Spontak, Ph.D.).

A crucial step in obtaining pure hydrogen is separating it from other compounds—mainly CO_2—that often accompany hydrogen in industrial chemical reactions. Advanced membrane technology may prove to be the key to the successful, economical production of molecular hydrogen for the eventual consumer market. Size-sieving glassy polymer membranes can separate H_2 on the basis of its small size. Alternatively, reverse-selective rubbery polymers can expedite the passage and, hence, removal of CO_2 due to its relatively high solubility in such membranes alone or in conjunction with dissociative chemical reactions. Transition-metal membranes and their alloys can adsorb H_2 molecules, dissociate the molecules into H atoms for transport through interstitial sites, and subsequently recombine the H atoms to form molecular H_2 again on the opposite membrane side. Microporous amorphous silica and zeolite membranes comprising thin films on a multilayer porous support exhibit good sorption selectivity and high diffusion mobilities for H_2, leading to high H_2 fluxes. Finally, carbon-based membranes, including carbon nanotubes, may be viable for H_2 separation on the basis of selective surface flow and molecular sieving. One approach to achieve higher gas selectivity is to cross-link polymer membranes, thus restricting the ability of gases of various sizes to readily permeate at an unimpeded rate. Cross-linking can occur through a number of means: UV and ion irradiation, plasma treatment, or chemical and thermal techniques. In this study, a chemical technique has been chosen to cross-link the polyimide Matrimid®. Polyimides are well-established as gas-separation membranes due to their intrinsically low free-volume and correspondingly high H_2 selectivity relative to other gases

`

such as CO_2. Prior studies have established that H_2/CO_2 selectivity can be improved by cross-linking polyimides with diamines differing in spacer length. In this first set of work, we follow the evolution of macroscopic and microscopic properties of a commercial polyimide over long cross-linking times (t_x) with 1,3-diaminopropane. According to spectroscopic analysis, the cross-linking reaction saturates after ~24 h, whereas tensile, nanoindentation and stress-relaxation tests reveal that the material stiffens, and possesses a long relaxation time that increases, with increasing t_x. Although differential scanning calorimetry shows that the glass transition temperature decreases systematically with increasing tx, permeation studies indicate that the permeabilities of H_2 and CO_2 decrease, while the H_2/CO_2 selectivity increases markedly, with increasing t_x. At long t_x, the polyimide becomes impermeable to CO2, suggesting that it could be used as a barrier material. Alternatively, polymer nanocomposites continue to receive considerable attention as multifunctional hybrid materials, with most nanocomposites fabricated by physical dispersion of surface-functionalized nanoscale objects. In the second study, we explore the viability of growing Pd-containing nanoparticles from Na_2PdCl_4 in two different polymers – hyper-cross-linked polystyrene (HPS) and an aromatic polyimide (PIm). In HPS, single Pd-containing nanoparticles possessing a relatively narrow size distribution (*ca*. 1-4 nm) are observed to form upon reduction of the divalent $PdCl_4^{-2}$ ions and cluster more readily if the reducing agent is introduced as a liquid. Single nanoparticles with a broad size distribution ranging from ~2 to 16 nm develop in PIm, which simultaneously undergoes chemical cross-linking during ion reduction. The conditions yielding Pd incorporation in PIm are explored through the use of instrumental neutron activation analysis. Such Pd-containing hybrid materials hold promise in molecular catalysis and gas separations. Results from these studies give prospect

`

that these materials, with a great deal of future research, could be developed for H_2 separations applications.

`

Modification of Polymer Membranes: A Study of Cross-linking and In-Situ Growth of Palladium-Containing Nanoparticles in Polymer Matrices

by
Christopher M. Aberg

A thesis submitted to the Graduate Faculty of
North Carolina State University
In partial fulfillment of the
Requirements for the Degree of
Master of Science

Chemical Engineering

Raleigh, North Carolina

June 2nd, 2008

APPROVED BY:

_____	_____
Dr. Richard J. Spontak Committee Chair	Dr. C. Maury Balik
_____	_____
Dr. Saad Khan	Dr. Orlin Velev

DEDICATION

I dedicate this body of work to my family, friends, and teachers and professors, all of whom, no matter how big or small, had an effect on my life and my education. Thank you for your support, advice, or help over all of these years.

BIOGRAPHY

Christopher M. Aberg (Chris) grew up in Maryland and attended high school in the Science and Technology Program at Eleanor Roosevelt High School, from which he graduated in June, 1999. For college, he attended University of Maryland, Baltimore County (UMBC) where he received the prestigious Meyerhoff Scholarship and majored in Chemical Engineering. He graduated from UMBC in December, 2003 and began attending North Carolina State University (NC State) in August, 2004, starting as a Ph.D. degree candidate in Chemical Engineering. Having previously worked with Dr. Richard Spontak and Dr. Nikunj Patel (a graduate student at the time) during the summer of 2003 in the NC State NSF Green Engineering program, Chris accepted a research assistantship in the Polymer Morphology Group ("The Fellowship of the Polymer") in late fall 2004. He passed the qualifying exam and entered into the Ph.D. degree program in April, 2005. After considerable introspection and internal struggle, Chris decided that despite his great interest and deep curiosity in science and math, he no longer wanted to pursue the Ph.D. degree and agreed upon completing his MS degree. Though he has at times struggled with the work, as many graduate students do, he looks back on the experience as a positive, enriching one. Of particular note is that his research took him to Trondheim, Norway where he did research for a month at the Norwegian Institute of Science and Technology (NTNU) in September, 2006. Chris started working in environmental consulting, specifically in air quality, for Trinity Consultants, Inc. in the Research Triangle Park in Durham, NC in April, 2007 and continues to work there. He has been working full time for the last year of his MS degree work.

ACKNOWLEDGMENTS

Family. Friends. Dr. Spontak and the PMG (past and present, especially Mohamed Seyam, Evren Ozcam, Jacob Majikes, and Anand Patel), Dr. Jon Samseth (SINTEF), Dr. May-Britt Hagg (NTNU), NC State technical staff (Mr. Scott Lasell, Mrs. Birgit Andersen), NC State Chemical Engineering faculty and staff (especially the patient staff in the office).

Funding Sources:

SINTEF/NTNU

NASA/University of Florida

TABLE OF CONTENTS

LIST OF TABLES

LIST OF FIGURES

CHAPTER 1

Hydrogen Purification: An Important Step Toward a Hydrogen-Based Economy

Tina M. Nenoff and Richard J. Spontak, Guest Editors, and Christopher M. Aberg

Printed in MRS Bulletin:

T.M. Nenoff, R.J. Spontak, and C.M. Aberg, *MRS Bulletin* **31** (2006) p. 735.

Abstract

Production of pure molecular hydrogen is essential to the realization of the proposed "hydrogen economy" that will ultimately provide hydrogen as a clean, renewable source of energy; eliminate the industrialized world's dependence on petroleum; and reduce the generation of greenhouse gases linked to global warming. A crucial step in obtaining pure hydrogen is separating it from other compounds—mainly CO_2—that often accompany hydrogen in industrial chemical reactions. Advanced membrane technology may prove to be the key to the successful, economical production of molecular hydrogen.

Size-sieving glassy polymer membranes can separate H_2 on the basis of its small size. Alternatively, reverse-selective rubbery polymers can expedite the passage and, hence, removal of CO_2 due to its relatively high solubility in such membranes alone or in conjunction with dissociative chemical reactions. Transition-metal membranes and their alloys can adsorb H_2 molecules, dissociate the molecules into H atoms for transport through interstitial sites, and subsequently recombine the H atoms to form molecular H_2 again on the opposite membrane side. Microporous amorphous silica and zeolite membranes comprising thin films on a multilayer porous support exhibit good sorption selectivity and high diffusion mobilities for H_2, leading to high H_2 fluxes. Finally, carbon-based membranes, including carbon nanotubes, may be viable for H_2 separation on the basis of selective surface flow and molecular sieving. A wide variety of materials challenges exist in hydrogen purification, and the objective of this issue of *MRS Bulletin* is to address those challenges and their potential solutions from basic principles.

Introduction

Although hydrogen comprises 80% of all known matter in the universe—excluding the elusive "dark matter" whose nature is currently not known—it is not available in its free molecular form on Earth. Here, it is tied up in the water that covers two-thirds of the planet, in the valuable hydrocarbon deposits that lie under the Earth's surface, and in countless other compounds. To obtain molecular hydrogen as a source of fuel requires the development of methods capable of separating hydrogen from carbon, oxygen, nitrogen, and other elements to which it is chemically bound. In some cases, such as in steam reforming of natural gas, described by the reaction

$$CH_4 + 2H_2O \rightarrow CO_2 + 4H_2\,, \qquad (1)$$

the separation of hydrogen from carbon and oxygen is accomplished on an industrial scale. However, molecular hydrogen is accompanied by CO_2 as a reaction product, which requires another separation step to produce a stream of pure hydrogen.

The challenges of producing hydrogen on an industrial scale are tremendous, but so are the potential rewards: a source of clean, renewable fuel, which produces only water when burned; decreased production of polluting greenhouse gases; and abundant energy for most of the industrialized world, ending our reliance on petroleum resources that are diminishing

and becoming increasingly expensive. While much attention has been recently and rightfully paid to H_2 storage and fuel cell development, H_2 separation and purification remain important considerations to achieving a "hydrogen economy". Furthermore, significant materials advances in membrane technology for H_2 gas separation are needed to drive reductions in existing H_2 production costs. The purpose of this issue of *MRS Bulletin* is to address the materials challenges that exist in hydrogen purification and present examples of the different types of membranes currently being studied for efficient and robust H_2 production.

The Drive Toward a Hydrogen Economy

In January 2003, a U.S. presidential directive announced the $1.2 billion Hydrogen Fuel Initiative, which has since generated tremendous interest in a "hydrogen economy" within the United States and catalyzed international cooperation efforts to bring such a global future to fruition. As it is envisioned, this hydrogen economy is one in which molecular H_2 is produced from coal, natural gas, nuclear energy, or renewable sources such as biomass, wind, and solar energy. Following production, H_2 would be distributed and stored, with its eventual use in fuel cells to generate energy, mostly for powering automobiles but also potentially for providing electricity and heat to residential, commercial, and industrial facilities. According to the U.S. Department of Energy (DOE), this overarching objective can be divided into four major research thrusts: production, distribution/transportation, storage, and fuel cell technology.[1] Clearly, H_2 production—of which purification is a major step—is vital in the eventual adoption of H_2 as an energy source.

Currently more than $125 USD/barrel, petroleum prices continue to rise (see Figure 1a for NYMEX light sweet crude oil). Since both oil production and refinery capacity in the United States are approaching steady-state, but the consumption of oil is steadily increasing (see Figure 1b), U.S. dependence on foreign petroleum sources has increased substantially (from 35% to 55% since 1973) and is projected to be as high as 68% by 2025.[2] With a growing worldwide population and the emergence of developing nations such as China and India, the demand for dwindling oil reserves will continue to rise. Finally, fossil fuels pose a substantial threat to the environment from the emission of greenhouse gases into the atmosphere, one of the leading causes presumed to be responsible for global warming. Rising global energy requirements, as well as accompanying economic and environmental implications, corroborate a genuine need to explore other energy options such as H_2.

The Current Status of Hydrogen Production

On a worldwide basis, 41 million tons/yr of H_2 are produced via industrial processes, with steam reforming of natural gas accounting for 80% of the hydrogen generated.[3] Of the total 850 billion m^3(STP)/yr of H_2 supplied globally, a little over half, 450 billion m^3(STP)/yr, is produced intentionally, while the remainder results as a by-product from petrochemical processing at refineries. Besides its potential as an energy source, hydrogen is a versatile chemical with a wide range of commercial uses. It is essential in processes developed for the removal of sulfur from petrochemicals (hydrodesulfurization), as well as for the production of syngas (a mixture composed primarily of CO and H_2), ammonia, methanol and higher alcohols, urea, and hydrochloric acid. Furthermore, H_2 is routinely

employed as a reducing agent for metals in Fischer–Tropsch reactions, a process used to generate hydrocarbon fuels by reacting H_2 and CO in the presence of a transition-metal catalyst, and to modify petroleum products and oils by hydrogenation or hydrocracking.[4–8]

In large-scale chemical plants, such as those currently used to generate H_2, separation and purification operations account for at least 50%, and sometimes up to 80%, of the capital investment.[9] Consider, for instance, that H_2 obtained from steam reforming of natural gas consumes about 74 MJ/kg of H_2 at ~23 bar on a production basis of 32.2 billion kg/yr. An estimated 470 billion MJ/yr could be saved with only a 20% improvement in the separation/purification train after the reformer.[10] Saved energy translates into a lower production cost, which is synergistic with the ultimate goal of making H_2 economically competitive relative to current gasoline prices.[8] Whether H_2 is produced from foreign or domestic fossil fuel reserves, nuclear energy, or biomass, the need will always exist for efficient ways to separate it from other diluent gases. Advanced membrane technology may prove to be the most effective means of conducting this separation step.

Membrane Separation Technology

A membrane is a thin, permeable interface that serves to separate two regions in a chemical system. In biology, the cellular membrane is a porous protecting surface that regulates the transport of molecules into or out of the cell. In industrial chemical processes, a membrane can be used to separate compounds based on the size of the molecule, the difference in solubility of the molecules in the membrane, dissociative diffusion mechanisms, or other processes.

In this issue of *MRS Bulletin*, we discuss five types of advanced membrane technologies: polymer, metal, silica, zeolite, and carbon. Size-sieving glassy polymer membranes can separate H_2 on the basis of its small size. Alternatively, reverse-selective rubbery polymers can expedite the passage and, hence, removal of CO_2 due to its relatively high solubility in such membranes alone or in conjunction with dissociative chemical reactions. Transition-metal membranes and their alloys can adsorb H_2 molecules, dissociate the molecules into H atoms for transport through interstitial sites, and subsequently recombine the H atoms to form molecular H_2 again on the opposite membrane side. Microporous amorphous silica and zeolite membranes comprising thin films on a multilayer porous support exhibit good sorption selectivity and high diffusion mobilities for H_2, leading to high H_2 fluxes. Finally, carbon-based membranes, including carbon nanotubes, may be viable for H_2 separation on the basis of selective surface flow and molecular sieving.

Polymeric Membranes for Gas Separation

In the past decade, a considerable amount of attention has been paid to polymeric membranes in the application of gas separations. Polymeric membranes such as Polysep systems (UOP) and PRISM systems (Monsanto, Air Products and Chemicals Inc.) are currently used to recover hydrogen from refinery, petrochemical, and chemical process streams.[3] Both examples are based on asymmetric membrane materials, fashioned in either spiral-wound sheet-type contactors (Polysep) or hollow fibers (PRISM) and composed of a single polymer or layers of different polymers, with the active layer being a polyimide. Typically, polymeric membranes are used in lower-temperature hydrogen recovery such as

from the tail stream of a pressure swing adsorption (PSA) unit. While the relative temperature sensitivity of polymers compared with dense ceramic or transition -metal membranes is a drawback, polymeric membranes have a number of advantages. Membranes created from polymers are generally less expensive (due to the abundance and price of precursor materials), easier to process, and more mechanically tunable than their inorganic counterparts.

Gas permeation through a dense polymer membrane is most often described with the solution-diffusion model, given by the following equation:

$$P = DS. \tag{2}$$

Here, P is the permeability coefficient routinely expressed in Barrers, where

$$1 \text{ Barrer} = 10^{-10} \text{ m}^3\text{(STP)cm}/(\text{cm}^2 \text{ s cm Hg}); \tag{3}$$

D is the diffusion coefficient, often given in units of cm^2/s; and S is the solubility coefficient in units of $\text{cm}^3\text{(gas)}/[\text{cm}^3\text{(polymer)cmHg}]$. The preferential ability of a polymer membrane to permeate one gas (A) over another gas (B) is referred to as the ideal selectivity ($\alpha_{A/B}$), as can be seen in the following equation:

$$\alpha_{A/B} = \frac{P_A}{P_B} = \frac{D_A}{D_B}\frac{S_A}{S_B}. \tag{4}$$

The selectivity can also be defined as the product of the diffusivity selectivity and the solubility selectivity of gases A and B. The diffusivity selectivity (D_A/D_B) is governed by the size difference of penetrant gases and the size-sieving ability of a polymer material. An important factor that influences the diffusivity selectivity is the available free volume, nanoscale voids not occupied by polymer chains at nanoscale dimensions through which penetrant gases migrate. In a polymer possessing relatively little free volume, as in the case of glassy polymers, only gas molecules able to fit within existing void regions can diffuse through the membrane. The diffusivity selectivity is also sensitive to temperature conditions: an increase in temperature tends to enlarge the polymer free volume, thereby increasing the diffusion coefficient of penetrant gases. Solubility selectivity (S_A/S_B), on the other hand, is governed by the solubility of gas A relative to the solubility of gas B in the polymer. Typically, solubility increases with increasing size and condensability of a gas penetrant, but decreases with increasing temperature due to reduced chemical interactions.

Glassy polymers ($T_g > T_{operating}$) are dominated by diffusivity selectivity and thus are often employed to remove lighter gases such as H_2, whereas rubbery polymers ($T_g < T_{operating}$) are dominated by solubility selectivity and are therefore often used to remove heavier gases like CO_2. Here, T_g denotes the glass-transition temperature of the polymer. As can be seen in Figure 2, polymeric membranes are generally subject to a tradeoff between selectivity and permeability or flux.[11,12] Furthermore, Figure 2a shows why glassy polymers are often preferred over rubbery materials for H_2-specific separations, given the desire for high product stream purity, a function of the selectivity. Conversely, Figure 2b illustrates why reverse-selective rubbery polymers are preferred for CO_2 removal. The cutting edge of polymeric

membrane research takes place when materials are found that can break this upper limit, achieving both high selectivity and high permeability.

Polymeric Membranes for H_2 Permselective Separation

In the first article in this issue, Perry et al. discuss the historical development of polymeric membranes for hydrogen separation, followed by a detailed mathematical treatment of the diffusivity and solubility parameters involved. They introduce the concepts of "hydrogen-selective" membranes, which allow hydrogen to pass through based on its small size, and "hydrogen-rejective" membranes, which favor the passage of higher-solubility molecules such as CO_2 through the membrane while blocking the less-soluble H_2 molecules. As mentioned previously, glassy polymers are often used for the separation of H_2 and CO_2 due to their ability to sieve penetrant gases on the basis of molecular size—and more specifically, the molecular kinetic diameter (see Table I). Since H_2 and CO_2 do not vary significantly in size, and CO_2 has a tendency to be readily soluble in some polymers, separation of these two gases can often be difficult. Furthermore, depending upon the chain structure of a given polymer, CO_2 can act as a plasticizing agent, effectively reducing the polymer glass-transition temperature T_g and increasing chain mobility, thus increasing its passage through the expanded free volume. As a result, over a wide range of polymers, H_2/CO_2 selectivity only varies between 0.5 and 2.5, according to Orme et al.[13]

Despite these findings, novel material advances have been made that have resulted in higher H_2/CO_2 selectivities. One such study examined the addition of alkyl groups onto novel poly(aryl ether ketone)s at 30°C and 100°C. Inevitably, the addition of alkyl groups in the

polymer backbone inhibits chain packing and therefore increases the free volume available for molecular transport, resulting in higher gas permeabilities. Wang et al.[14] found that with increasing alkyl group sizes, the permeabilities of H_2 and CO_2 both increased, but the selectivity between the two gases decreased. Interestingly, however, by increasing the temperature to 100°C, the H_2/CO_2 selectivity likewise increases for each respective polymer, with appreciably improved H_2 permeabilities.

A considerable amount of work has been conducted with polyimides and their derivatives, largely because of their high T_g and tight chain packing. A study of interest that involves outside-the-box thinking was performed by exposing polybenzimidazole (T_g = 435°C) to temperature ranges that are not normally examined in routine gas transport studies.[15] Pure- and mixed-gas permeabilities have been measured up to 340°C, a temperature at which methanol-reforming is usually conducted. For pure gases, the permeability of H_2 reached a maximum of 18 Barrer (at ~250°C), which is relatively low. The corresponding H_2/CO_2 selectivity is, however, reported to be as high as 20.

While research has been conducted with poly(amide-imide) block copolymers,[16] the emerging concept of polyimide mixed-matrix composite materials has provided some promising results in gas permeation studies. Yong et al.[17] report that combinations of polyimide (Matrimid®), zeolite materials, and 2,4,6-triaminopyrimidine (TAP) at 35°C yield relatively good He/CO_2 selectivity results. While the permeabilities are relatively low, the results illustrate that the incorporation of particles typically used for size-sieving of H_2 can generate a composite material (see Figure 3) capable of improved selectivity. Smaihi et al.[18]

generated hybrid imide-siloxane systems containing silica particles to achieve high both H_2 permeabilities and selectivities.

Other noteworthy advances include a multilayer polysulfone/silicone rubber composite membrane yielding a high H_2/N_2 selectivity at 50°C;[19] incorporation of a poly(ethylene oxide) layer into a polysulfone/silicone rubber composite, resulting in a H_2/N_2 selectivity that is higher than the selectivity of any one of the integrated components at 35°C, [20] and an alumina-supported styrene-divinylbenzene, with high H_2/CH_4 selectivities.[21] Unfortunately, none of these studies provide CO_2 data, so their overall value remains speculative at this point.

Polymeric Membranes for CO2 Permselective Separation

Carbon dioxide is a highly permeable gas, largely because it is an acid gas with a quadrupolar moment and high solubility in a number of polymers, particularly rubbery polymers that possess polar chemical species. Such reverse-selectivity can be used to promote CO_2 migration into the permeate stream, leaving H_2 pressurized in the rententate stream. The net result is removal of the CO_2 contaminant and recovery of the H_2 product at high pressure, thereby eliminating the need for costly H_2 recompression prior to use or storage. These membranes have resulted in CO_2/H_2 selectivities as high as 10 in a polyphosphazene composed of poly(dichlorophosphazene) modified with 2-(2-methoxyethoxy)ethanol.[22] Similar[23,24] and, depending on temperature, even higher[24,25] CO_2/H_2 selectivities have been observed in cross-linked poly(ethylene glycol) membranes.

In the second article in this issue, Hägg and Quinn examine one type of hydrogen-rejective membrane referred to as a polymeric facilitated-transport membrane. These membranes selectively permeate CO_2 by means of a reversible chemical reaction between the penetrant gas and the membrane material. In addition, the membrane provides a barrier to H_2 permeation. The net result is removal of the CO_2 contaminant and recovery of the H_2 product at high pressure, thereby eliminating the need for recompression prior to use or storage. A wide range of polymeric materials have been investigated, including ion-exchange resins, hydrophilic polymers blended with CO_2-reactive salts, polyelectrolytes, fixed-site carrier polymers, and biologically inspired materials.

Some glassy, high free-molecular-volume polymers are inherently CO_2-selective, but their more attractive aspect is their significantly high permeabilities. Poly(1-trimethylsilyl-1-propyne) (PTMSP), poly(1-methyl-1-pentyne) (PMP), and poly(tertbutylacetylene) (PTBA), all substituted polyacetylenes, have H_2 permeabilities of ~19,000 Barrer, 5800 Barrer, and 300 Barrer, respectively, but their CO_2/H_2 selectivities are all only ~2 at 25°C.[26,27] A random copolymer composed of poly[2,2-bis(trifluoromethyl)-4,5-difluoro-1,3-dioxole] and tetrafluoroethylene (TFE/BDD, 87/13 mol basis), as well as Teflon®, both exhibit H_2 permeabilities of over 3000. However, they exhibit even lower CO_2/H_2 selectivities of slightly greater than 1 at 25°C.[28,29] Most of these membranes, along with polydimethylsiloxane (PDMS), are better suited for the removal of larger (C_3+) organic vapors over light gases such as hydrogen,[30] although PDMS does exhibit a CO_2/H_2 selectivity of ~4.3 at 35°C.[31]

Inorganic Membranes for H2 Purification

Much effort has recently been devoted to the synthesis of inorganic membranes because of their potential applications in the domains of gas separation, pervaporation, and reverse osmosis, as well as in the development of chemical sensors and catalytic membranes.[32–36] Inorganic membranes, which possess good thermal stability and chemical inertness, enjoy several important advantages over polymer membranes for many industrial applications. Improvement needs continue to focus on areas of membrane integrity and manufacturing costs.

Alloys and Metals

Metallic materials are of great interest for hydrogen-selective membranes.[10] The article by Sholl and Ma describes metal membranes for high-temperature applications. The physical mechanism of H_2 permeation through metal membranes is quite different from porous membranes: metal membranes function by adsorbing and dissociating gaseous H_2 on the metal surface exposed to the feed stream and subsequent diffusion of atomic H through interstitial sites in the metal. Recombination of atomic H into H_2 on the downstream membrane side completes the transport of H_2 across the membrane. Because of this mechanism, metal membranes can achieve essentially perfect selectivity for H_2 when exposed to gas mixtures, because transport of species other than hydrogen through the membrane is restricted to defects in the film. Effective membranes can be prepared by depositing thin metal films on macroporous supports. These membranes can be 100% selective toward hydrogen since hydrogen is transported in dissociated form, which yields

ultrapure hydrogen with little or no greenhouse gas contamination. Despite such performance, porous membranes can still be useful to drive the reaction. More work is needed to explore practical opportunities in this area. Of the metals currently of interest, Pd remains the most promising for H_2-selective membranes, even with its mechanical limitations, including embrittlement, cracks, pinhole film defects, delamination, and sulfur sensitivity.[10,32,37–42]

Furthermore, for Pd membranes to be economically attractive in H_2 separations, they have one major shortcoming that must be addressed prior to their wide-scale implementation in industrial processes: their flux must be improved by a factor of 2–4 for use in steam reformers or water–gas shift (WGS) reactors.[10] As a result, current research is focused on the consistent preparation of thin Pd films, measuring ~5 mm thick, that can still afford high selectivity. Thin Pd membranes deposited on porous supports, such as porous alumina or porous metal, are able to withstand the operating conditions typical of H_2 manufacture processes. Sol-gel processing[43] and chemical vapor deposition (CVD)[39,40,44] have thus far been the methods of choice to prepare such thin films. Sol-gel modification provides good selectivity and permeability, in contrast to CVD methods, which yield membranes with reduced permeability but enhanced selectivity. The sol-gel method, however, suffers from poor reproducibility. A variety of synthetic methods have been reported in addition to those already listed,[44,45] including electroless plating,[10,45–49] where films exhibit high permeances for long operational times while retaining H_2/N_2 selectivities on the order of 1000.

Silicas and Zeolites

High-temperature porous membranes (e.g., silica, silicalites, and zeolites) have also been investigated for applications in steam reforming,[51,52] dry reforming,[53–55] and WGS reactions.[56,57] These materials eliminate the need for scarce precious metals. In addition, they are less expensive and exhibit higher permeances than Pd-based membranes. Moreover, they are inert to H_2 embrittlement.

Verweij et al. discuss microporous amorphous silica and zeolite membranes synthesized as thin films on a multilayer porous support. The membranes possess a network of connected micropores measuring ~0.5 nm in diameter. Net transport of small molecules on this network occurs under the driving force of a gradient in chemical potential. Favorable combinations of sorption selectivity and diffusion mobility in the membrane materials lead to high H_2 fluxes and good selectivity with respect to other gases. The membranes also show potential for application in H_2 separation under harsh conditions. Amorphous silica membranes show very high H_2 fluxes because they can be made very thin, but; all-silica MFI-type zeolite (termed silicalite) membranes are expected to demonstrate better operational stability. To make the membranes a viable option, improvements are needed to reduce the occurrence of membrane defects, decrease manufacturing costs, and enhance reproducibility and operational stability.

To date, the most promising results for a membrane separation with steam reforming have been achieved with a silica zirconia composite membrane prepared by sol-gel coating.[51] However, the presence of water vapor may significantly affect the performance of these silica membranes over time, particularly if operated at relatively low temperatures.[10] Recent studies

on silica-based zeolite membranes (see Figure 4) have confirmed that H_2O adsorption at temperatures >100°C interferes with H_2 selectivity by enhancing CO_2 permeance (see Figure 4).[58]

Microporous silicas are very promising due to their low cost, high stability, and high permeance. Recently, these membranes have also produced exceptional H_2 selectivities, with the best H_2/N_2 selectivities exceeding 10,000 for membranes prepared by CVD.[10,58–61]

An extension of the silica membranes work is the development of hybrid metal-coated silica systems, such as the Al-coated SiO_2 permselective membranes studied and reported by Oyama.[61] They are likewise prepared by CVD of a thin SiO_2 layer on a porous alumina substrate, resulting in a non-continuous network of solubility sites. The submicrometer-thick silica-on-alumina composite motif utilizes progressive size gradation, thereby promoting enhanced permeability of hydrogen over CO_2, N_2, CO, and CH_4.

Another method for avoiding costly and fragile Pd for H_2 purification relies on the use of nanoporous membranes. Zeolite membranes in particular combine pore size and shape selectivity with the inherent mechanical, thermal, and chemical stability necessary for long-term operation. The effective pore size distribution of the zeolite membrane, and hence its separation performance, is intrinsically governed by the choice of the zeolitic phase.[62–65] This applies when molecular size exclusion sieving is dominant and no other diffusion pathways bypass the network of well-defined zeolitic channels (otherwise, viscous flow through grain boundaries prevails). The optimum thickness of the zeolite film is always a compromise between separation performance and overall transmembrane flux, and should be tailored to the needs of the application envisioned. Very thin (~0.5 μm) *H*-galloaluminosilicate ZSM-5

type (MFI) membranes on alumina have recently been synthesized[66] and found to exhibit high fluxes (He permeance around 80×10^{-7} mol/m^2- s- Pa) coupled with separation factors essentially in the Knudsen diffusion regime ($He/SF_6 \approx 0.9$ Knudsen factor). Large-surface-area MFI membranes have been grown with a high success rate and exhibit good selectivity characteristics ($H_2/SF_6 > 3$ Knudsen factor) but low H_2 permeance, on the order of $1.5\ 10^{-8}$ mol/m^2- s- Pa.[67]

Due to the need for carbon sequestration associated with H_2 production from fossil fuels, zeolite membranes selective for CO_2 gas separations have also been studied and include the faujasite (FAU) and the silica/aluminophosphate (SAPO-4) framework families. For example, Dong and co-workers[68] reported that the addition of water vapor to the CO_2/N_2 feed gas drastically reduced CO_2 and N_2 permeances and altered the membrane selectivity at low temperature (<80°C) but enhanced CO_2 selectivity at elevated temperature (140–200°C). Noble and Falconer have likewise demonstrated that their SAPO-4 zeolite membranes can be used to separate CO_2 from CH_4 under a variety of pressures and temperatures, with high selectivities at 30 atm and 50°C.[69]

Carbon-Based Membranes

In her article, Pietraß discusses the use of carbon membranes and carbon nanotubes as hydrogen separation devices. Carbon membranes have been prepared as unsupported or supported materials. Typical precursors are organic polymers that are converted to pure carbon materials by treatment at high temperature in an inert atmosphere (carbonization).

Among the unsupported membranes, capillary tubes or hollow fibers and flat membranes have been fabricated to date.

Selective surface flow membranes (SSF™) were introduced in 1993 by Rao and Sircar.[70] These porous carbon membranes are formed by cross-linking and subsequent carbonization of poly(vinylidene chloride)-acrylate terpolymer latex polymer. The permeability of hydrogen in a mixture with hydrocarbons was reduced by several orders of magnitude over that of pure hydrogen, indicating that hydrocarbon-selective adsorption hindered the pore diffusion of hydrogen, thus making these membranes extremely promising for hydrogen separation. The advantages of these membranes are multifold. Since adsorption occurs on the high-pressure side, the partial pressure of the component to be adsorbed can be low, and the partial pressure gradient across the membrane does not need to be high to attain separation. The driving force for mass transfer across the membrane is the difference in the concentration of the adsorbed species.

In addition, carbon nanotubes are being investigated for possible use in hydrogen separation. The unique porous structure of an array of CNTs that can be millimeters long at diameters of molecular dimensions has prompted studies to investigate transport through these tubes. The smoothness of the interior in defect-free nanotubes gives rise to greater transport capacity than conventional carbon-based membranes. Hydrogen separations are expected to be effective for very small nanotube diameters.

Conclusions

Worldwide, a variety of membranes have been and continue to be studied and optimized for the robust and economically efficient large-scale production of H_2. Each type of membrane possesses strengths and current weaknesses. However, strides are being continually reported to improve each membrane type to eventually meet the H_2 energy goals established by the U.S. Department of Energy and its global counterparts.

While polymeric membranes have come a long way over the past decade, it is obvious that more work is required in order to create competitive technologies that will help to reduce production costs for a sustainable hydrogen economy. In the short term, polymeric membranes must be further developed for either H_2- or CO_2-selective applications. Ideally, H_2-selective membranes should exhibit H_2/CO_2 selectivities that exceed 15–20 at 200°C, which is the current range for commercial membranes, whereas CO_2-selective membranes should target CO_2/H_2 selectivities that are double the current commercial membranes. Greater stability and improved performance at elevated temperatures (e.g., at syngas conditions of 200°C) would significantly benefit the involvement of polymer membranes in commercial H_2 activities. Long-term research strategies should be examined for mixed-matrix membranes and the development of organic–inorganic hybrid materials that could yield unexpected but highly desirable properties.[71] Polymeric membranes possess a great deal of potential, provided novel concepts are conceived to meet both short-term and long-term hydrogen separation goals.

Inorganic membranes hold the potential for full and near-term industrial implementation due to their tunable nature and high-temperature/high-pressure stability.

However, a few materials-related hurdles remain to be overcome. Concerns associated with these materials include increasing the selectivity and flux for metal membranes, as well as the level of reproducibility in porous membranes. Compared with organic membranes, inorganic membranes currently are expensive to manufacture. Introduction into large-scale production facilities is, however, anticipated to result in more competitive costs approaching $\$100/ft^2$. The marriage of H_2-selective membranes with advances in materials-related nanotechnology, including nanotube synthesis and designer nanoporosity, holds tremendous promise for the development of stable inorganic membranes capable of achieving the gas separation goals necessary to ultimately realize a hydrogen economy.

Acknowledgments

Sandia is a multiprogram laboratory operated by Sandia Corporation, a Lockheed Martin Company, for the U.S. Department of Energy's National Nuclear Security Administration, under contract DE-AC04–94AL85000. T. M. Nenoff thanks the U.S. DOE Hydrogen, Fuel Cells, & Infrastructure Technologies Program for continued support. R.J. Spontak gratefully acknowledges support from the U.S. DOE under contract DE-FG02-99ER14991, the Research Council of Norway under the NANOMAT Program, and the STC Program of the National Science Foundation (CHE-9876674).

REFERENCES

[1] "Hydrogen, Fuel Cells & Infrastructure Technologies Program. Multi-Year Research, Development and Demonstration Plan. Planned program activities for 2003–2010" (U.S. Department of Energy, Washington, DC, 2003).

[2] S.G. Chalk and J.J. Romm, *Chem. & Eng. News* **83** (34) (2005) p. 30.

[3] Committee on Alternatives and Strategies for Future Hydrogen Production and Use, National Research Council, National Academy of Engineering, *The Hydrogen Economy: Opportunities, Costs, Barriers and R&D Needs* (National Academy Press, Washington, DC, 2005).

[4] *Kirk-Othmer Concise Encyclopedia of Chemical Technology, 4th ed.* (John Wiley & Sons, New York, 1999).

[5] "Gas Processing 2002," *Hydrocarbon Process.* (May 2002).

[6] "Petrochemical Processes 2003," *Hydrocarbon Process.* (March 2003).

[7] R.A. Meyers, *Handbook of Petroleum Refining Processes, 3rd ed.* (McGraw-Hill, New York, 2004).

[8] H.A. Wittcoff, B.G. Reuben, and J.S. Plotkin, *Industrial Organic Chemicals, 2nd ed.* (John Wiley & Sons, New Jersey, 2004).

[9] 7. S.G. Chalk and J.J. Romm, *Chem. & Eng. News* **83** (34) (2005) p. 30.

[10] "Hydrogen, Fuel Cells & Infrastructure Technologies Program. Multi-Year Research, Development and Demonstration Plan. Planned program activities for 2003–2010" (U.S. Department of Energy, Washington, DC).

[11] J.M. Prausnitz, R.N. Lichtenthaler, and E.G. de Azevedo, *Molecular Thermodynamics of Fluid Phase Equilibria, 3rd ed.* (Prentice Hall, 1999).

[12] J.A. Ritter and A.D. Ebner, *DOE/ITP/Chemicals & Chemicals Industry Vision 2020 Technology Partnership* (December 2005); J.A. Ritter and A.D. Ebner *Sep. Sci. Technol* (2006) submitted.

[13] L. Robeson, *J. Membr. Sci.* **62** (1991) p. 165.

[14] B.D. Freeman, *Macromolecules* **32** (1999) p. 375.

[15] C.J. Orme, M.L. Stone, M.T. Benson, and E.S. Peterson, *Sep. Sci. Technol.* **38** (2003) p. 3225.

[16] Z.G. Wang, T.L. Chen, and J.P. Xu, *Macromolecules* **33** (2000) p. 5672.

[17] D.R. Pesiri, B. Jorgensen, and R.C. Dye, *J. Membr. Sci.* **218** (2003) p. 11.

[18] M. Langsam and D.V. Laciak, *J. Polym. Sci., Part A: Polym. Chem.* **38** (2000) p. 1951.

[19] H.H. Yong, N.C. Park, Y.S. Kang, J. Won, and W.N. Kim, *J. Membr. Sci.* **188** (2001) p. 151.

[20] M. Smaihi, J.C. Schrotter, C. Lesimple, I. Prevost, C. Guizard, *J. Membr. Sci.* **161** (1999) p. 157.

[21] X.S. Feng, P.H. Shao, R.Y.M. Huang, G.L. Jiang, and R.X. Xu, *Sep. Purif. Technol.* **27** (2002) p. 211.

[22] Z. Ye, Y. Chen, H. Li, G. He, and M. Deng, *Mater. Chem. & Phys.* **94** (2005) p. 288.

[23] J. Hradil, V. Krystl, P. Hrabanek, B. Bernauer, and M. Kocirik, *React. Funct. Polym.* **61** (2004) p. 3.

[24] C.J. Orme, M.K. Harrup, T.A. Luther, R.P. Lash, K.S. Houston, D.H. Weinkauf, and F.F. Stewart, *J. Membr. Sci.* **186** (2001) p. 249.

[25] N.P. Patel, A.C. Miller, and R.J. Spontak, *Adv. Mater.* **15** (2003) p. 729; *Adv. Funct. Mater.* **14** (2004) p. 699.

[26] N.P. Patel, C.M. Aberg, A.M. Sanchez, M.D. Capracotta, J.D. Martin, and R.J. Spontak, *Polymer* **45** (2004) p. 5941.

[27] H.Q. Lin, E. van Wagner, B.D. Freeman, L.G. Toy, and R.N.P. Gupta, *Science* **311** (2006Patel, A.C. Miller, and R.J. Spontak, *Adv. Mater.* **15** (2003) p. 639729.

[28] A. Morisato and I. Pinnau, *J. Membr. Sci.* **121** (1996) p. 243.

[29] A. Morisato, H.C. Shen, S.S. Sankar, B. Freeman, I. Pinnau, and C.G. Casillas, *J. Polym. Sci., Part B: Polym. Phys.* **34** (1996) p. 2209.

[30] T.C. Merkel, V. Bondar, K. Nagai, B.D. Freeman, and Y.P. Yampolskii, *Macromolecules* **32** (1999) p. 8427.

[31] I. Pinnau and L.G. Toy, *J. Membr. Sci.* **109** (1996) p. 125.

[32] I. Pinnau and Z. He, *J. Membr. Sci.* **244** (2004) p. 227.

[33] T.C. Merkel, V.I. Bondar, K. Nagai, B.D. Freeman, and I. Pinnau, *J. Polym. Sci., Part B: Polym. Phys.* **38** (2000) p. 415.

[34] J.N. Armor, *J. Membr. Sci.* **147** (1998) p. 217.

[35] J. Caro, M. Noack, P. Kolsch, and R. Schafer, *Microporous Mesoporous Mater.* **38** (2000) p. 3.

[36] A.S.T. Chiang and K.-J. Chao, *J. Phys. & Chem. Solids* **62** (2001) p. 1899.

[37] M. Noack, P. Kolsch, R. Schafer, P. Toussaint, and J. Caro, *Chem. Eng. Technol.* **25** (2002) p. 221.

[38] S.G. Thoma, D.E. Trudell, F. Bonhomme, T.M. Nenoff, *Microporous Mesoporous Mater.* **50** (2001) p. 33.

[39] A.-G. Collot, "Prospects for hydrogen from coal," *IEA Clean Coal Center, London,* (2003).

[40] S. Uemiya, *Top. Catal.* **29** (2004) p. 79.

[41] E. Kikuchi, *Catal. Today* **56** (2000) p. 97.

[42] E. Kikuchi, Y. Nemoto, M. Kajiwara, S. Uemiya, and T. Kojima, *Catal. Today* **56** (2000) p. 75.

[43] S.N. Paglieri and J.D. Way, *Sep. Purif. Methods* **31** (2002) p. 1.

[44] K.S. Rothenberger, Y.H. Ma, F. Bustamante, R.P. Killmeyer, I.P. Mardilovich, B.D. Morreale, R.M. Enick, and A.V. Cugini, *J. Membr. Sci.* **224** (2004) p. 55.

[45] H.B. Zhao, G.X. Xiong, J.H. Gu, S.S. Sheng, H. Bauser, N. Stroh, and K. Pflanz, *Catal. Today* **25** (1995) p. 237.

[46] G. Barbieri, V. Violante, F.P. Dimaio, A. Criscuoli, and E. Drioli, *Ind. Eng. Chem. Res.* **36** (1997) p. 3369.

[47] V. Jayaraman, Y.S. Lin, M. Pakala, and R.Y. Lin, *J. Membr. Sci.* **99** (1995) p. 89.

[48] Y.M. Lin, G.L. Lee, and M.H. Rei, *Catal. Today* **44** (1998) p. 343.

[49] Y.M. Lin, S.L. Liu, C.H. Chuang, and Y.T. Chu, *Catal. Today* **82** (2003) p. 127.

[50] J.N. Keuler, L. Lorenzen, and S. Miachon, *Sep. Sci. Technol.* **37** (2002) p. 379.

[51] L. Paturzo and A. Basile, *Ind. & Eng. Chem. Res.* **41** (2002) p. 1703.

[52] X.L. Pan, N. Stroh, H. Brunner, G.X. Xiong, and S.S. Sheng, *Sep. Purif. Technol.* **32** (2003) p. 265.

[53] T. Tsuru, T. Tsuge, S. Kubota, K. Yoshida, T. Yoshioka, and M. Asaeda, *Sep. Sci. Technol.* **36** (2001) p. 3721.

[54] S. Kurungot and T. Yamaguchi, *Catal. Lett.* **92** (2004) p. 181.

[55] T. Ioannides and X.E. Verykios, *Catal. Lett.* **36** (1996) p. 165.

[56] P. Ferreira-Aparicio, I. Rodriguez-Ramos, and A. Guerrero-Ruiz, *Appl. Catal., A* **237** (2002) p. 239.

[57] D. Lee, P. Hacarlioglu, and S.T. Oyama, *Top. Catal.* **29** (2004) p. 45.

[58] S. Giessler, L. Jordan, J.C.D. da Costa, and G.O. Lu, *Sep. Purif. Technol.* **32** (2003) p. 255.

[59] Y. Hasegawa, K. Kusakabe, and S. Morooka, *J. Membr. Sci.* **190** (2001) p. 1.

[60] J. Dong, W. Liu, Y.S. Lin, *AIChE J.* **46** (2000) p. 1957; L. Li, K. Adams, J. Dong, and T.M. Nenoff, *J. Membr. Sci.* (2006) in preparation.

[61] A.K. Prabhu, R. Radhakrishnan, and S.T. Oyama, *Appl. Catal., A* **183** (1999) p. 241.

[62] A.K. Prabhu and S.T. Oyama, *Chem. Lett.* (1999) p. 213.

[63] A.K. Prabhu and S.T. Oyama, *J. Membr. Sci.* **176** (2000) p. 233.

[64] Z.A.E.P. Vroon, K. Keizer, M.J. Gilde, H. Verweij, and A.J. Burggraaf, *J. Membr. Sci.* **113** (1996) p. 293.

[65] E.R. Geus, M.J. den Exter, and H.J. van Bekkum, *Chem. Soc. Faraday Trans.* **88** (1992) p. 3101.

[66] W.J.W. Bakker, F. Kapteijn, J. Poppe, and J.A. Moulijn, *J. Membr. Sci.* **117** (1996) p. 57–78.

[67] C. Bai, M.-D. Jia, J.L. Falconer, and R.D. Noble, *J. Membr. Sci.* **105** (1995) p. 79.

[68] J. Hedlund, J. Sterte, M. Anthonis. A.J. Bons, B. Carstensen, N. Corcoran, D. Cox, H. Deckman, W. De Gijnst, P.-P. de Moor, F. Lai, J. McHenry, W. Mortier, J. Reinoso, and J. Peters, *Microporous Mesoporous Mater.* **52** (2002) p. 179.

[69] M. Noack, P. Kolsch, R. Schafer, P. Toussaint, I. Sieber, and J. Caro, *Microporous Mesoporous Mater.* **49** (1–3) (2001) p. 25.

[70] X.H. Gu, J.H. Dong, and T.M. Nenoff, *Ind. Eng. Chem. Res.* **44** (2005) p. 937.

[71] S. Li, J.G. Martinek, J.L. Falconer, R.D. Noble, and T.Q. Gardner, *Ind. Eng. Chem. Res.* **44** (2005) p. 3220.

[72] M.B. Rao, and S. Sircar, *J. Membr. Sci.* **85** (1993) p. 253.

[73] T.C. Merkel, B.D. Freeman, R.J. Spontak, Z. He, I. Pinnau, P. Meakin, P., and A.J. Hill, *Science* **296** (2002) p. 519.

FIGURES AND TABLES

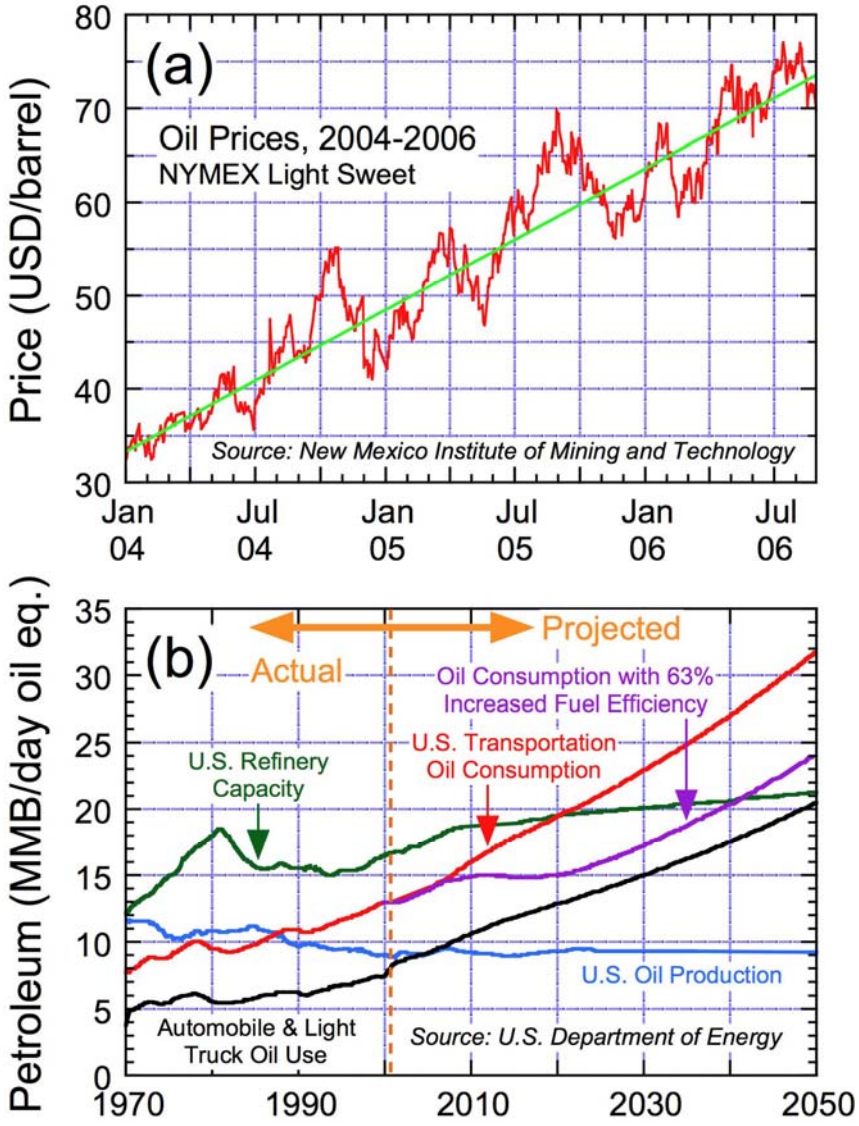

Figure 1-1. US oil prices and projected use. (a) The price of NYMEX sweet crude oil from January 2004 to August 2006, according to the New Mexico Institute of Mining and Technology. The green line is a linear fit to the data. (Prices taken from http://octane.nmt.edu/ marketplace/prices/.) (b) Long-range (actual and projected) U.S. dependence on petroleum with time, according to the U.S. Department of Energy.

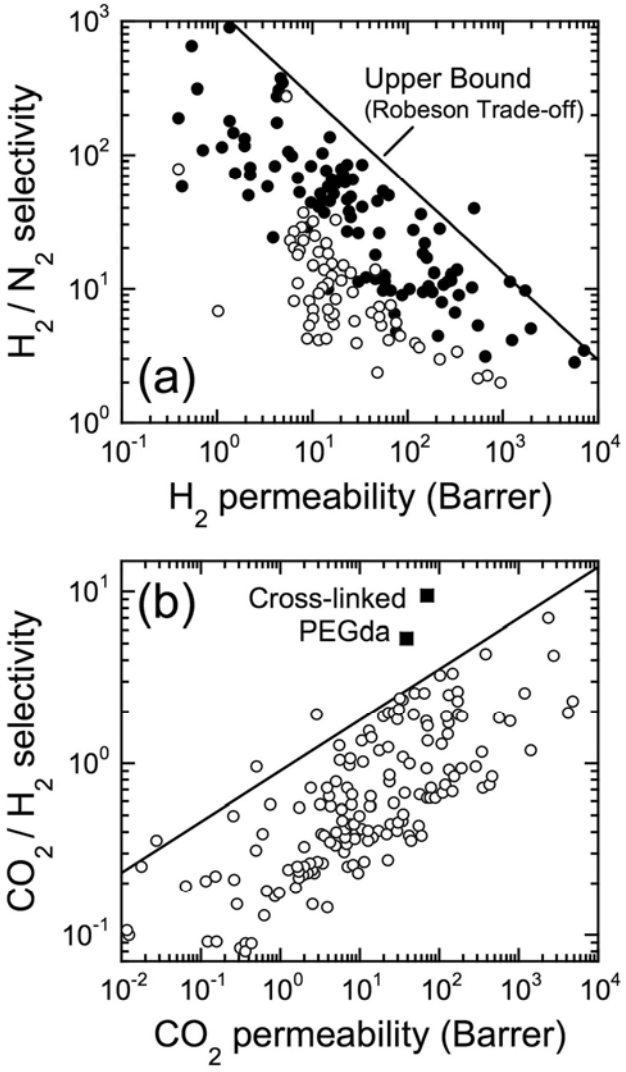

Figure 1-2. Relationships between permeability and selectivity in glassy and rubbery polymers. Relationships between (a) H_2/N_2 selectivity and H_2 permeability[11,12] (adapted from ref. 12 and reproduced with permission from the American Chemical Society) and (b) CO_2/H_2 selectivity and CO_2 permeability[23] over a wide range of polymers. In (a), rubbery and glassy polymers are depicted by open and filled symbols, respectively, whereas such delineation is not made in (b). The empirical upper bound known as the Robeson tradeoff is identified by the solid line in (a) and (b). Highly CO_2-selective polyether (PEGda) membranes are identified by filled squares in (b).

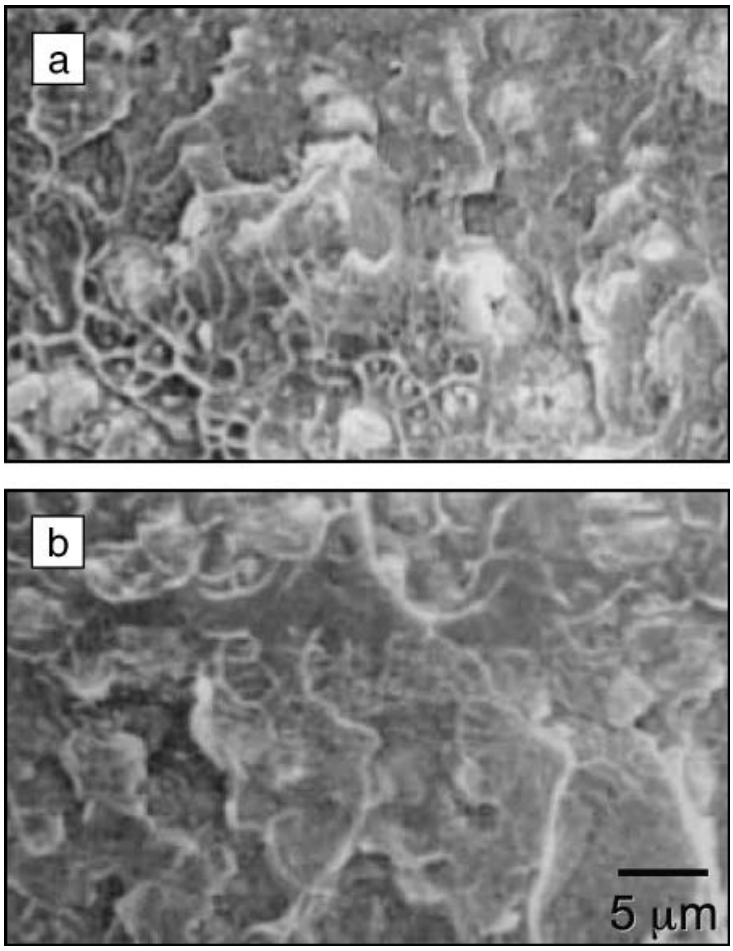

Figure 1-3. Matrimid-zeolite composite membranes. Scanning electron microscopy cross-sections of (a) a Matrimid®/4A zeolite (0.38 nm pore size)/TAP (1.00/0.43/0.21 by weight) and (b) a Matrimid®/13X zeolite (0.74 nm pore size)/TAP (1.00/0.43/0.14 by weight) composite membranes with He/N_2 selectivities of 1282 and 575, respectively. (Adapted from ref. 17 and reproduced with permission from Elsevier Science B.V.)

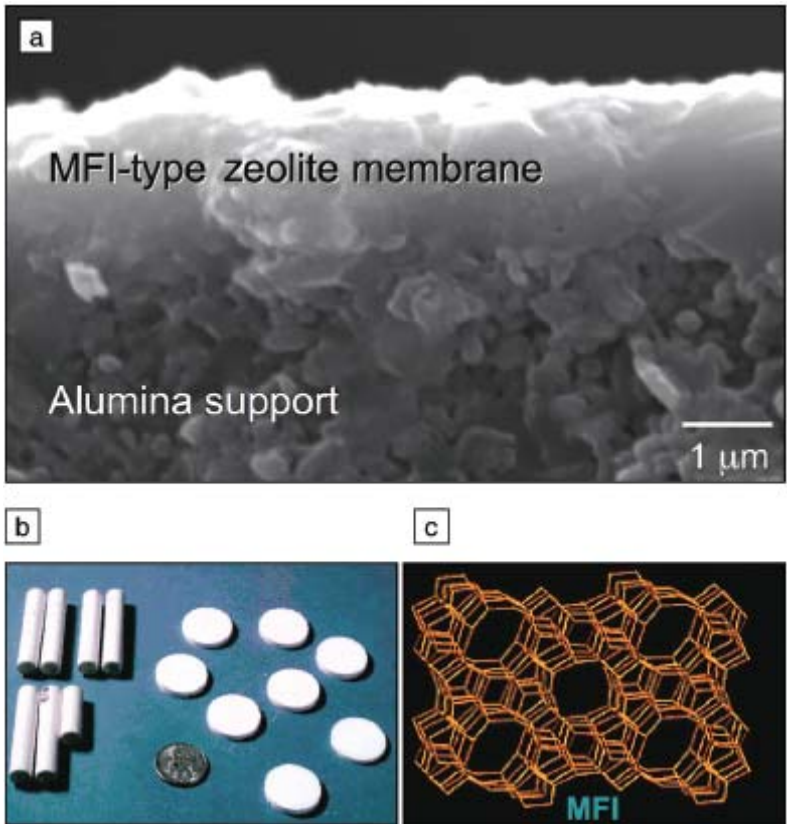

Figure 1-4. MFI-type zeolite membranes. Scanning electron microscopy cross-section of (a) an MFI-type zeolite membrane on alumina support[58] with inserts of (b) the membrane ceramic supports and (c) the MFI structure (adopted from the IZA database website, www.iza-structure.org/databases).

Table 1-1: Light Gas Molecules Commonly Found in H_2 Purification Feed Streams and Their Kinetic Diameters.[10]

Molecule	Kinetic sieving diameter (nm)
He	0.260
H_2	0.289
NO	0.317
CO_2	0.330
Ar	0.340
O_2	0.346
N_2	0.364
CO	0.376
CH_4	0.380

CHAPTER 2

Advances in the Separation of H_2 and CO_2 from Gas Mixtures via Cross-Linked Polymer Membranes

Christopher M. Aberg,[†] **Greg G. Qiao**[§] and **Richard J. Spontak**[†‡]

Departments of [†]Chemical & Biomolecular Engineering and [‡]Materials Science & Engineering
North Carolina State University, Raleigh, NC 27695

[§]Department of Chemical & Biomolecular Engineering, University of Melbourne
Melbourne, Australia

Introduction

In both the political and scientific communities of the US and abroad, a growing interest in alternative energy sources has been steadily emerging. There are many approaches primarily focused on, but not limited to, the reduction of carbon dioxide emissions and it is important to note that they are all worthy of debate. With that said, it is not the intention of this article to spend its time in the debate over which method has the greatest potential for future implementation, but rather to focus on the potential of a foreseeable hydrogen-based economy in this discussion of the separation of hydrogen (H_2) and carbon dioxide (CO_2) using cross-linked polymer membranes. In keeping with the goals of responsible energy management, polymer membranes have emerged over the last two decades as a relatively low cost, low energy demand alternative to the pressure-swing adsorption units used for the purification of gases.[1,2] The primary challenge of polymer membranes is the separation of gas pairs that are relatively similar in size such as H_2 and CO_2. Fundamentally, the desired goal is to increase the selectivity for one gas molecule over another, either by size or solubility. One approach to achieve higher gas selectivity is to cross-link polymer membranes, thus restricting the ability of gases of various sizes to readily permeate at an unimpeded rate.

Cross-linking of Polymers

Cross-linking is the chemical process by which two molecules are joined together by a covalent bond. As can be seen in a simple scheme in *Figure 1*, polymeric cross-linking is

the formation of networks by the joining of polymer chains by grafted molecules, internal functional groups, and/or functional end groups. The cross-linking of polymers has been a relatively simple, useful synthetic way to modify polymers for over a century. One of the more recognizable uses of cross-linking is in the vulcanization of rubber to increase rigidity for its use in tires for our various forms of transportation. Though often over-looked, cross-linking also occurs in nature on a fairly regular basis such as when mollusks attach to surfaces or transglutaminases in the body cross-linking proteins.

As early as 1940, the diffusion and sorption of gases were being studied in polymer systems incorporating cross-links, and it was at this time their ability to achieve a greater level of selectivity was discovered and reported.[3] By 1968, Barrer et al. were studying highly cross-linked copolymers composed of tetraethyleneglycoldimethacrylate (TEGDM) and ethylacrylate (EA) that exhibited selectively high solubility for CO_2, lending to a separation factor over N_2 of 45 at 30°C in the polymer containing 40% TEGDM.[4] These data and the data from other studies helped spawn a new branch of research and development in membrane technology. Since then, as will be reviewed in this article, in roughly the past decade, gas separation studies involving cross-linked membranes have not strayed too far from their original focus on industrially important gas-pairs, such as H_2/CO_2, CO_2/CH_4, CO_2/N_2, and O_2/N_2.

Some interesting research however, has been extended outside of these common gas separations. One study thermally cross-linked a poly(amide imide) with poly(ethylene adipate) that selectively permeated the larger vapors benzene, toluene, and methanol over the

comparatively smaller gases CO_2, O_2, and N_2.[5] Another study cross-linked a copolyimide with poly(ethylene glycol) (PEG) for the selective separation of ethylene oxide and ethylene, improving the solubity for ethylene oxide by the increased polarity added by the PEG linkage.[6] Poly(dimethyl siloxane) (PDMS) was cross-linked by hydrosilylation in the study of the durability of the polymer to molecular chlorine gas (Cl_2) and the permeation of Cl_2.[7]

Pervaporation transport has also incorporated cross-linked polymers such as in the stabilization of poly(ether imide) support membranes using poly(ethylene glycol) diglycidyl ether.[8] Phenol recovery from process water by pervaporation can be enhanced by the esterification crosslinking reaction of 6FDA-6FpDA/DABA 2:1 copolyimide with 1,10 decanediol.[9] A similar method was employed for the pervaporation dehydration of an isopropanol/water mixture. The cross-linking modification of the P84-copolyimide with short chain diamines (*p*-xylenediamine, ethylenediamine) has been proposed as an efficient, economical approach to this separation.[10]

While research attention has traditionally focused on gas-pair or vapor separations, cross-linking of polymers has been employed in less common industrial separations as well. An atypical, albeit interesting study involved a poly(vinyl alcohol)/glutaraldehyde network for the purification of the biologically significant compounds creatinine, IgG, and Fab.[11] Membranes for the nanofiltration of salts have been generated by the cross-linking of poly(amidoamine) dendrimers and trimesoyl chloride on phenolphthalein poly(ether ether ketone) ultrafiltration membranes.[12] Furthermore, cross-linking has been used to increase

hydrolytic stability in proton exchange membranes (PEMs) for their use in fuel cells, with little change to the proton conductivities.[13]

As in the vulcanization of rubber, cross-linking is not just restricted to the intentional use in filtration, purification, and separation; it can also be used to make a polymer more mechanically robust, as in the example of poly(dimethylsiloxane) (PDMS) and polyurethane (PU).[14] Furthermore, cross-linked polymers can be used as size-restrictive networks in which materials such as polyaniline (PANI) dispersed particles can be generated, as they were in PDMS.[15]

It is clearly evident that cross-linking is a straightforward, versatile way to modify the physical characteristics of polymers. In this article, the efforts in the research community to address the separation of hydrogen and carbon dioxide by controlling diffusion and solubility through cross-linking will be reviewed.

Common Cross-Linking Methods

In generating polymer networks for gas separations, a number of common techniques have been used to induce cross-linking. This section will cover these methods.

UV Irradiation

UV light is an electro-magnetic radiation that exists at wavelengths shorter than visible light. Because the waves are of a shorter length, and hence a higher frequency, they carry with them a larger amount of energy. In UV photochemical cross-linking, the radiation

is harnessed as an energy source to break bonds generating radicals within a polymer or of a cross-linking agent leading to the formation of a network of polymer chains.

Ion Irradiation

Ion irradiation works in a similar fashion to UV irradiation in that it provides an energetic source to generate radicals in the polymer or a cross-linking agent. H+ ion irradiation has been shown to cross-link Matrimid by a couple of different processes based upon ion fluence.[16] Low dosages of low energy ion irradiation using beams such as Ar, He, H_2, and NH_3 induce compaction of the surface layer of polymers due to processes like cross-linking.[17] Care must be taken in the process though because carbonization can occur at higher doses, resulting in lower permeabilities.[18]

Plasma Treatment

Plasma treatment is another way that is employed to cross-link polymers. Cross-linking is initatied by the generation of radical sites when electrons, atoms, and radicals in the plasma attack the surface of a polymeric membrane. In a related manner, the plasma treatment can be used as a means of depositing a cross-linked polymer film generated by monomeric units. Plasma polymerization of silicon organic vapors (hexamethyldisiloxane [HMDSO] and hexamethyldisilazane [HMDSN]) led to cross-linked polymer films deposited onto porous aluminum oxide membranes (pore diameter of 20nm). The plasma-polymerized

HMDSO achieved a nitrogen permeability on the same order of magnitude as silicon rubber (~10^2 Barrer) with higher separation factors for CO_2 (α = 8.1) and C_4H_{10} (α = 21) over N_2.[19]

Chemical/Thermal

There are many methods by which polymers can be chemically and/or thermally modified to induce cross-linking but it appears that some are more prominent than others. Two common chemical techniques that are employed to cross-link polymer membranes (specifically polyimides) are the esterification reaction or the methanol/diamine methodology. Through the cross-linking and thermal annealing of the 6FDA-DAM:DABA (2:1) polyimide, the CO_2 permeability and swelling, thus the diffusion coefficient, can be stabilized. The free carboxylic acid group –COOH of the diaminobenzoic acid graft (DABA) can be esterified with 1,4-cyclohexanedimethanol and upon the thermal annealing step, cross-linking occurs as illustrated by *Figure 2*.[20]

Another chemical route, which has its roots in a US Patent, is a cross-linking reaction that occurs at room temperature when a polyimide is immersed in a mixture of methanol and a short-chain diamine.[21] More on this novel technique will be covered later in this review. The CO_2 plasticization effect can be particularly problematic in thin films, and thus one of the proposed means by which to address this problem has been to cross-link ultra-thin dense polyimide films of 6FDA-durene with *p*-xylenediamine. Zhou et al. showed this to be an effective means to reduce plasticization and it leads to greater CO_2 stability.[22]

Thermal cross-linking, much like UV, ion, and plasma treatments, can be used as a driving force providing energy to either activate radicals within functional groups or endgroups on a polymer backbone or to generate radicals on thermally active cross-linking agents, leading to the formation of a network.

Chemical Cross-linking of Polyimides and Other Polymers

Based on the research interests of the authors, extra attention will be paid on the chemistry of cross-linking of polyimides and other polymers before addressing the ways in which cross-linking methods have conferred varied separation abilities onto those polymers.

Generally speaking, there are two main classes of polymers used for constructing gas membranes for H_2 and CO_2 separation membranes. One class is formed based on conventional cross-linking methods, mainly being polyimide-based polymers. The other is formed using free radical cross-linking chemistry. In the 1st type, linear polyimides are initially formed and the membrane is constructed through a physical method such as casting or spin coating. The formed membranes are then submerged into a solution with cross-linkers and the cross-linking reaction takes places from the surface to the inside of the membrane by penetration of cross-linkers. The cross-linking may also be formed during the membrane formation by addition of cross-linker to the casting solution provided that there is a controlled delayed onset of the cross-linking reaction. In the 2nd type, cross-linking is carried out when the membrane is formed during the polymerization. Therefore, polymer formation,

cross-linking and membrane construction occur simultaneously. The encompassing membrane cross-linking classifications are illustrated in *Figure 3*.

Conventional Cross-linking

Three different techniques have been used in the chemical cross-linking of polyimides: 1) cross-linking though polymer backbone by using diamines via reaction with carbonyl groups[21,23-34]; 2) synthesis of polyimides which incorporate pendant cross-linkable functional groups; 3) synthesis of branched polyimides.

I. Crosslinking through Polymer Backbone

This method has been extensively studies recently due to its simplicity. The carbonyl groups are vulnerable to reaction by amines. Because of this, it is possible to allow reaction between a polyimide membrane and a diamine leading to a cross-linked membrane. The amine groups react with a carbonyl group on the imide ring yielding two amide groups. This reaction is illustrated in *Figure 4*. The crosslinking agent may be added either during or after membrane formation. This method of cross-linking has been used with a large number of diamines or multi amines. *Table 1* lists some recently reported amines as crosslinkers, including dendrimers with amine functionality at its peripheral of the branch ends.

Epoxides and diamines can been added to polyimide casting solutions.[35,36] The membranes can then be thermally treated to form an epoxy network within the polyimide membrane. Because the diamines can react with the carbonyl groups on the polyimide prior

to formation of the epoxy network, there is the possibility of the formation of a polyimide/epoxy hybrid structure. This reaction scheme is illustrated in *Figure 5*.

Copolyimides which include an acetylene linkage in their back bone have been synthesized by Chung and coworkers.[37] Heating to 400 ^{o}C of these membranes can cause cross-linking to occur (the authors suggest that a Diels-Alder cycloaddition takes place). This work was used to fabricate carbon membranes (by heating to 800 ^{o}C). The synthesis of these copolyimides is illustrated in *Figure 6*.

II. Crosslinking through Pendent Groups

Polyimides have been synthesized which include pendent carboxylic acid functional groups. The presence of these groups allows crosslinking of the membranes via reactions with alcohols or metal ions. A good explanation of the chemistry here can be found in elsewhere.[38] *Figures 7, 8* and *9* display typical examples of the monomers used, the reaction with diols and reaction with aluminum ions.

The pendent primary amine groups in chitosan allow for a great deal of crosslinking chemistry to be carried out. An example of a crosslinking agent is trimesoyl chloride which reacts with chitosan to form a crosslinked structure. Feng and coworkers have soaked chitosan membranes in trimesoyl chloride/hexane solutions to yield crosslinked membranes.[39] Other crosslinking agents that have been used on chitosan include sulfuric acid, glutaraldehyde, 1,6-hexamethylene disocyanate, sulfosuccinic acid, epichlorohydrin and 2,4-toluylene diisocyanate.

Polymer/silica hybrid membranes constitute another method of forming cross-linked membranes. By synthesizing polymers which contain silanes, membranes can be fabricated. Heating of these membranes can cause alcohols to be eliminated and the formation of Si-O bonds between the silica groups – yielding polymer/silica crosslinked hybrid membranes. It is important to note that these membranes can be formed with the silane in either the backbone or a pendent group. *Figure 10* displays the former, while *Figure 11* illustrates the latter. A large number of papers in this area have been published.

III. Branched polymers

Highly branched polyimide/polyethylene oxide membranes have been synthesised by Okamoto and co-workers.[42] The authors react the monomer 6FDA with a triamine compound in various ratios. This yields a hyper branched species with surplus anhydride units (see *Figure 12*). This species was then functionalised with polyethylene oxide arms. Because of the hyper branched core, these membranes possess regions similar to crosslinked polymers, however, they are soluble in solution. By adjusting the ratio of 6FDA to triamine, it should be possible to generate fully crosslinked membranes.

Free Radical Crosslinking

Free radical crosslinking can be used in the fabrication of crosslinked gas separation membranes. The most common means of fabricating these films involves free radical polymerization of a liquid polyethylene glycol with either dimethacrylate or diacrylates as

end groups. As illustrated in *Figure 13*, an acrylate monomer, which can be functionalized, is crosslinked with diacryalte or crosslinker with more than two acryl or methacryl groups. The diacrylate may be linked by a L segments which can introduce a soft or hydrophilic component to the network. A very common studied is the ethylene oxide oligomers used as L segment. The R3 in monomer can also be linked to an ethylene oxide oligomers to enhance the permeability of CO2. The free radical polymerization can be initiated by thermal, redox or UV methods. A initiator is premixed with the monomer and crosslinked precursors, followed by casting the solution to a desired shape and the external reaction condition, either heat, time or UV light, is applied to cause the polymerization to take place in situ. Some literature examples of these types of membranes are listed in Table 2. This style of membrane has the significant advantage of ease of creating a wide range of copolymers by using a blend of monomers. It does however carry a serious disadvantage of limiting the types of membrane morphologies to dense flat sheet membranes.

H_2 Selective Cross-linked Membranes

Gas separations involving the transport of hydrogen through the polymer membrane to the permeate side are virtually solely based upon the ability of a membrane to selectively diffuse molecules on the basis of size. Thus, the goal is to be able to tailor the diffusivity of a gas through a polymer membrane by controlling cross-linking reaction parameters such as time, temperature, and material selection. In this section, the efforts to control such

parameters in the attempt to achieve optimal gas transport characteristics in the various types of cross-linking will be covered.

UV/Photochemical

In 1994, Kita et al. generated a polyimide and two copolyimides containing benzophenone (BTDA-TMPD, BTDA/6FDA-TMPD [1:1], BTDA/6FDA-TMPD [1:3]) and cross-linked these polymers by UV irradiation for various time periods resulting in relatively high H_2/CO_2 selectivities. The polyimide composed of BTDA-TMPD (3,3',4,4'-benzophenone tetracarboxylic dianhydride & 2,4,6-tridianhydride) demonstrated selectivities of 16.1 and 28.3 after 10 and 30 minutes of UV irradiation exposure, respectively. The hydrogen permeabilities decreased with increasing irradiation, assuredly due to the restricted chain mobility due to cross-linking. The incorporation of 6FDA (2,2-bis[3,4-dicarboxyphenyl]hexafluoropropane dianhydride) likely opened up the free volume due to the bulky fluorine groups in the dianhydride, resulting in higher permeabilities with increasing 6FDA content, but upon cross-linking the co-polyimides did not yield selectivities that were competitive with the compared BTDA-TMPD polyimide.[50] Similar findings were presented in the UV irradiation of the polyimide BTDA-4MPDA (4MPDA: 2,3,5,6-tetramethyl phenylenediamine) in that there is a two fold decrease in the permeability of H_2. Unfortunately, no CO_2 data was provided, but the selectivity of H_2 over N_2 was 949.0 after 8 hrs of UV irradiation exposure.[51]

It is a common theme that, as the exposure time of the polymers to UV irradiation is increased resulting in a greater degree of cross-linking, the permeabilities of gas penetrants will decrease due to the decrease in their diffusion coefficient through the polymer. While this effect is not easily overcome through the use of UV irradiation as a means to cross-link, parameters such as the temperature of permeation can be adjusted resulting in a smaller decrease in the permeability of hydrogen.[52]

In a set of three studies conducted with synthesized polyarylates, UV irradiation was used to initiate cross-linked polymer membranes. The various polyarylates showed promise in their relatively high H_2 permeabilities, though their selectivity over CO_2 was not very impressive.[53,54]

Ion Irradiation

Toth et al. demonstrated in 1996 that the H_2 transport properties of two organosilicon polymers, polyvinyltrimethylsilane (PVTMS) and polydimethylsiloxane (PDMS), could be modified by treatment with various fast atom bombardments. The permeation depended upon the material, PVTMS having inherently higher diffusion coefficients, and the choice of particle beam source ($Ar > He > H_2 > NH_3$).[17] Unfortunately the polymer membrane thicknesses were not reported along with no CO_2 data, however the permeance of all gases decreased, but more so for those of larger size, thus resulting in higher H_2 selectivities in all cases.

Plasma Treatment

A study conducted by Hu et al. established recently that Ar-plasma treatment of poly(methyl-methacrylate) (PMMA) membranes leads to surface cross-linking. The technique is relatively successful in suppressing CO_2 plasticization, and at longer durations (5 and 10 min.) of the highest power (300W) of the Ar-plasma treatment, He/CO_2 selectivities are above 100 with He permeabilities maintaining around 14 Barrer. With increasing power of the plasma treatment, the He permeabilities surprisingly increased due to an etching effect that does not occur at the lower power plasma treatment acting synergistically with the cross-linking.[55]

Chemical/Thermal

The methanol/diamine modification of polyimides first appeared in a scientific journal in the year 2001. It is relatively similar to the esterification cross-linking reaction, but differs in that it does not require any prior modification to the polyimide and it does not require any heat to initiate the reaction, as it occurs spontaneously at room temperature. In this initial study, Liu et al. reported the findings for helium (He) gas permeation through the 6FDA-durene polyimide that had been cross-linking with *p*-xylenediamine. Cross-linking was demonstrated through gel content and ATR-FTIR measurements. A clear emergence of amide characteristic peaks (C=O stretching) coupled with the decrease of imide peaks (symmetric, asymmetric C=O stretching) suggested to the researchers that they had converted the imide groups to amide groups, supporting the cross-linking scheme in *Figure 4*. It is

believed that the short-chain diamines create links between separate polyimide chains, thus restricting the molecular mobility of the polymer, reducing the CO_2 plasticization effect. After 60 minutes of immersion time in the MeOH/diamine solution, 6FDA-durene was sufficiently crosslinked such that the He permeability reduced from 362 Barrer to 34.4 Barrer increasing the He/CO_2 selectivity from 0.8 to 16.1.[23] It is important to note that they did not report permeability values for H_2, but rather He in its place, but considering the similarity in kinetic diameter between the two, the permeability and selectivity should only decrease slightly based upon size.

Since this first study, a great deal of work has been done with moderately impressive results by employing this diamine modification technique on the polyimides Matrimid and 6FDA-durene using a variety of diamino-cross-linkers (*p*-xylenediamine, diaminobutane dendrimers, ethylenediamine [EDA], 1,3-cyclohexanebis(methylamine), 1,3-propanediamine [PDA], and 1,4-butanediamine[BuDA]).[24,27,29,30,34] The most recent research reported permselective properties impressively above the Robeson Trade-off Line by cross-linking 6FDA-durene with three various sized linear short-chain aliphatic diamines, EDA, PDA, and BuDA. As can be seen in *Figure 14*, membranes maintained ideal permeabilities of 10 Barrer or more with standout selectivity performances by the polyimide membranes modified with PDA for 5 and 10 minutes.[34] Even binary mixed gas tests revealed gas transport properties in these cross-linked membranes on or above the permselective trade-off line.

Because the currently most abundant source of molecular hydrogen is the water-gas shift reaction from the steam-reforming of methane, operating conditions tend to be at high

temperatures and pressures. Thus, it is in the interest of keeping energy costs down to have membranes that will be able to perform at these operating conditions. Amongst the polyimides that have been cross-linked by the methanol/diamine method an interesting phenomenon occurs. First identified by Kawakami et al. in 1996, thermal treatments to fluoropolyimides lead to densified structures and the formation of charge transfer complexes (CTCs).[56] Similar effects were shown to occur in Matrimid, improving plasticization resistance.[57-59] Recent studies by Shao et al. looked at the coupled effect of diamino cross-linking followed by thermal treatment. It was found that the effect induced by the thermal treatment was two fold; the thermal annealing reversed the room temperature spontaneous cross-linking by diamines along with the formation of CTCs, leading to the densification of the polymer membrane. This densification leads to great CO_2 plasticization resistance at pressures above 300 up to 720 psia.[29,30] It is believed that the strong ability to form CTCs in the cross-linked membranes is in large part due the novel diamino-modification method. This may be due to conformational changes that occur during cross-linking that allow for the formation of CTCs upon thermal treatment, aligning intramolecular electron donating or accepting π-bonds as seen in Figure 15. This has lead to the previously mentioned plasticization resistance while maintaining relatively high H_2 permeabilities (>100 Barrer) lending to a H_2/CO_2 selectivity of 3.41 at optimum membrane modification conditions.[30]

Other novel chemical cross-linking methodologies have been proposed to generate membranes appropriately intended for H_2/CO_2 separations. One study followed a similar approach as the methanol/diamine cross-linking reaction, but employed hexane as the

swelling agent/solvent, yielding relatively competitive results for 6FDA-durene modified with N,N-dimethylaminoethyleneamine for 24 hours (P_{He} = 91.3 Barrer, $\alpha_{He/CO2}$ = 7.87).[60] Another study generated Langmuir-Blodgett bilayer "glued" films through ionic cross-linking that have a He/CO_2 selectivity of 150 but with low permeabilities.[61]

Simple thermal treatments have also been shown to cross-link polyimide blend, poly(ether imide), and polyarylate membranes with relatively average H_2(He)/CO_2 transport properties.[62,63,64] Either due to severe thermal conditions required or mediocre membrane performance this route of cross-linking modification has not been focused upon greatly for the creation of H_2/CO_2 separation

CO_2 Selective Cross-linked Membranes

One aspect of using H_2-selective cross-linked polymers for the separation of hydrogen and carbon dioxide is that H_2 permeates through the membrane to the permeate side where it will subsequently need to be recompressed for its eventual use. Such an energy intensive process may offset the financial advantage to using polymeric membranes over adsorption unit operations. A proposed way to address this problem is to employ the use of reverse-selective polymeric membranes that will selectively permeate CO_2 based upon its high solubility in rubbery polymers that contain polar chemical species. This would result in H_2 remaining in the retentate stream, eliminating the need for a costly recompression step for an end-use goal.

In the removal of H_2 by its permeation through cross-linked polymer membranes, the type of polymer plays a relatively important role based upon its thermal/chemical resistance and the characteristic fractional free volume, but as shown in the previous section, it appears that the cross-linking modification technique plays as important a role if not more so. Conversely, in CO_2-selective permeation, the type of polymer plays a significantly more important role because the solubility of CO_2 in the polymer has a much larger effect on the overall permeation rather than the diffusion coefficient. For this reason, this section will place a significant importance on the types of polymers employed rather than the techniques used to cross-link them, without undermining the effect that cross-linking performs.

Cross-linked polydimethylsiloxane (PDMS) networks are known to exhibit very high gas permeabilities favoring larger gas molecules over smaller penetrants due to the high chain mobility. While the permeability for CO_2 is higher than that of H_2, the highest reported pure cross-linked PDMS selectivity is only about 4.3. Based upon gas permeation studies, PDMS is more suitable for the larger gases and vapors over the smaller gases. A similar CO_2/H_2 selectivity was found in cross-linked poly(dicyclohexylpolysiloxane) (PDCHS), but it was discovered that with an even lower cross-link density than PDMS, PDCHS impedes the movement of the larger vapors due to the fact that the cycloaliphatic groups occupy more free volume.[65]

Polyphosphazenes are hybrid polymers that contain an inorganic backbone of phosphorous and nitrogen, each phosphorous atom possessing two organic pendant groups. Nucleophilic substitution processes have resulted in a wide range of pendant groups attached

to the inorganic backbone, lending versatility to the polymer based upon the pendant groups substituted. Early studies showed that In one study, varied amounts of three pendant groups were added followed by subsequent cross-linking for the purpose of gas separations. First, 2-(2-methoxyethoxy)ethanol (MEE) was substituted onto the backbone to add a polar hydrophilic nature to the polymer. Second, 4-methoxyphenol was added to provide hydrophobicity and the ability to form films. Finally, 2-allylphenol was added for its aid in cross-linking. Cross-linking was initiated by the UV irradiation activation of 1,1'-azo-bis(cyclohexanecarbonitrile). It was found that as the MEE content increases, the CO_2 permeability increases, such that at 100% MEE the P_{CO2} is 250 Barrer and the CO_2/H_2 selectivity is 10.[66] A similar study conducted found the same effect due to the ether-linkage containing MEE, and added that as temperature increases, so does the CO_2 permeability, but the selectivity decreases.[67]

A great deal of research has been spent on the CO_2 reverse-selective properties of polyethers, taking advantage of the polar ether-linkages that increase the solubility of carbon dioxide in the polymers.[43-46,49,68-72] In 1999, Hirayama et al. generated a cross-linked PEO membrane composed of 70/30 wt% methoxy-terminated poly(ethylene glycol) methacrylate (MEMA) and poly(ethylene glycol) diamethacrylate (EDMA) that resulted in a CO_2 permeability of 200 Barrer and a CO_2/H_2 selectivity of 19.2.[43] Since then, a number of a number of studies have focused on various elements of polyethers. Variation in the pre-cross-linked molecular weight of poly(ethylene glycol) diacrylate (PEGda) showed that as the molecular weight increases, the permeability of all gases increase but preferentially for

CO_2 as the cross-linked polymers become more rubbery due to the increased distance between cross-links.[44] Similarly, it was found in a study of poly(propylene glycol) diacrylate (PPGda) that the increased aliphatic content and therefore reduced ether-linkage content led to a reduction in CO_2/H_2 selectivity though there was an increase in all gas permeabilities.[45] Given the outcomes of the previous studies, blends of PEGda and PPGda led to results that show that selectivity increases with increasing PEGda content but permeability increases with increasing PPGda content (*Figure 16*).[46] PPGda was further investigated by Roharjo et al. when it was cross-linked with poly(propylene glycol) methyl ether acrylate (PPGmea). As the content of the PPGmea branches increases, the fractional free volume increases, resulting in higher gas diffusivities and an increase in the CO2/H2 selectivity to a value of ~4.6.[49] In a study on the effect of cross-linking in PEGda, it was found that cross-link density does not necessarily affect gas diffusion and permeation, the glass transition temperature (T_g), or the fractional free volume in polymer networks. By controlling the cross-link density, while maintaining similar chemical composition of the membranes it was shown that the changes in P and D are more a result of the changes in T_g than changes in the cross-link densities.[68] Lin et al. also found that sorption isotherms of CO_2 in cross-linked PEGda can be fit using the Flory-Huggins model.[69] Changes in gas permeability can be well described by a free volume model in PEO membranes generated from PEGda and poly(ethylene glycol) methyl ether acrylate (PEGmea). As the PEGmea content increases, the size of free volume elements is increased, leading to an increase in CO_2 permeability and CO_2/H_2 selectivity. At 99 vol% PEGmea and a temperature of 35°C, the permeability of CO_2

is 570 Barrer and the CO_2/H_2 selectivity is 12.[70] When the membrane is composed of a 70/30 wt% mixture of PEGmea and PEGda, mixed gas results are found to be dependent upon temperature where selectivity decreases with increasing temperature, but only mildly dependent on the gas mixture or partial pressure.[71] Another study found that the permeability of the highly sorbing CO_2 increases with an increase in its fugacity or concentration in cross-linked PEGda, while the permeability of the light gas H_2 is independent of fugacity.[72]

An area of research that has received recent attention in the selective separation of CO_2 over H_2 is facilitated transport.[73] The difference between a solubility-selective polymer membrane and a facilitated transport polymer membrane is that CO_2 permeates by a reversible reaction between the gas and the polymer. If X represents a carrier species with which CO_2 reacts, forming an adduct X-CO_2. This adduct diffuses through the polymer due the pressure difference between the retentate and permeate sides, where at the end free X and CO_2 are reformed. The reaction chemistry dictates how effective X performs as a carrier. Effective facilitated transport occurs when reactions are fast, particularly the decomposition step. The other gas penetrants such as hydrogen will operate by diffusion only. Cross-linked polymers for facilitated transport have been studied and published in the patent literature with moderately successful results, the best of which having a CO_2/H_2 selectivity of 75.[74,75] More recently, however, cross-linked poly(vinyl alcohol) polymers containing both mobile and fixed carriers were reported to have CO2 permeabilities as high as 8200 Barrer and CO2/H2 selectivities as high as 450.[76] Based upon these results, facilitated transport may hold the future of CO_2 selective separations of carbon dioxide and hydrogen.

Cross-linked Membranes for Other Industrially Important Gas Separations

The Separation of CO_2 and CH_4

For as much attention that has been spent on the separation of hydrogen and carbon dioxide using cross-linked polymers, it would be unfair to disregard the efforts that have been applied to other industrially important gas separations. The separation of CO_2 and CH_4 is significantly important to the purification of low quality natural gas that contains above 30 mol% CO_2. A great deal of the size-selective polyimides and other polymers that can be used for the separation of H_2 and CO_2 have an equal if not amplified ability to separate carbon dioxide and methane. The cross-linking must be controlled however to allow the passage of CO_2 at relatively high permeabilities, while restricting the diffusion of CH_4.

While some suggestion UV irradiation[77], plasma treatments[78], or thermal treatments[79] for cross-linking of membranes intended for the separation of CO2 and CH4, many studies have suggested the previously mentioned transesterification or MeOH/diamine techniques. The studies involving the transesterification cross-linking reaction of polyimides have been met with moderately good success.[38,80-83] In a 6FDA-DAM/DABA 2:1 polyimide cross-linked with butylenes glycol, 50/50 CO_2/CH_4 mixed gas results showed a CO2 permeability of 158 Barrer and a selectivity of 33.[83] Those polyimides cross-linked by the MeOH/diamine method in which the diamine-containing cross-linker is a dendrimer have also shown some promise.[28,31,32] The highest ideal CO_2 permeability was 160 Barrer with a selectivity of 36.

Efforts have been spent using both methods on the modification of hollow fibers, the best CO_2/CH_4 selectivity achieved being 101 by employing the MeOH/diamine modification.[25,26,84,85]

A great deal of the CO_2 selective cross-linked polymer membranes can also be used for CO_2/CH_4 separations. The increased CO_2 solubility and the more limited diffusion coefficient and solubility for CH_4 make these relatively ideal polymers to employ in the separation of the two gases. Facilitated transport, however, proves to be the most ideal CO_2-selective way to purify carbon dioxide and methane.[86,87] The study by Wang et al. demonstrated a pure CO_2/CH_4 selectivity of 524.4 and a mixed selectivity of 46.8.

The Separation of CO_2 and N_2

The separation of CO_2 and N_2 is industrially important for the purification of air, but more interestingly has been said it could be applied as a means to utilize gases in the Martian atmosphere. In general many of the size-sieving membranes and CO_2-selective membranes are well suited for CO_2/N_2 separations.

By utilization of facilitated transport, a CO_2 soluble selective form of transport, a water-swollen hydrogel (WSH) cross-linked membrane of poly(vinyl alcohol) and glutaraldehyde (1/0.04 mol%) achieved a CO_2 permeability of nearly 140 Barrer. This permeability was discovered under a CO_2/N_2 (20/80) mixed gas feed at an upstream pressure of 179 cmHg and a downstream pressure of 0.4 cmHg at 25°C after 10hrs of permeation. Upon a CO_2/N_2 (10/90) mixed gas feed of similar conditions aside from an altered

downstream pressure (3.4 cmHg), the permeability at steady state conditions (10 hrs) was about 60 Barrer with a selectivity to N_2 of nearly 75. Finally, the addition of $KHCO_3$ (2N) and $NaASO_2$ (.5N) resulted in a decrease in the CO_2 permeability (~40 Barrer) however lending to an increase in the selectivity over N2 to nearly 100. While it was believed that the addition of the $KHCO_3$ and $NaASO_2$ would lend to increased transport performance, as tends to be the case in facilitated transport, the additives reduced the swelling ratio in the presence of water to from 108% to 61%.[88]

CONCLUSIONS

Cross-linking provides a relatively simple, yet effective route by which one can manipulate the gas transport properties of a polymer membrane intended for the separation of H_2 and CO_2. Challenges however, still exist. For instance, many of the suggested techniques by which to cross-link polymer membranes would have to be a post-fabrication step, thus increasing capital costs in an industrial setting. As a result, some research efforts have been focused on the application of membranes for large-scale applications, such as the development of hollow fiber membranes from cross-linked polyimides. Furthermore, very few cross-linked materials have been able to achieve results that challenge the Robeson trade-off line. This problem is quite fundamental in that the higher the cross-link density in the polymer, the lower the diffusion coefficient will be for gas molecules.

There have been some suggestions extending or incorporating the idea of cross-linked polymers to improve gas transport properties. José et al. studied the introduction of silica

into a PDMS network which resulted in a hybrid organic-inorganic composite membrane achieving a higher CO_2 permeability and CO_2/H_2 selectivity (~7) than PDMS alone, mildly addressing the problem of the relatively low CO_2/H_2 selectivity in the pure polymer membrane.[89] Another study has focused on the use of a PDMS network as a precursor to generate a SiO_x surface layer by UV-ozone treatment.[90] A study concentrated on the incorporation of silica (TEOS) into a cross-linked polymer resin (α,ω-diamine polypropylene oxide) resulting in an increased O_2 permeability.[91] Similar work was performed in the incorporation of silica in the generation of hybrid imide-siloxane copolymers lending to relatively fair H_2/CO_2 selectivities (~7) while maintaining H_2 permeabilities above 100 Barrer at 190°C.[92] Furthermore, as was mentioned earlier, high ion irradiation dosages can eventually lead to the carbonization of a polymer surface, generated a carbon molecular sieve membrane (CMSM).[18] This is a method that, if controlled, can cross-link the surface of a polymer. Cross-linked polyimides generated by the MeOH/diamine method can also serve as precursors to CMSMs.[93,94]

Cross-linking may not be the answer to address the separation of similarly sized gas pairs. Krol et al. suggested in their study of the separation of propylene and propane that cross-linking may in fact not be necessary to suppress plasticization, but rather that well controlled heat treatments could provide the optimal separation conditions.[58] Given the larger size of their penetrants, this is not very surprising as cross-linking constricts the polymer chain mobility to a detrimental degree in their study, though this does not rule out cross-linking for the separation of smaller penetrant gases. A final anti-plasticization

alternative to cross-linking is demonstrated in the homogeneous blending of Matrimid and either polysulfone or the P84 copolyimide, resulting in CO_2 permeabilities that fall in between the permeabilities of their pure constituents.[95]

In closing, as is most certainly the usual case, as research on the subject of cross-linking continues it is bound to lead to creative and innovative technological advances in polymer membrane gas separations. Controllable, selective transport of hydrogen, carbon dioxide, and other gases can be achieved as researchers gain further knowledge on how to manipulate the free volume or chemical groups of a polymer such that the diffusive or solubility characteristics can be controlled.

REFERENCES

[1] W.J. Koros, Evolving beyond the the thermal age of separation processes: Membranes can lead the way, *AIChE Journal,* **50** (2004) 2326.

[2] T.M. Nenoff, R.J. Spontak, C.M. Aberg, Membranes for hydrogen purification: An important step toward a hydrogen-based economy, *MRS Bulletin,* **31** (2006) 735.

[3] R.M. Barrer, Permeability of organic polymers, *Trans. Faraday Soc.*, **36** (1940) 644.

[4] R.M. Barrer, J.A. Barrie, P.S.-L. Wong, The diffusion and. solution of gases in highly crosslinked copolymers, *Polymer*, **9** (1968) 609.

[5] V. Sindelar, P. Sysel, V. Hynek, K. Friess, M. Sipek, N. Castaneda, Transport of gases and organic vapors through membranes made of poly(amide-imide)s crosslinked with poly(ethylene adipate), *Collect. Czech. Chem. Commun.*, **66** (2001) 533.

[6] B. Schiewe, C. Staudt-Bickel, A. Vuin, G. Wegner, Membrane-based gas separation of ethylene/ethylene oxide mixtures for product enrichment in microreactor technology, *ChemPhysChem*, **2** (2001) 211.

[7] M.S. Eikeland, M.-B. Hägg, M.A. Brook, M. Ottøy, A. Lindbråthen, Durability of poly(dimethylsiloxane) when exposed to chlorine gas, *J. Appl. Polym. Sci.*, **85** (2002) 2458.

[8] W. Albrecht, J. Schauer, Th. Weigel, A. Lendlein, Preparation of novel composite membranes: Reactive coating on microporous poly(ether imide) support membranes, *J. Membr. Sci.*, **269** (2006) 49.

[9] F. Pithan, C. Staudt-Bickel, Crosslinked copolyimide membranes for phenol recovery from process water by pervaporation, *ChemPhysChem*, **4** (2003) 967.

[10] X. Qiao, T.-S. Chung, Diamine modification of P84 polyimide membranes for pervaporation dehydration of isopropanol, *AIChE Journal*, **52** (2006) 3462.

[11] W.S. Dai, T.A. Barbari, Hollow fiber-supported hydrogels with mesh-size asymmetry, *J. Membr. Sci.*, **171** (2000) 79.

[12] L. Lianchao, W. Baoguo, T. Huimin, C. Tianlu, X. Jiping, A novel nanofiltration membrane prepared with PAMAM and TMC by in situ interfacial polymerization on PEK-C ultrafiltration membrane, *J. Membr. Sci.*, **269** (2006) 84.

[13] S. Sundar, W. Jang, C. Lee, Y. Shul, H. Han, Crosslinked sulfonated polyimide networks as polymer electrolyte membranes in fuel cells, *J. Polym. Sci.*, **43** (2005) 2370.

[14] K. Madhavan, B.S.R. Reddy, Synthesis and characterization of poly(dimethylsiloxane-urethane) elastomers: Effect of hard segments of polyurethane on morphological and mechanical properties, *J. Polym. Sci. Pt. A: Polym. Chem.*, **44** (2006) 2980.

[15] D. Zhou, S. Subramaniam, J.E. Mark, In situ synthesis of polyaniline in poly(dimethylsiloxane) networks using an inverse emulsion route, *J. Macromol. Sci. Pt. A. – Pure and Appl. Chem.*, **42** (2005) 113.

[16] L. Hu, X. Xu, J.B. Ilconich, S. Ellis, Maria Coleman, Impact of H+ ion irradiation on Matrimid®. I. Evolution in chemical structure, *J. Appl. Polym. Sci.*, **90** (2003) 2010.

[17] A. Tóth, V.S. Khotimsky, I. Bertóli, G. Marletta, Particle-beam treatment of organosilicon gas separation membranes: A novel way of controlling their mass transport properties, *J. Appl. Polym. Sci.*, **60** (1996) 1883.

[18] J. Won, M.H. Kim, Y.S. Kang, H.C. Park, U.Y. Kim, S.C. Choi, S.K. Koh, Surface modification of polyimide and polysulfone membranes by ion beam for gas separation, *J. Appl. Polym. Sci.*, **75** (2000) 1554.

[19] J. Weichart, J Müller, Plasma polymerization of silicon organic membranes for gas separation, *Surf. Coat. Technol.*, **59** (1993) 342.

[20] J.D. Wind, S.M. Sirard, D.R. Paul, P.F. Green, K.P. Johnston, W.J. Koros, Carbon dioxide-induced plasticization of polyimide membranes: Pseudo-equilibrium relationships of diffusion, sorption, and swelling, *Macromolecules*, **36** (2003) 6433.

[21] R.A. Hayes, Amine-modified polyimide membranes, US Patent No. 4,981,497, 1991.

[22] C. Zhou, T.S. Chung, R. Wang, Y. Liu, S.H. Goh, The accelerated CO_2 plasticization of ultra-thin polyimide films and the effect of surface chemical cross-linking on plasticization and physical aging, *J. Membr. Sci.*, **225** (2003) 125.

[23] Y. Liu, R. Wang, T.-S. Chung, Chemical cross-linking modification of polyimide membranes for gas separation, *J. Membr. Sci.*, **189** (2001) 231.

[24] P.S. Tin, T.-S. Chung, Y. Liu, R. Wang, S.L. Liu, K.P. Pramoda, Effects of cross-linking modification on gas separation performance of Matrimid membranes, *J. Membr. Sci.*, **225** (2003) 77.

[25] Y. Liu, T.-S. Chung, R. Wang, D.F. Li, M.L. Chng, Chemical cross-linking modification of polyimide/poly(ether sulfone) duel-layer hollow-fiber membranes for gas separation, *Ind. Eng. Chem. Res.*, **42** (2003) 1190.

[26] C. Cao, T.-S. Chung, Y. Liu, R. Wang, K.P. Pramoda, Chemical cross-linking modification of 6FDA-2,6-DAT hollow fiber membranes for natural gas separation, *J. Membr. Sci.*, **216** (2003) 257.

[27] L. Shao, T.-S. Chung, S.H. Goh, K.P. Pramoda, Transport properties of cross-linked polyimide membranes induced by different generations of diaminobutane (DAB) dendrimers, *J. Membr. Sci.*, **238** (2004) 153.

[28] T.-S. Chung, M.L. Chng, K.P. Pramoda, Y. Xiao, PAMAM dendrimer-induced cross-linking modification of polyimide membranes, *Langmuir*, **20** (2004) 2966.

[29] L. Shao, T.-S. Chung, S.H. Goh, K.P. Pramoda, Polyimide modification by a linear aliphatic diamine to enhance transport performance and plasticization resistance, *J. Membr. Sci.*, **256** (2005) 46.

[30] L. Shao, T.-S. Chung, S. H. Goh, K. P. Pramoda, The effects of 1,3-cyclohexanebis(methylamine) modification on gas transport and plasticization resistance of polyimide membranes, *J. Membr. Sci.*, **267** (2005) 78.

[31] Y. Xiao, T.-S. Chung, M.L. Chng, Surface characterization, modification chemistry, and separation performance of polyimide and polyamidoamine dendrimer composite films, *Langmuir*, **20** (2004) 8230.

[32] Y. Xiao, L. Shao, T.-S. Chung, D.A. Schiraldi, Effects of thermal treatments and dendrimers chemical structures on the properties of highly surface cross-linked polyimide films, *Ind. Eng. Chem. Res.*, **44** (2005) 3059.

[33] E. Powell, X. Duthie, S. Kentish, G.G. Qiao, G. Stevens, Reversible diamine cross-linking of polyimide membranes, *J. Membr. Sci.*, **291** (2007) 199.

[34] T.-S. Chung, L. Shao, P.S. Tin, Surface modification of polyimide membranes by diamines for H2 and CO2 separation, *Macromol. Rapid Commun.*, **27** (2006) 998.

[35] K. Nagai, N. Booker, A. Mau, J. Hodgkin, S. Kentish, G. Stevens, A. Geertsema, Gas permeation properties of polyimide/epoxy composite materials, *Polymeric Materials: Science & Engineering*, **85** (2001) 91.

[36] X. Duthie, S. Kentish, E. Powell Clem, G.G. Qiao, K. Nagai, G. Stevens, Plasticization suppression in grafted polyimide-epoxy network membranes, *Ind. Eng. Chem. Res.*, **46** (2007) 8183.

[37] Y. Xiao, T.-S. Chung, H.-M. Guan, M.D. Guiver, Synthesis, cross-linking and carbonization of co-polyimides containing internal acetylene units for gas separation, *J. Membr. Sci.*, **302** (2007) 254.

[38] J.D. Wind, C. Staudt-Bickel, D.R. Paul, W.J. Koros, The effects of crosslinking chemistry on CO2 plasticization of polyimide gas separation membranes, *Ind. Eng. Chem. Res.*, **41** (2002) 6139.

[39] S. Xiao, X. Feng, R.Y.M. Huang, Trimesoly chloride crosslinked chitosan membranes for CO2/N2 separation and pervaporation dehydration of isopropanol, *J. Membr. Sci.*, **306** (2007) 36.

[40] M.-H. Tsai, S.-L. Huang, P.-C. Chiang, C.-J. Chen, Morphology, dynamic mechanical properties, and gas separation of crosslinking silica-containing polyimide nanocomposite thin film, *J. Appl. Polym. Sci.,* **106** (2007) 3185.

[41] C. Hibshman, C.J. Cornelius, E. Marand, The gas separation effects of annealing polyimide-organosilicate hybrid membranes, *J. Membr. Sci.*, **211** (2003) 25.

[42] Y. Yin, M. Yoshino, J. Fang, K. Tanaka, H. Kita, K.-I. Okamoto, Synthesis and gas permeation properties of star-like poly(ethylene oxides)s using hyperbranched polyimide as central core, *Polymer Journal*, **36** (2004) 294.

[43] Y. Hirayama, Y. Kase, N. Tanihara, Y. Sumiyama, Y. Kusuki, K. Haraya, Permeation properties to CO2 and N2 of poly(ethylene oxide)-containing and crosslinked polymer films, *J. Membr. Sci.*, **160** (1999) 87.

[44] N. Patel, A.C. Miller, R.J. Spontak, Highly CO2-permeable and selective polymer nanocomposite membranes, *Adv. Mater.*, **15** (2003) 729.

[45] N. Patel, A.C. Miller, R.J. Spontak, Highly CO2-permeable and -selective membranes derived from crosslinked poly(ethylene glycol) and its nanocomposites, *Adv. Funct. Mater.*, **14** (2004) 699.

[46] N. Patel, M.A. Hunt, S. Lin-Gibson, S. Bencherif, R.J. Spontak, Tunable CO2 transport through mixed polyether membranes, *J. Membr. Sci.*, **251** (2005) 51.

[47] M.A. Borns, S. Kalakkunnath, D.S. Kalika, V.A. Kusuma, B.D. Freeman, Dynamic relaxation characterisitics of crosslinked poly(ethylene oxide) copolymer networks: Influence of short chain pendant groups, *Polymer*, **48** (2007) 7316.

[48] S. Kelman, H. Lin, E.S. Sanders, B.D. Freeman, CO2/C2H6 separation using solubility selective membranes, *J. Membr. Sci.*, **305** (2007) 57.

[49] R.D. Raharjo, H. Lin, D.F. Sanders, B.D. Freeman, S. Kalakkunnath, D.S. Kalika, Relation between network structure and gas transport in crosslinked poly(propylene glycol diacrylate), *J. Membr. Sci.*, **283**

[50] H. Kita, T. Inada, K. Tanaka, K. Okamoto, Effect of photocrosslinking on permeability and permselectivity of gases through benzophenone-containing polyimide, *J. Membr. Sci.*, **87** (1994) 139.

[51] Y. Liu, C. Pan, M. Ding, J. Xu, Effect of crosslinking distribution on gas permeability and permselectivity of crosslinked polyimides, *Euro. Polym. Journal*, **35** (1999) 1739.

[52] Y. Liu, M. Ding, J. Xu, Gas permeabilities and permselectivity of photochemically crosslinked polyimides, *J. Appl. Polym. Sci.*, **58** (1995) 485.

[53] C.T. Wright, D.R. Paul, Gas sorption and transport in UV-irradiated polyarylate copolymers based on tetramethyl bisphenol-A and dihydroxybenzophenone, *J. Membr. Sci.*, **124** (1997) 161.

[54] M.S. McCaig, D.R. Paul, Effect of UV crosslinking and physical aging on the gas permeability of thin glassy polyarylate films, *Polymer*, **40** (1999) 7209.

[55] C.-C. Hu, C.-Y. Tu, Y.-C. Wang, C.-L. Li, K.-R. Lee, J.-Y. Lai, Effects of plasma treatment on CO2 plasticization of poly(methyl methacrylate) gas-separation membranes, *J. Appl. Polym. Sci.*, **93** (2004) 395.

[56] H. Kawakami, M. Mikawa and S. Nagaoka, Gas transport properties in thermally cured aromatic polyimide membranes, *J. Membr. Sci.*, **118** (1996) 223.

[57] A. Bos, I.G.M. Punt, M. Wessling, H. Strathmann, Suppression of CO2-plasticization by semiinterpenetrating polymer network formation, *J. Polym. Sci Pt. B: Polym. Phys.*, **36** (1998) 1547.

[58] J.J. Krol, M. Boerrigter, G.H. Koops, Polyimide hollow fiber gas separation membranes: Preparation and the suppression of plasticization in propane/propylene environments, *J. Membr. Sci.*, **184** (2001) 275.

[59] J.N. Barsema, S.D. Klijnstra, J.H. Balster, N.F.A. van der Vegt, G.H. Koops, M. Wessling, Intermediate polymer to carbon gas separation membranes based on Matrimid PI, *J. Membr. Sci.*, **238** (2004) 93.

[60] Y. Liu, M.L. Chng, T.-S. Chung, R. Wang, Effects of amidation on gas permeation properties of polyimide membranes, *J. Membr. Sci.*, **214** (2003) 83.

[61] J. Li, V. Janout, S.L. Regen, Glued Langmuir-Blodgett bilayers having unusually high He/CO2 permeation selectivities, *Langmuir*, **21** (2005) 1676.

[62] M. Rezac, E.T. Sorensen, H.W. Beckham, Transport properties of crosslinkable polyimide blends, *J. Membr. Sci.*, **136** (1997) 249.

[63] C.T. Wright, D.R. Paul, Feasibility of thermal crosslinking of polyarylate gas-separation membranes using benzocyclobutene-based monomers, *J. Membr. Sci.*, **129** (1997) 47.

[64] M. Rezac, B. Schoberl, Transport and thermal properties of poly(ether imide)/acetylene-terminated monomer blends, *J. Membr. Sci.*, **156** (1999) 211.

[65] D.P. Dworak, H. Lin, B.D. Freeman, M.D. Soucek, Gas permeability analysis of photo-cured cyclohexyl-substituted polysiloxane films, *J. Appl. Polym. Sci.*, **102** (2006) 2343.

[66] C.J. Orme, M.K. Harrup, T.A. Luther, R.P. Lash, K.S. Houston, D.H. Weinkauf, F.F. Stewart, Characterization of gas transport in selected rubbery amorphous polyphosphazene membranes, *J. Membr. Sci.*, **186** (2001) 249.

[67] P. Jha, L.W. Mason, J.D. Way, Characterization of substituted polyphosphazene membranes – pure and mixed gas results, *Ind. Eng. Chem. Res.*, **45** (2006) 6570.

[68] H. Lin, T. Kai, B.D. Freeman, S. Kalakkunnath, D.S. Kalika, The effect of cross-linking on gas permeability in cross-linked poly(ethylene glycol diacrylate), *Macromolecules*, **38** (2005) 8381.

[69] H. Lin, B.D. Freeman, Gas and vapor solubility in cross-linked poly(ethylene glycol diacrylate), *Macromolecules*, **38** (2005) 8394.

[70] H. Lin, E. Van Wagner, J.S. Swinnea, B.D. Freeman, S.J. Pas, A.J. Hill, S. Kalakkunnath, D.S. Kalika, Transport and structural characteristics of crosslinked poly(ethylene oxide) rubbers, *J. Membr. Sci.*, **276** (2006) 145.

[71] H. Lin, E. Van Wagner, B.D. Freeman, L.G. Toy, R.P. Gupta, Plasticization-enhanced hydrogen purification using polymeric membranes, *Science*, **311** (2006) 639.

[72] H. Lin, B.D. Freeman, Gas permeation and diffusion in cross-linked poly(ethylene glycol diacrylate), *Macromolecules*, **39** (2006) 3568.

[73] M.-B. Hägg, R. Quinn, Polymeric facilitated transport membranes for hydrogen purification, *MRS Bulletin,* **31** (2006) 750.

[74] W.S.W. Ho, Membranes comprising salts of amino acids in hydrophilic polymers, US Patent No. 5,611,843 (1997).

[75] W.S.W. Ho, Membranes comprising amino acid salts in polyamine polymers and blends, US Patent No. 6,099,621 (2000).

[76] J. Zou, W.S.W. Ho, CO2-selective polymeric membranes containing amines in crosslinked poly(vinyl alcohol), *J. Membr. Sci.*, **286** (2006) 310.

[77] P. Tiemblo, J Guzman, E. Riande, E.F. Salvador, C. Peinado, Gas transport properties in crosslinked polymers. I. Aliphatic polyurethane-acrylate-based adhesives, *J. Polym. Sci. Pt. B: Polym. Phys.*, **39** (2001) 786.

[78] S. Borisov, V.S. Khotimsky, A.I. Rebrov, S.V. Rykov, D.I. Slovetsky, Y.M Pashunin, Plasma fluorination of organosilicon polymeric films for gas separation applications, *J. Membr. Sci.*, **125** (1997) 319.

[79] A. Bos, I.G.M. Punt, M. Wessling, H. Strathmann, Plasticization-resistant glassy polyimide membranes for CO2/CH4 separations, *Sep. Purif. Technol.*, **14** (1998) 27.

[80] C. Staudt-Bickel, W.J. Koros, Improvement of CO2/CH4 separation characteristics of polyimides by chemical crosslinking, *J. Membr. Sci.*, **155** (1999) 145.

[81] C. Staudt-Bickel, Cross-linked copolyimide membranes for the separation of gaseous and liquid mixtures, *Soft Materials*, **1** (2003) 277.

[82] J.D. Wind, C. Staudt-Bickel, D.R. Paul, W.J. Koros, Solid-state covalent cross-linking of polyimide membranes for carbon dioxide plasticization reduction, *Macromolecules*, **36** (2003) 1882.

[83] J.D. Wind, D.R. Paul, W.J. Koros, Natural gas permeation in polyimide membranes, *J. Membr. Sci.*, **228** (2004) 227.

[84] D.W. Wallace, J. Williams, C. Staudt-Bickel, W.J. Koros, Characterization of crosslinked hollow fiber membranes, *Polymer*, **47** (2006) 1207.

[85] J. Ren, R. Wang, T.-S. Chung, D.F. Li, Y. Liu, The effects of chemical modifications on morphology and performance of 6FDA-ODA/NDA hollow fiber membranes for CO2/CH4 separation, *J. Membr. Sci.*, **222** (2003) 133.

[86] C. Yi, Z. Wang, M. Li, J. Wang, S. Wang, Facilitated transport of CO2 through polyvinylamine/polyethylene glycol blend membranes, *Desalination*, **193** (2006) 90.

[87] Z. Wang, C. Yi, Y. Zhang, J. Wang, S. Wang, CO2-facilitated transport through poly(N-vinyl-g-sodium aminobutyrate-co-sodium acrylate)/polysulfone composite membranes, *J. Appl. Polym. Sci.*, **100** (2006) 275.

[88] Y.-I Park, K.-H. Lee, Preparation of water-swollen hydrogel membranes for gas separation, *J. Appl. Polym. Sci.*, **80** (2001) 1785.

[89] N.M. Jose, L.A.S.A. Prado, I.V.P. Yoshida, Synthesis, characterization, and permeability evaluation of hybrid organic-inorganic films, *J. Polym. Sci. Pt. B: Polym. Phys.*, **42** (2004) 4281.

[90] M. Ouyang, R.J. Muisener, A. Boulares, J.T. Koberstein, UV-ozone induced growth of SiOx surface layer on a cross-linked polysiloxane film: Characterization and gas separation properties, *J. Membr. Sci.*, **177** (2000) 177.

[91] I. Park, H. Peng, D.W. Gidley, S. Xue, T.J Pinnavaia, Epoxy-silica mesocomposites with enhanced tensile properties and oxygen permeability, *Chem. Mater.*, **18** (2006) 650.

[92] M. Smaihi, J.-C. Schrotter, C.Lesimple, I. Prevost, C. Guizard, Gas separation properties of hybrid imide-siloxane copolymers with various silica contents, *J. Membr. Sci.*, **161** (1999) 157.

[93] P.S. Tin, T.-S. Chung, Novel approach to fabricate carbon molecular-sieve membranes based on consideration of interpenetrating networks, *Macromol. Rapid Commun.*, **25** (2004) 1247.

[94] P.S. Tin, T.-S. Chung, S. Kawi, M.D. Guiver, Novel approaches to fabricate carbon molecular sieve membranes based on chemical modified and solvent treated polyimides, *Microporous and Mesoporous Mat.*, **73** (2004) 151.

[95] A. Bos, I. Punt, H. Strathmann, M. Wessling, Supression of gas separation membrane plasticization by homogenous polymer blending, *AIChE Journal*, **47** (2001) 1088.

FIGURES AND TABLES

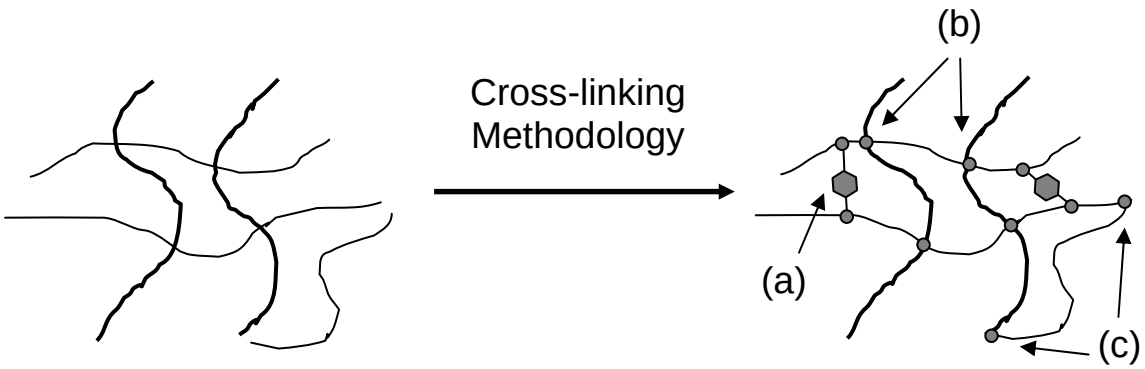

Figure 2-1. Cross-link network generation scheme. This figure demonstrates a simple scheme by which to understand the multiple ways in which a polymer can be cross-linked to generate a network: (a) multifunctional grafted small molecules, (b) internal functional groups, (c) functional end-groups.

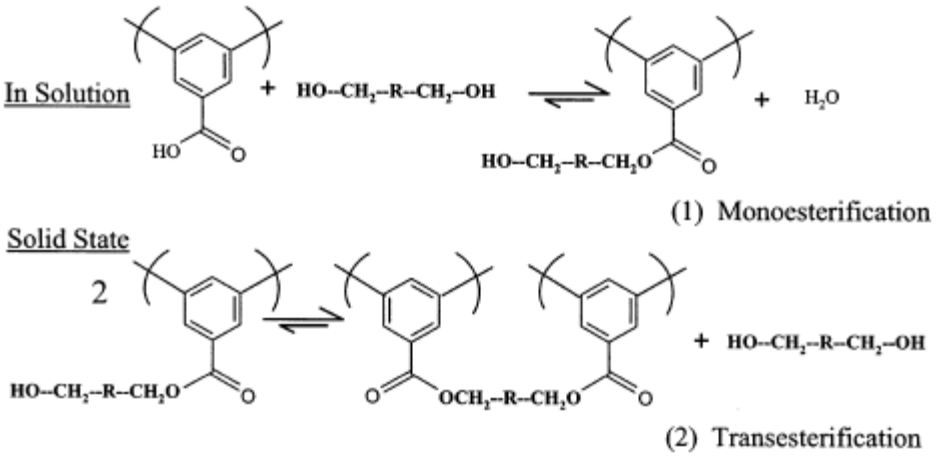

Figure 2-2. Transesterification cross-linking reaction of DABA-containing polyimide. Transesterification cross-linking reaction of DABA-containing polyimide upon addition of a diol and a thermal step. (Adapted from Ref. 20)

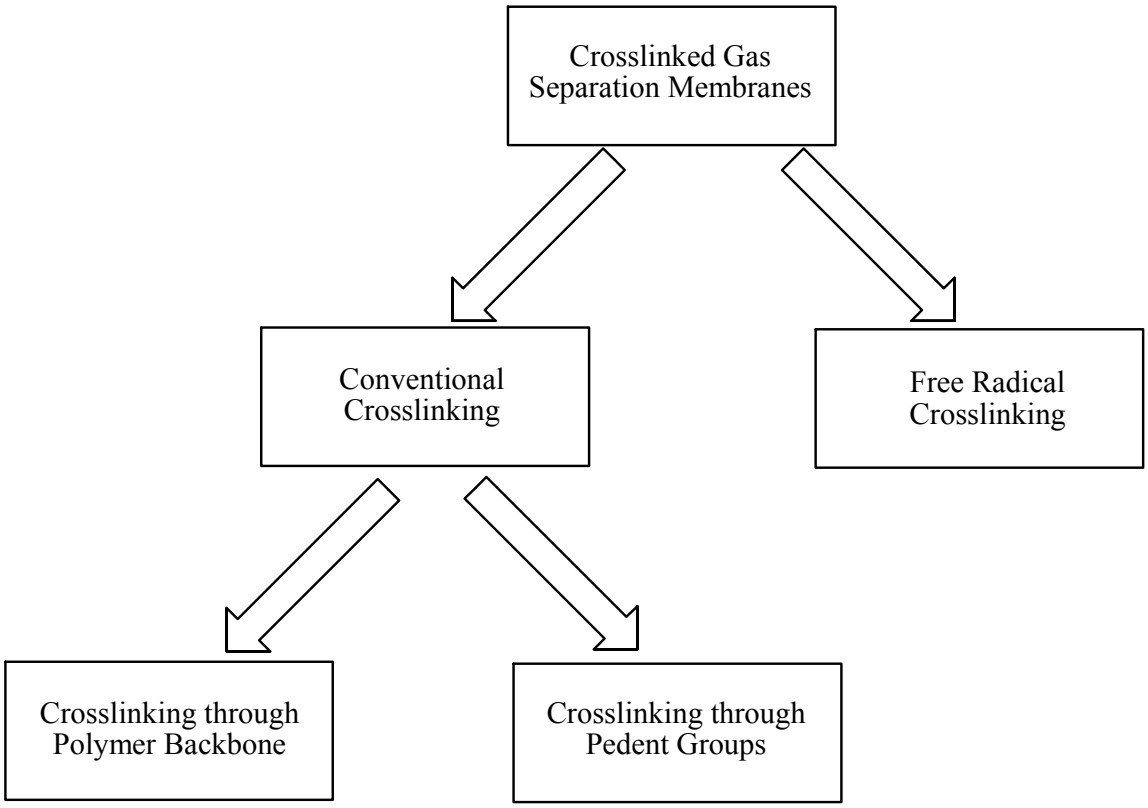

Figure 2-3. Cross-linking polyimides. This flowchart comprehensively demonstrates the various methods of cross-linking polyimides.

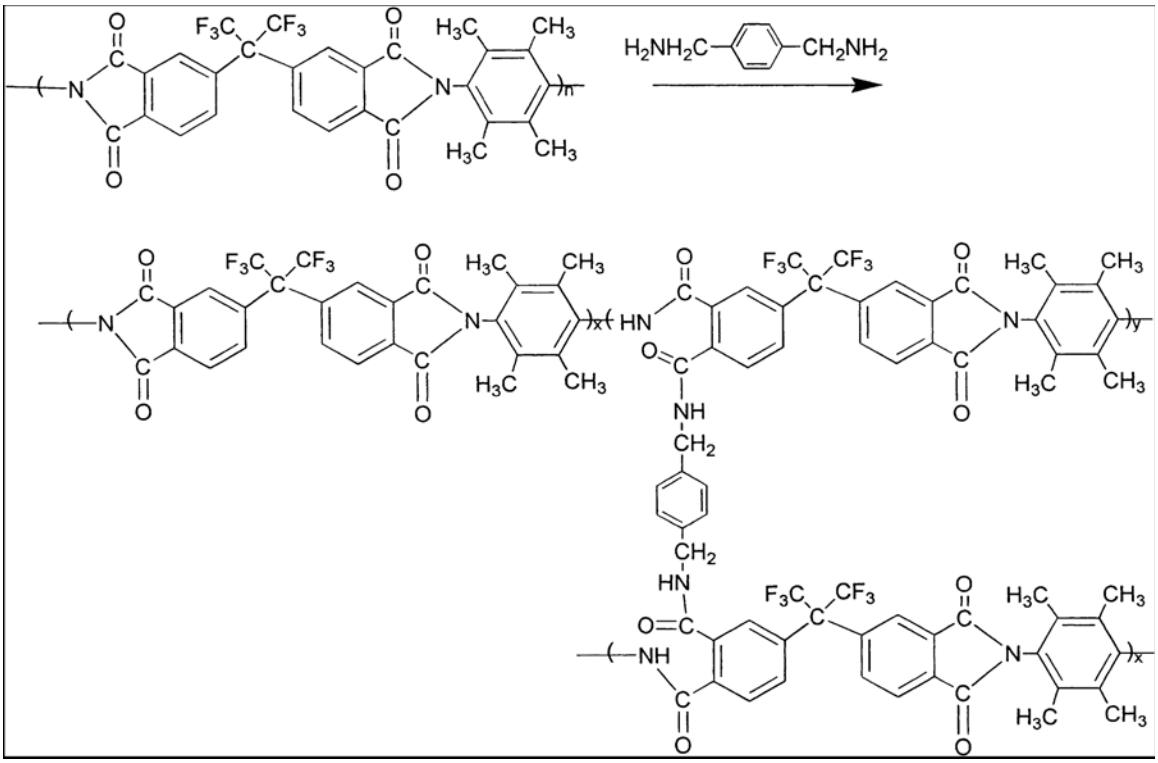

Figure 2-4. Diamino-modification cross-linking reaction scheme. (Adapted from Ref. 23)

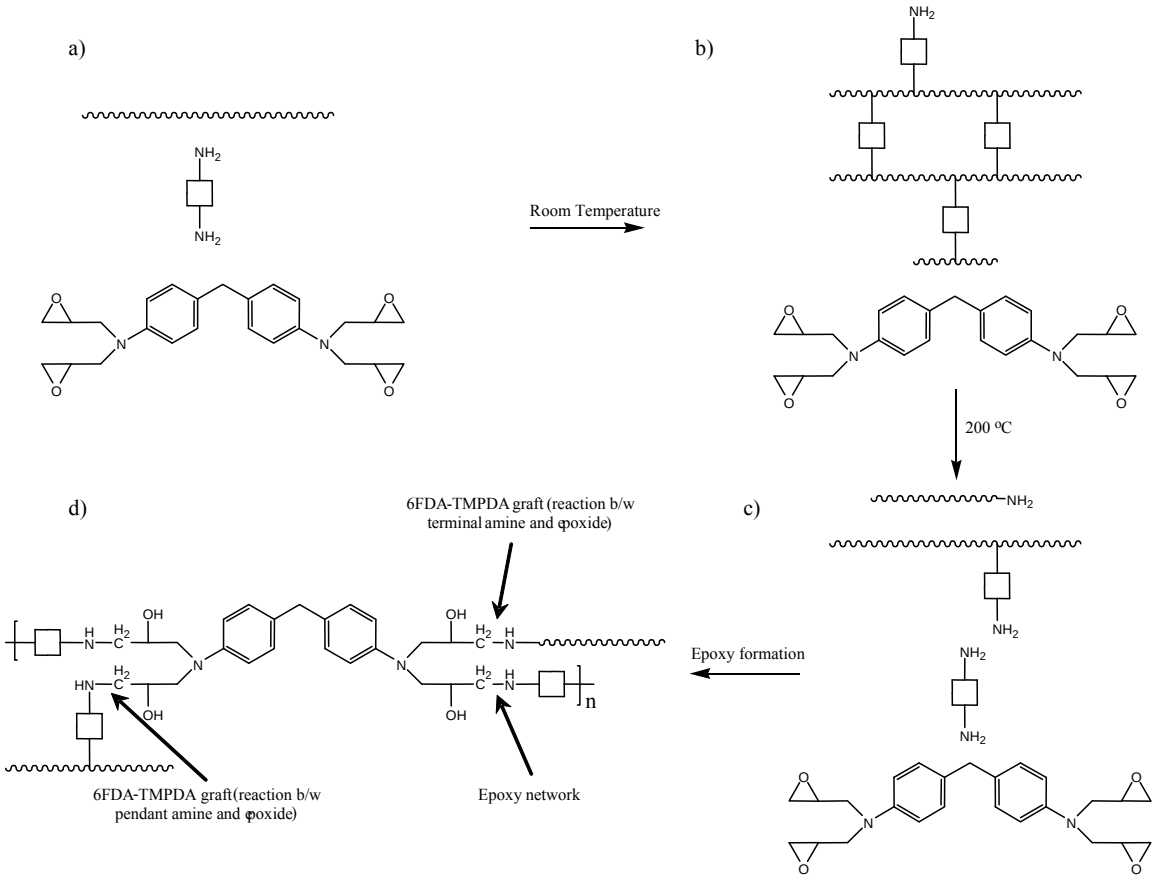

Figure 2-5. Polyimide-diamine reaction variations. Scheme illustrating some of the different types of bonding which can be formed during the reactions between polyimides, diamines and epoxides.

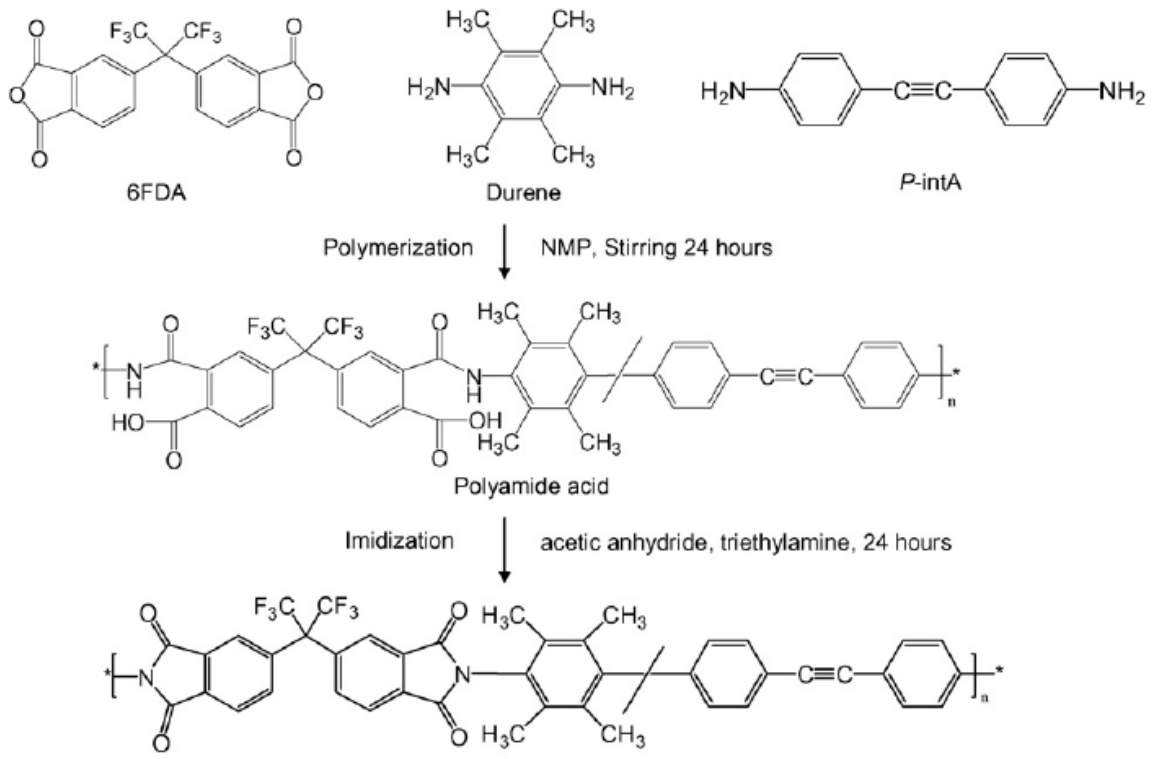

Figure 2-6. Synthesis of copolyimides containing internal acetylenes (Adapted from Ref. 37).

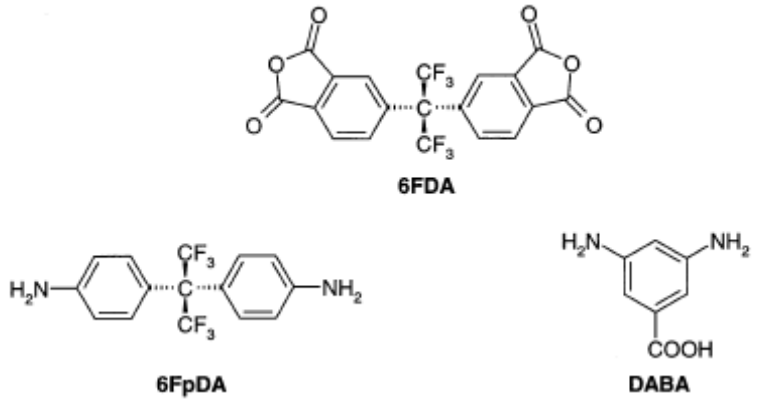

Figure 2-7. Monomers used in synthesis copolymers containing pendent carboxylic acid groups (Adapted from Ref. 38).

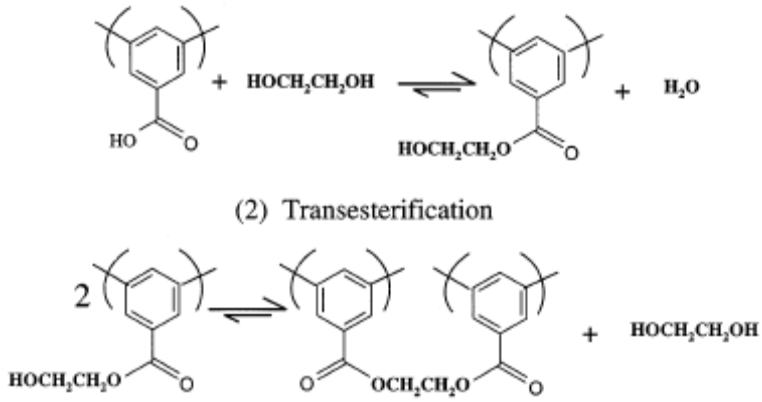

Figure 2-8. Transesterification reaction (Adapted from Ref. 38).

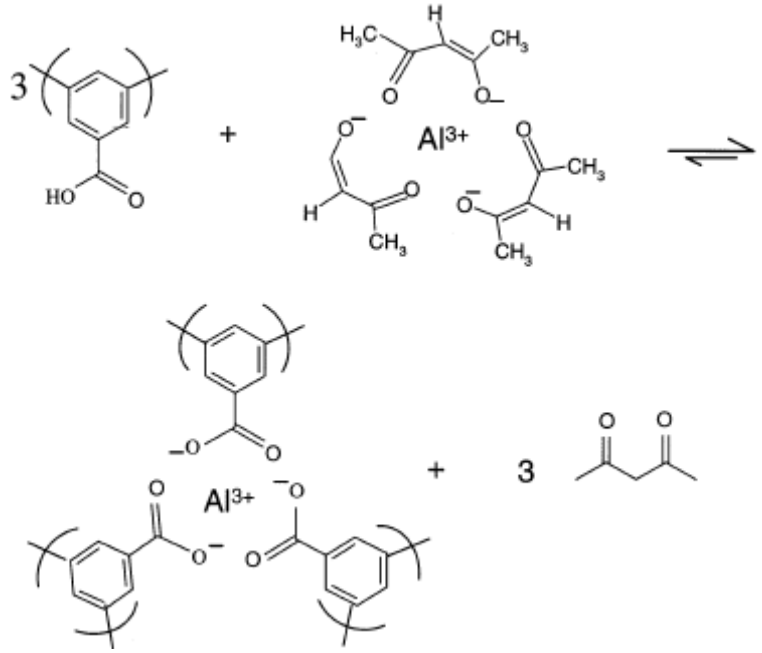

Figure 2-9. Reaction between polymer containing pendent carboxylic acid groups and aluminium cations (Adapted from Ref. 38).

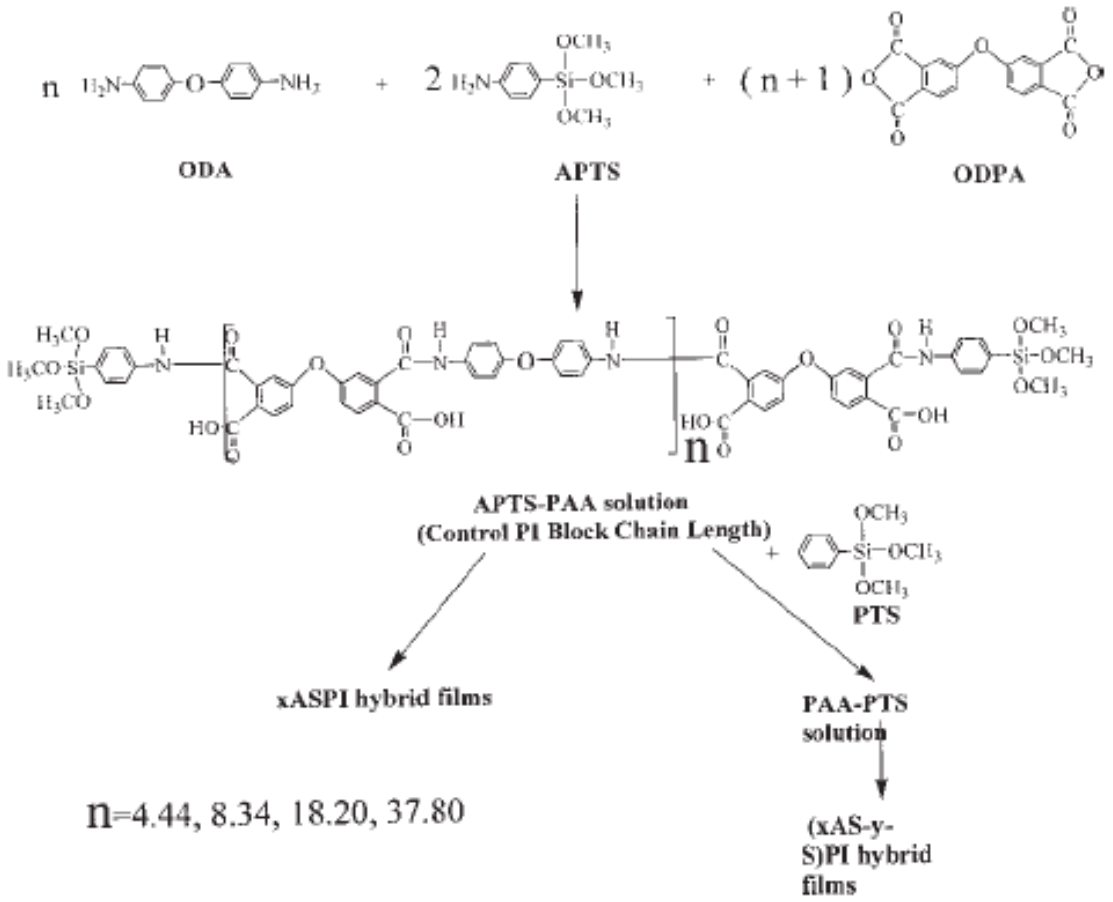

Figure 2-10. Preparation of polymer/silica hybrid membranes with silica in the polymer end group (Adapted from Ref. 40).

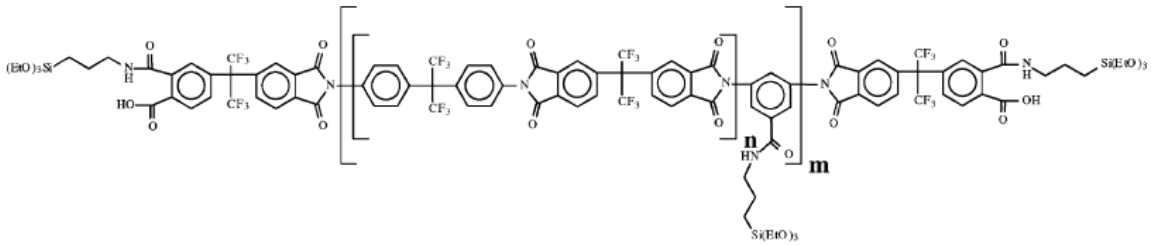

Figure 2-11. Polymer/silica hybrid membranes with silica in pendent groups (Adapted from Ref. 41).

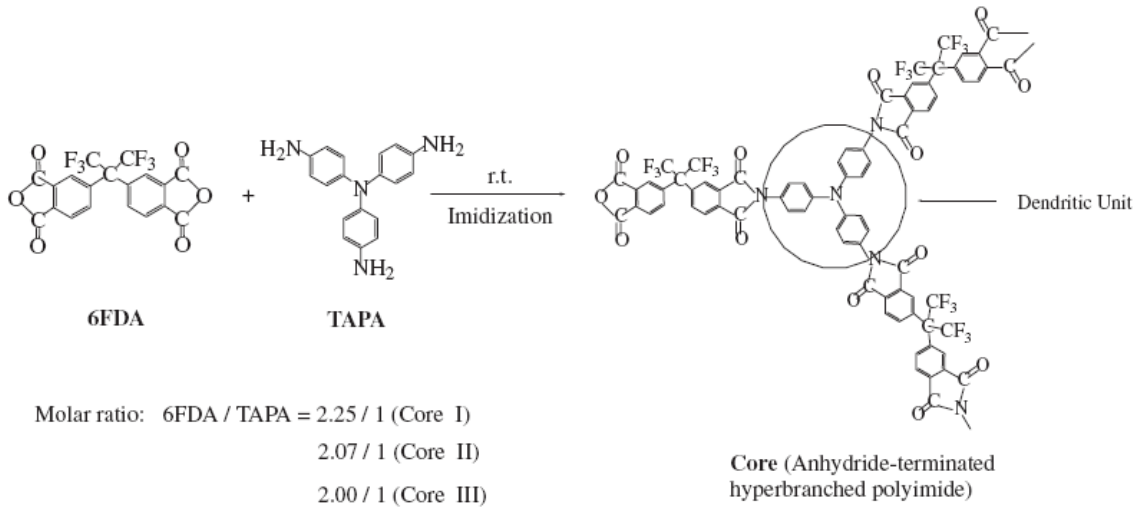

Figure 2-12. Synthesis of hyper branched core (Adapted from Ref. 42).

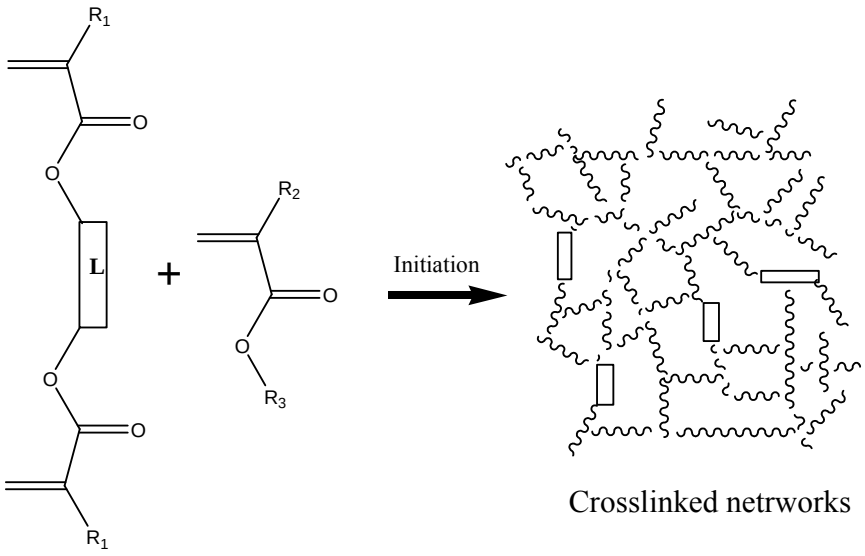

Figure 2-13. Polymer membrane network formed from free radical polymerization.

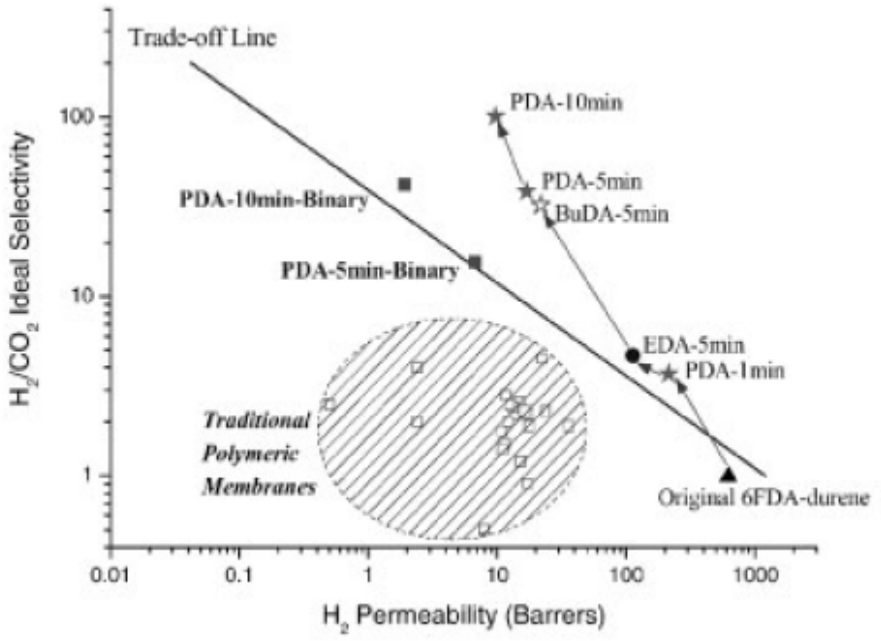

Figure 2-14. Permselective trade-off line for H_2 and CO_2. This figure is showing the ideal-gas and mixed-gas performance of linear short-chain aliphatic modified polyimides (Adapted from Ref. 34).

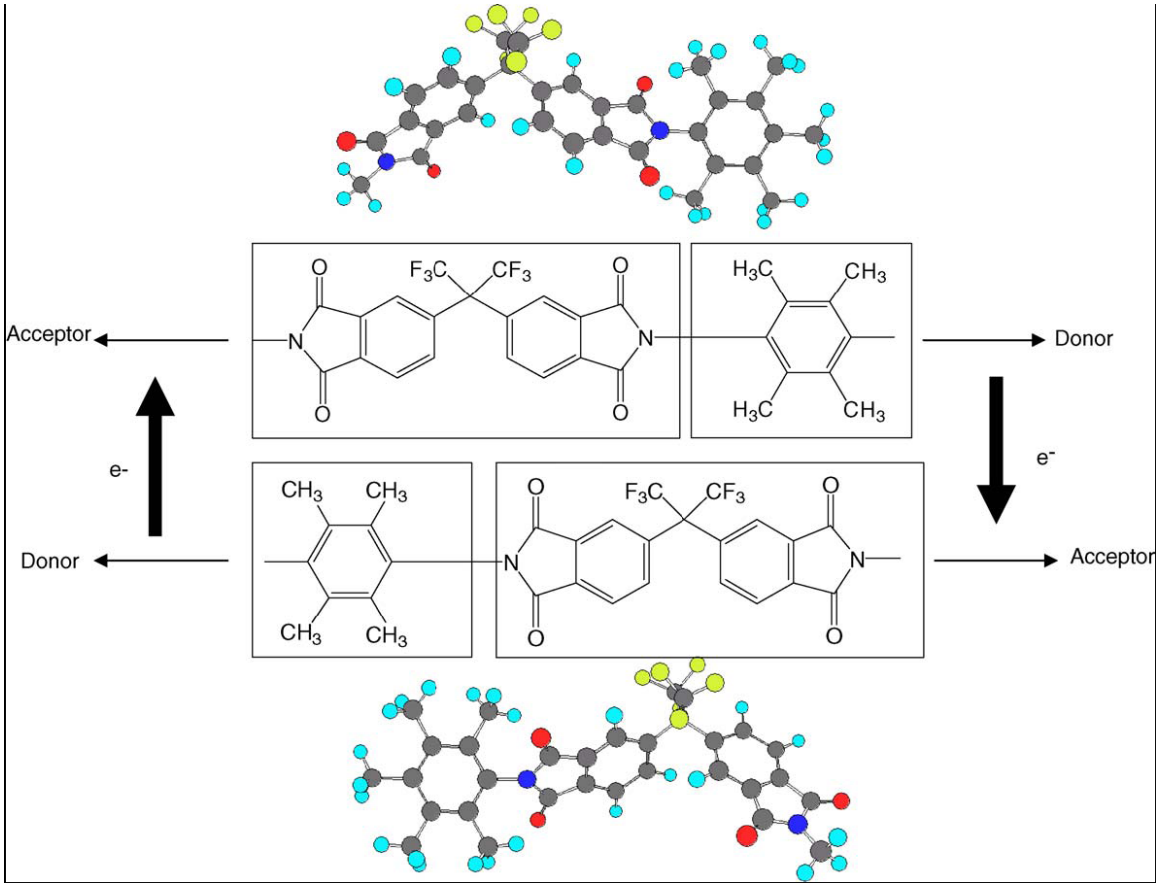

Figure 2-15. Scheme of charge transfer complex orientation with electron donors and acceptors (Adapted from Ref. 60).

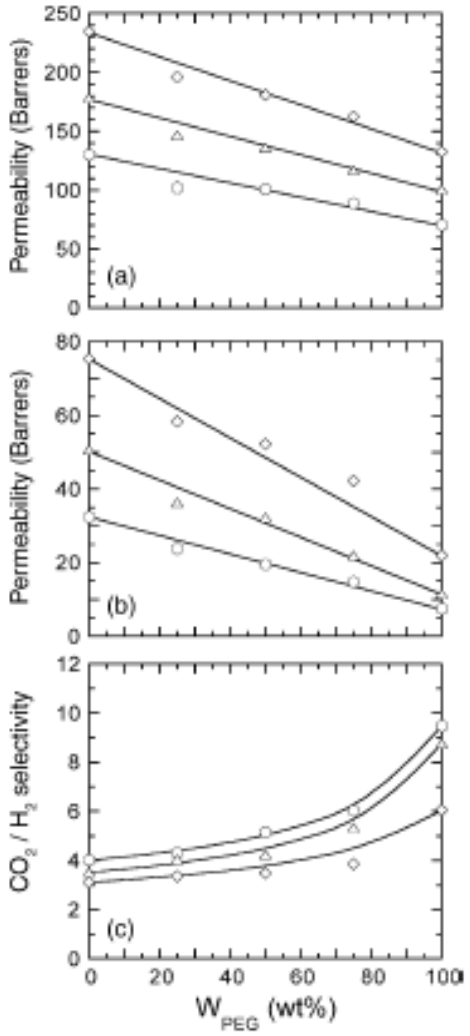

Figure 2-16. Gas transport variations of cross-linked polyethers. Variation of (a) CO_2 permeability, (b) H_2 permeability and (c) CO_2/H_2 selectivity with composition (WPEG) in PEGda/PPGda mixed membranes at three different temperatures (in ◦C): 23 (open circle), 35 (open triangle) and 50 (open diamond) (Adapted from Ref. 46).

Table 2-1. Selected Diamines used as Cross-linking Agents

Crosslinking agent	Structure	Reference
1,3-diaminobenzene	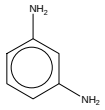	[33]
PAMAM Dendrimer	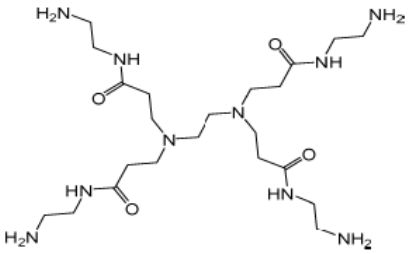	[28]
p-xylenediamine	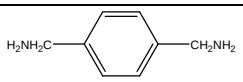	[23, 24, 26]
DAB-AM-4 G1 Dendrimer	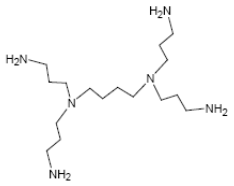	[27]
DAB-AM-8 G2 Dendrimer	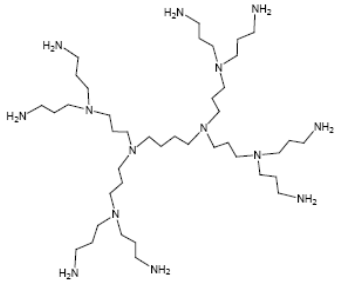	[27]
DAB-AM-16 G3 Dendrimer	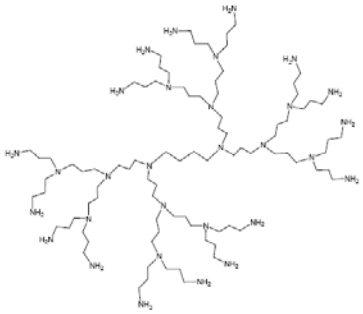	[27]

Table 2-1 (continued).

1,3-cyclohexanebis(methylamine)	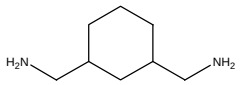	[30]
1,2-diaminoethane	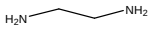	[29]
1,3-diaminopropane		[34]
1,6-diaminohexane		[21]
Tris(2-aminoethyl)amine	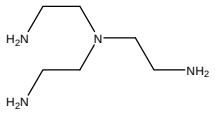	[21]
Triethylenetetraamine	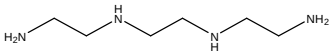	[21]
Pentaethylenehexaamine	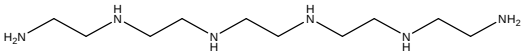	[21]
JEFFAMINE ED-900	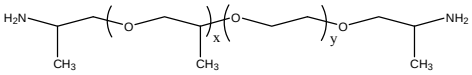	[21]
Polyethyleneimine	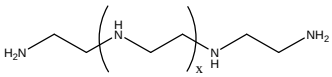	[21]

Table 2-2. Selected Examples of Cross-linked Polyethylene Oxides

Monomer	Structures	Initiator	Reference
Polyethylene glycol dimethacrylate	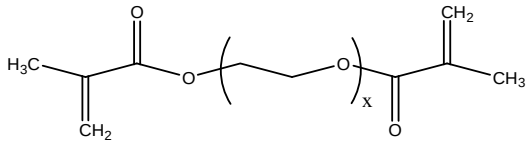	Plasma Treatment	[43]
2,2-bis(4-methacryloxy polyethoxyphenyl)propane	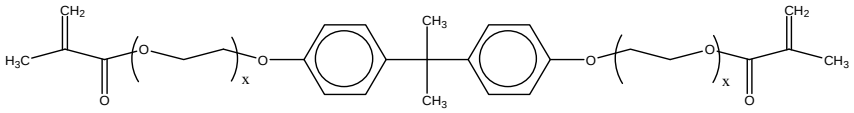	Plasma Treatment	[43]
Polyethylene glycol diacrylate	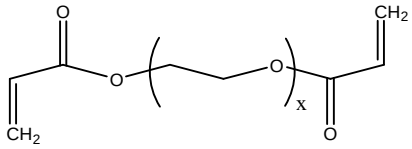	AIBN	[44, 45]

Table 2-2 (continued).

Poly(ethylene glycol)diacrylate blended with poly(ethylene oxide), poly(propylene glycol)diacrylate, 2-aminoethyl methacrylate hydrochloride or poly(ethylene glycol)urethane dimethacrylate	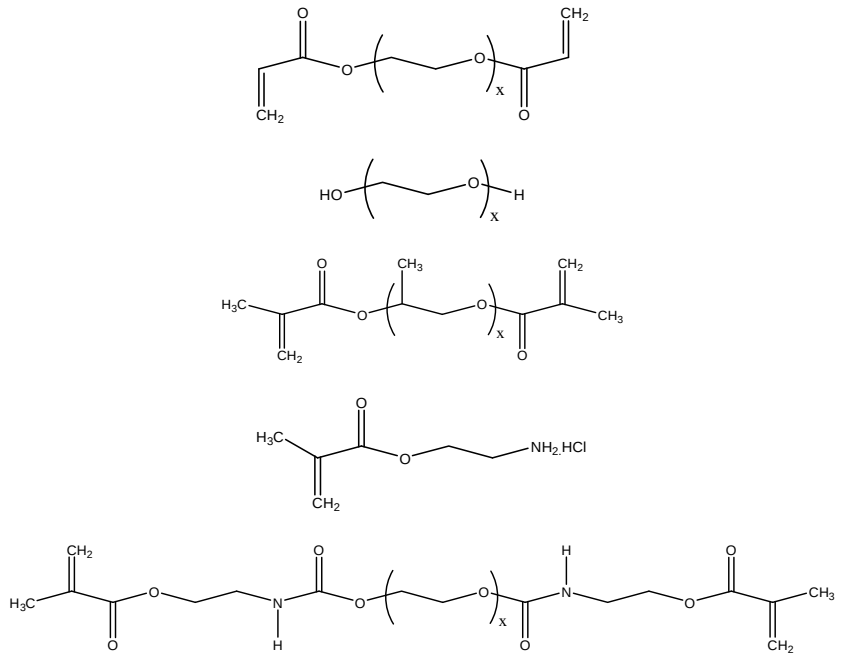	AIBN	[46]

Table 2-2 (continued).

Poly(ethylene glycol) diacrylate blended with ethylene glycol methyl ether acrylate, 2-hydroxy ethyl acrylate, or diethylene glycol ethyl ether acrylate	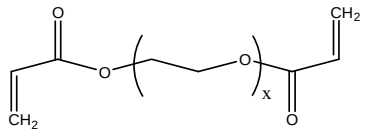 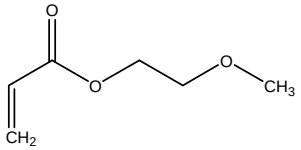 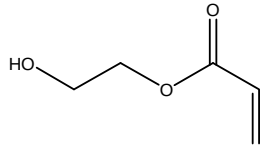 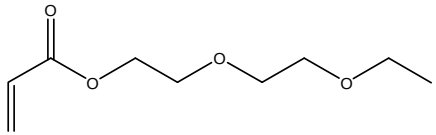	1-hydroxyl-cyclohexyl phenyl ketone + uv light	[47]

Table 2-2 (continued).

Poly(ethylene glycol) diacrylate and poly(ethylene glycol) methyl ether acrylate blend	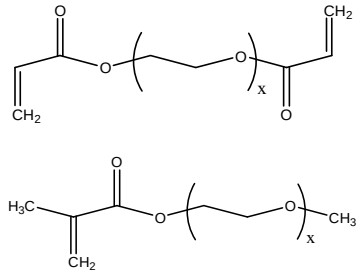	1-hydroxyl-cyclohexyl phenyl ketone + uv light	[48]
Copolymers from poly(propylene glycol) diacrylate and poly(propylene glycol) methyl ether acrylate	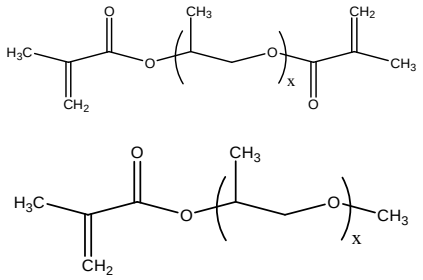	1-hydroxyl-cyclohexyl phenyl ketone + uv light	[49]

CHAPTER 3

Extended Chemical Cross-linking of a Thermoplastic Polyimide: Macroscopic and Microscopic Property Development

Christopher M. Aberg,[†] **Ali E. Ozcam,**[†] **Jacob M. Majikes**,[‡] **Mohamed A. Seyam**[†] and **Richard J. Spontak**[†‡]

[†] Department of Chemical & Biomolecular Engineering, North Carolina State University, Raleigh, NC 27695, USA

[‡]Department of Materials Science & Engineering, North Carolina State University, Raleigh, NC 27695, USA

(in press in *Macromolecular Rapid Communications*)

Abstract

Polyimides are well-established as gas-separation membranes due to their intrinsically low free-volume and correspondingly high H_2 selectivity relative to other gases such as CO_2. Prior studies have established that H_2/CO_2 selectivity can be improved by cross-linking polyimides with diamines differing in spacer length. In this work, we follow the evolution of macroscopic and microscopic properties of a commercial polyimide over long cross-linking times (t_x) with 1,3-diaminopropane. According to spectroscopic analysis, the cross-linking reaction saturates after ~24 h, whereas tensile, nanoindentation and stress-relaxation tests reveal that the material stiffens, and possesses a long relaxation time that increases, with increasing t_x. Although differential scanning calorimetry shows that the glass transition temperature decreases systematically with increasing t_x, permeation studies indicate that the permeabilities of H_2 and CO_2 decrease, while the H_2/CO_2 selectivity increases markedly, with increasing t_x. At long t_x, the polyimide becomes impermeable to CO_2, suggesting that it could be used as a barrier material.

Introduction

As the worldwide availability of fossil fuel reserves diminishes, the need to convert from oil to an alternative source of fuel steadily increases. Hydrogen has emerged as the most promising candidate,[1,2] and various technologies built around proton fuel cells have witnessed tremendous interest and growth over the past few years.[3-5] As pointed out elsewhere,[6,7] an important and often overlooked aspect of using H_2 is that it is largely produced from petrochemical reactions that yield mixed gas streams. The water-gas shift

reaction is responsible for generating the largest quantity of H_2 for fuel and chemical consumption in the world today,[8] but the resultant gas stream contains H_2 diluted with CO_2, in which case it is necessary to purify H_2. This can be achieved in one of two ways using dense polymeric membranes. The throughput of a gas penetrating a polymer is generally expressed as the permeability (P), which is the product of the solubility (S) and diffusivity (D). The quality of separation is referred to as the ideal selectivity of gas A to gas B ($\alpha_{A/B}$) and is given by the ratio P_A/P_B, which can be rewritten as $\alpha_{S,A/B}\alpha_{D,A/B}$, where $\alpha_{S,A/B}$ and $\alpha_{D,A/B}$ denote the solubility and diffusion selectivity, respectively. Elastomers derived from polymers with a low glass transition temperature (T_g), such as poly(ethylene glycol),[9-12] remove CO_2 due to the intrinsically high solubility of CO_2 in such polymer matrices. In this case, $\alpha_{S,CO_2/H_2} > \alpha_{D,CO_2/H_2} \approx 1$ and the membranes are classified as solubility-selective. Alternatively, glassy polymers routinely operate on the basis of diffusion selectivity.[13-15] Since molecular transport in the case of glassy polymers is limited by available free volume, H_2 is more permeable than CO_2 due to the smaller size of the H_2 molecules, and $\alpha_{D,H_2/CO_2} > \alpha_{S,H_2/CO_2}$.

One family of glassy polymers that have attracted considerable attention as H_2-selective membranes consists of aromatic polyimides, which typically possess T_gs beyond 200°C. These materials alone or in conjunction with physically incorporated nanoporous additives (e.g., carbon molecular sieves to yield mixed matrix membranes[16,17]) can achieve H_2/CO_2 selectivities in excess of 3.5.[18] Chung and co-workers[18-21] have repeatedly demonstrated that the gas separation efficacy of such polyimides can be further enhanced by

introducing diamine cross-links, which react with the carbonyl functionalities on the polyimide repeat unit to form interchain amide bridges. Various chemical considerations involving polyimide cross-linking have recently been reviewed by Powell and Qiao.[22] By systematically examining diamines differing in spacer length (from 2 to 4 methyl groups), Chung et al.[23] report that the H_2/CO_2 selectivity can be increased up to ~101 (a 100x increase relative to the virgin polyimide) after cross-linking with 1,3-diaminopropane (DAP) for 10 min at ambient temperature. A sensible explanation for this observation is that the introduction of interchain bridges forces the polyimide chains to pack more closely together than they would otherwise, thereby effecting a net reduction in the existing free volume (which serves to reduce the permeability of CO_2 to a greater extent than that of H_2). These results motivate the present study wherein DAP is introduced into a polyimide (PIm) for long cross-linking times, up to 72 h, at ambient conditions. To elucidate the effect of such long-time cross-linking on the PIm, we examine the time evolution of macroscopic properties (i.e., mechanical and thermal properties), as well as microscopic properties (i.e., gas permeation).

Experimental

The PIm employed in this study (Matrimid® 9725, a micropulverized form of Matrimid® 5218) was kindly provided in powder form by the MemFo group at the Norwegian University of Science and Technology (NTNU), whereas the DAP and reagent-grade methanol and dichloromethane were purchased from Sigma-Aldrich. All materials were used as-received. Dense polymer films were prepared by dissolving the PIm in dichloromethane to form a 2 wt% solution, followed by gravity filtration using glass fiber

filter circles (Fisherbrand G6, 1.6 μm) to remove any insoluble solids. Each solution was cast onto a metal plate and allowed to dry quiescently under ambient conditions for 24 h or more. The resultant films were subsequently dried in a vacuum oven for 48 h at 100°C to remove residual solvent. The chemical procedure described by Chung et al.[23] was used to cross-link the PIm at ambient temperature. Briefly, prior to immersion of 2 cm x 2 cm strips of PIm, DAP was added to methanol at a concentration of 10% w/v in a 50 mL beaker, which was subsequently sealed to avoid methanol evaporation. After a predetermined cross-link time (t_x) at ambient temperature, the PIm strip was removed and dried under ambient conditions for at least 5 days prior to analysis.

Fourier-transform infrared (FTIR) spectroscopy was performed on a Nicolet Nexus 470 spectrophotometer to follow the chemical conversion of the polyimide, whereas sol-gel analysis was used to ascertain the insoluble fraction upon cross-linking. Uniaxial extension at a constant crosshead speed of 3.3 mm/min and stress relaxation with a constant preload of 0.5 N were conducted at ambient temperature on an MTS-30G unit, with each test repeated at least 4x. Moduli were also measured by nanoindentation performed on a Hysitron Triboindenter equipped with a Berkovich diamond (150 nm) tip and operated with an indentation force of 8 mN (at a loading rate of 1 mN/s). At least 7 points were examined on each specimen. Thermal characteristics were measured by differential scanning calorimetry (DSC) on a TA Q2000 calorimeter operated under N_2 according to a 2-part cycle: heated to 360°C at 10°C/min, held at 360°C for 5 min, cooled to 40°C at -10°C/min, held at 40°C for 5 min, and repeated. Glass transition temperatures measured at the inflection point from the

second heating cycle were recorded. The permeabilities of H_2 and CO_2 through virgin and cross-linked PIm were measured from 25 to 125°C using the constant-volume/variable-pressure setup and procedure described earlier.[24]

Results and Discussion

Representative FTIR spectra acquired from the virgin PIm, as well as dry PIm films upon cross-linking with DAP for 1 and 48 h, are presented in Fig. 1a and confirm that the intensity of the vibrational modes associated with the polyimide (e.g., the symmetric C=O and C-N stretches at 1710 and 1380 cm^{-1}, respectively) decrease, while the intensity of the modes arising from the newly formed polyamide (e.g., the C=O and C-N stretches at 1650 and 1550 cm^{-1}, respectively) increase, with increasing t_x. These trends are clearly seen in Fig. 1b, which shows the change in peak absorbance (ΔA) relative to the FTIR spectrum of virgin PIm. Systematic changes in the peak intensities for all four vibration modes listed above are evident and indicate that reaction saturation occurs after about 24 h. Fitting the measured values of ΔA to a rate equation of the form $\Delta A_\infty\left(1-e^{kt_x}\right)$, where ΔA_∞ denotes the limit of ΔA at long t_x, yields rate constant (k) values ranging from 0.12 to 0.20 h^{-1}. Included in Fig. 1b are data collected from the peak associated with the C=C stretch of the aromatic moieties identified[25] at 1488 and 1512 cm^{-1}. Since the aromatic units remain unaffected by the cross-linking reaction, this absorbance is not anticipated to change with increasing t_x, which is confirmed in Fig. 1b. Complementary sol-gel analysis conducted for t_x up to 5 h (data not shown) reveals that the insoluble gel fraction due to chemical cross-linking reaches about

60% after 1 h of cross-linking and then slowly continues to increase thereafter, suggesting that cross-linking of the outer skin of the film hinders diffusion of DAP molecules into the film core, and thus slows the reaction front, as t_x increases. Taken together, these results establish that DAP cross-linking of PIm proceeds under the conditions employed and initially occurs quickly, but then slows upon saturation.

Classical studies of elastomers have focused on cross-linking low-T_g polymers as a straight-forward means by which to form rigid molecular networks. Few studies[26,27] have explored the strategy of cross-linking polymers to reduce undesirable CO_2 plasticization effects, and fewer yet have examined the corresponding changes in mechanical properties. In the case of elastomers, the modulus increases (to a limit) with increasing cross-linking as freely moving molten chains become progressively immobilized. Glassy polymers, on the other hand, intrinsically possess a high modulus, and so cross-linking is not anticipated to change the modulus of PIm appreciably at temperatures below T_g. This expectation is observed in Fig. 2, which shows the dependence of the tensile modulus (E) on t_x. Measured moduli up to t_x = 1 h are comparable in magnitude, within experimental uncertainty, to that of unmodified PIm. This observation, coupled with a similar trend for the ultimate stress (σ_{max}) in the inset of Fig. 2, confirms that cross-linking has little effect on mechanical properties at relatively short t_x. At longer t_x (12 h), both E and σ_{max} increase just beyond those of virgin PIm, whereas the elongation-to-break decreases markedly from ~30% (virgin PIm) to ~5%. When t_x is increased to 48 h, however, the films exhibit sufficient wrinkling[28] due to deswelling of the highly cross-linked PIm matrix to preclude conventional tensile

testing. Nanoindentation analysis, on the other hand, yields surface moduli that are slightly higher than, but in nonetheless favorable agreement with, those measured by extensional rheometry, and permits assessment of the modulus of films cross-linked for 48 h. The results in Fig. 2 establish that the stiffness of PIm increases systematically with increasing t_x.

The effect of extended cross-linking on the thermal properties of PIm is depicted in the DSC thermograms displayed in Fig. 3. The T_g of virgin PIm at $t_x = 0$ h is measured as 321°C, which agrees favorably with reported[16] values (onset at 302°C). At short cross-linking times ($t_x < 1$ h), the T_g decreases slightly (less than 6°C). At $t_x = 6$ h, the T_g diminishes to 295°C. This reduction in T_g with increasing t_x continues over the range of t_x examined, with T_g reaching 260°C at $t_x = 48$ h. The thermal data reported in Fig. 3 therefore indicate that DAP-induced cross-linking of PIm serves to systematically decrease T_g, which can occur by one of two mechanisms. The first is that cross-linking causes the polymer molecules to pack less effectively, thereby yielding a net increase in local free volume. This possibility is discounted, however, due to a decrease in the permeabilities of both H_2 and CO_2 upon cross-linking (discussed later), since a reduction in gas permeability is indicative of lower free volume available for molecular transport and, thus, improved chain packing. The second possible mechanism to account for the decrease in T_g evident in Fig. 3 pertains to the reactivity of DAP. As the number of DAP molecules within PIm increases due to cross-linking, DAP becomes progressively more soluble within the polymer matrix. Under such excess conditions, imbibed DAP molecules may react only with single chains and form dangling ends instead of the desired interchain bridges. Recall that the thermograms provided in Fig. 3 correspond to the second heating cycle. In the first heating cycle (data not shown),

endothermic events occurring at 113 and 180°C (and completely eliminated upon repeated cycling) are observed. Neither of these temperatures corresponds, however, to the normal boiling points of the organic liquids to which the PIm is exposed (40°C for dichloromethane, 65°C for methanol and 140°C for DAP). Although the cause of these endotherms is not established at present, the first endothermic peak may reflect further cross-linking of PIm, whereas the second one may arise due to reimidization.[20] Unreacted or partially reacted DAP molecules may likewise react (to a more limited extent) with the amide linkages subsequently formed by a single reaction of imide linkages and therefore induce chain scission.

A systematic reduction in and broadening of the PIm T_g upon extended cross-linking are consistent with a stochastic reduction in PIm molecular weight. At long t_x, a growing population of shortened PIm chains possessing a broad molecular weight distribution would exhibit a broad, lower T_g relative to virgin PIm. Since the chains remain highly cross-linked, properties evaluated in glassy PIm at low temperatures far removed from Tg would be expected to be less influenced by chain scission. Stress-relaxation data, for instance, wherein σ_n (the measured stress normalized with respect to the initial stress) is plotted as a function of time (t) in Fig. 4a and reveal that the decay in $\sigma_n(t)$ becomes less pronounced as the polymer becomes increasingly more cross-linked. [Films cross-linked for 48 h did not respond reproducibly to this test and are not included here for that reason.] This observation suggests that the chains in the cross-linked PIm are less mobile and thus unable to relax as easily as those comprising the virgin PIm at $T << T_g$, thereby providing a direct measure of network

development in the glassy state. Quantitative analysis of the $\sigma_n(t)$ curves requires a biexponential model of the form $\sigma_n = \phi_1 \exp(-t/\tau_S) + \phi_2 \exp(-t/\tau_L)$, where ϕ_1 and ϕ_2 are independent weighting parameters that should ideally sum to unity, and τ_S and τ_L represent short and long relaxation times, respectively.[29] In the regression analyses performed here, $\phi_1 + \phi_2$ is always within a few percent of 1. Regressed values of τ_S and τ_L are displayed in Fig. 4b and indicate that the two relaxation times differ by orders of magnitude. Short relaxation times measure on the order of seconds and show evidence of a plateau after ~1 h of cross-linking, whereas τ_L (measuring on the order of hours) does not change appreciably at short t_x but increases monotonically as t_x exceeds 1 h.

A primary motivation for this study is to discern the effect of long-time cross-linking on the transport properties of small molecules through PIm. Measured permeabilities of H_2 and CO_2 (after conditioning at the set temperature for 4-8 h under vacuum) are presented as a function of temperature (T) for virgin PIm, as well as for PIm cross-linked with DAP for 1 and 48 h, in Fig. 5. As anticipated, the permeabilities increase with increasing temperature and P_{H_2} is consistently larger than P_{CO_2}, verifying that this polymer in its native or cross-linked form is H_2-selective. Without cross-linking, α_{H_2/CO_2} varies from 5.4 at 50°C to 4.6 at 125°C. When the PIm is cross-linked for 1 h, both permeabilities decrease significantly, which is attributed to a net reduction in molecular pathways through which penetrant molecules can diffuse. The H_2/CO_2 selectivity, on the other hand, increases dramatically to ~49 at 50°C. At t_x = 48 h, however, P_{H_2} is very low, while P_{CO_2} is immeasurable, in which case highly cross-linked PIm acts as an effective barrier to permeation. An Arrhenius

representation of $P_{H_2}(1/T)$ is included in the inset of Fig. 5 and reveals two noteworthy features. The first is that Arrhenius behavior is observed at elevated temperatures, but deviates at lower temperatures, and the second is that the activation energy for permeation (E_P) increases systematically with increasing t_x. Since E_P is the product of the activation energy for diffusion (E_D) and the heat of solubilization (ΔH_S) and since it is unlikely that ΔH_S for H_2 changes substantially upon PIm cross-linking, the observed increase in E_P with increasing t_x is largely attributed to an increase in E_D due to a reduction in available diffusive pathways. In light of the cross-linking-induced changes in mechanical and thermal properties previously discussed, a simultaneous decrease in gas permeability and increase in E_D translates into a highly networked polymer matrix wherein existing voids are sufficiently small to substantially hinder the molecular transport of penetrant molecules, which may be of interest in barrier applications.

Conclusions

Extensive chemical cross-linking of PIm results in significant changes in mechanical, thermal and transport properties. Uniaxial tensile and nanoindentation measurements indicate that, at long reaction times, PIm is highly networked, as evidenced by an increase in modulus. Stress relaxation analysis confirms that the PIm chains comprising the network become increasingly immobilized as cross-linking proceeds. Thermal calorimetry, however, shows that the T_g of PIm decreases with increasing cross-linking, suggesting that the molecular weight distribution of the PIm chains is affected by long-time cross-linking.

Permeation tests reveal that cross-linking (*i*) decreases the permeability of H_2 and CO_2, (*ii*) increases the H_2/CO_2 selectivity and (*iii*) increases the activation energy of permeation. Taken together, long-time PIm cross-linking generates a material that differs considerably from virgin PIm in terms of macroscopic and microscopic property development.

Acknowledments

This work was supported by NASA through the Environmental Systems Commercial Space Technology Center at the University of Florida, the National Science Foundation, the Research Council of Norway under the NANOMAT Program and the NC State Undergraduate Research program. We thank Professor M.-B. Haag of NTNU for providing the PIm.

REFERENCES

[1] J. M. Ogden, *Phys. Today*, **2002**, *55*, 69.

[2] J. A. Turner, *Science*, **2004**, *305*, 972.

[3] M. Rikukawa, K. Sanui, *Prog. Polym. Sci.* **2000**, *25*, 1463.

[4] L. Schlapbach, A. Zuttel, *Nature*, **2001**, *414*, 353.

[5] M. A. Hickner, H. Ghassemi, Y. S. Kim, B. R. Einsla, J. E. McGrath, *Chem. Rev.* **2004**, *104*, 4587.

[6] T. M. Nenoff, R. J. Spontak, C. M. Aberg, *MRS Bull.* **2006**, *31*, 735.

[7] N. W. Ockwig, T. M. Nenoff, *Chem. Rev.* **2007**, *107*, 4078.

[8] J. A. Ritter, A. D. Ebner, *Sep. Sci. Tech.* **2007**, *42*, 1123.

[9] N. P. Patel, A. C. Miller, R. J. Spontak, *Adv. Mater.,* **2003**, *15*, 729.

[10] N. P. Patel, A. C. Miller, R. J. Spontak, *Adv. Funct. Mater*., **2004**, *14*, 699.

[11] H. Q. Lin, B. D. Freeman, *Macromolecules*, **2006**, *39*, 3568.

[12] H. Q. Lin, E. van Wagner, B. D. Freeman, L. G. Toy, R. P. Gupta, *Science*, **2006**, *311*, 639.

[13] V. P. Shantarovich, I. B. Kevdina, Y. P. Yampolskii, A. Y. Alentiev, *Macromolecules*, **2000**, *33*, 7453.

[14] T. C. Merkel, B. D. Freeman, R. J. Spontak, Z. He, I. Pinnau, P. Meakin, A. J. Hill, *Science*, **2002**, *296*, 519.

[15] W. Yave, K. V. Peinemann, S. Shishatskiy, V. Khotimskiy, M. Chirkova, S. Matson, E. Litvinova, N. Lecerf, *Macromolecules*, **2007**, *40*, 8991.

[16] D. Q. Vu, W. J. Koros, S. J. Miller, *J. Membr. Sci.*, **2003**, *211*, 311.

[17] T. S. Chung, L. Y. Jiang, Y. Li, S. Kulprathipanja, *Prog. Polym. Sci.* **2007**, *32*, 483.

[18] P. S. Tin, T. S. Chung, Y. Liu, R. Wang, S. L. Liu, K. P. Pramoda, *J. Membr. Sci.,* **2003**, *225*, 77.

[19] L. Shao, T. S. Chung, S. H. Goh, K. P. Pramoda, *J. Membr. Sci.*, **2004**, *238*, 153.

[20] L. Shao, T. S. Chung, S. H. Goh, K. P. Pramoda, *J. Membr. Sci.*, **2005**, *256*, 46.

[21] L. Shao, T. S. Chung, S. H. Goh, K. P. Pramoda, *J. Membr. Sci.*, **2005**, *267*, 78.

[22] C. E. Powell, G. G. Qiao, *J. Membr. Sci*., **2006**, *279*, 1.

[23] T. S. Chung, L. Shao, P. S. Tin, *Macromol. Rapid Commun.*, **2006**, *27*, 998.

[24] N. P. Patel, C. M. Aberg, A. M. Sanchez, M. D. Capracotta, J. D. Martin, R. J. Spontak, *Polymer*, **2004**, *45*, 5941.

[25] J. N. Barsema, S. D. Klijnstra, J. H. Balster, N. F. A. van der Vegt, G. H. Koops, M. Wessling, *J. Membr. Sci.*, **2004**, *238*, 93.

[26] J. D. Wind, C. Staudt-Bickel, D. R. Paul, W. J. Koros, *Ind. Eng. Chem. Res.* **2002**, *41*, 6139.

[27] C. E. Powell, X. J. Duthie, S. E. Kentish, G. G. Qiao, G. W. Stevens, *J. Membr. Sci.*, 2007, *291*, 199.

[28] J. Genzer, J. Groenewold, *Soft Matter*, **2006**, *2*, 310.

[29] R. J. Spontak, M. S. Vratsanos, *Macromolecules*, **2000**, *33*, 2290.

FIGURES AND TABLES

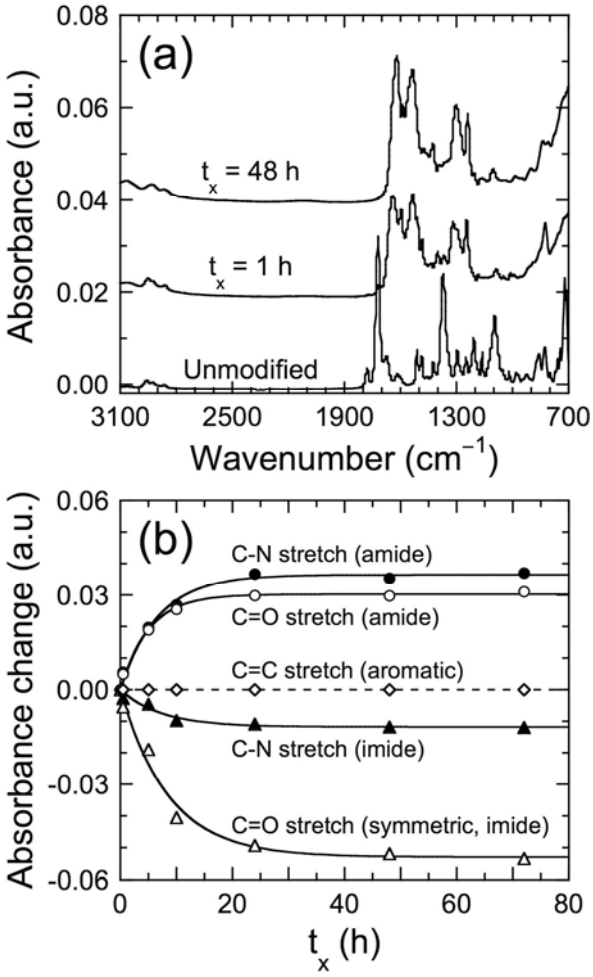

Figure 3-1. FTIR spectra and analysis acquired from umodified and cross-linked polyimide. (a) FTIR spectra acquired from unmodified PIm, as well as PIm cross-linked with DAP for 1 and 48 h. The intensities of characteristic imide vibrations decrease, while those of amide vibrations increase, with increasing cross-linking time (t_x). Details regarding the origin of these vibrations are provided in the text. (b) Variation of the change in absorbance (ΔA) for five characteristic vibrations (labeled) with t_x. The solid lines are regressed fits to the rate expression provided in the text, whereas the dashed line denotes the condition corresponding to $\Delta A = 0$.

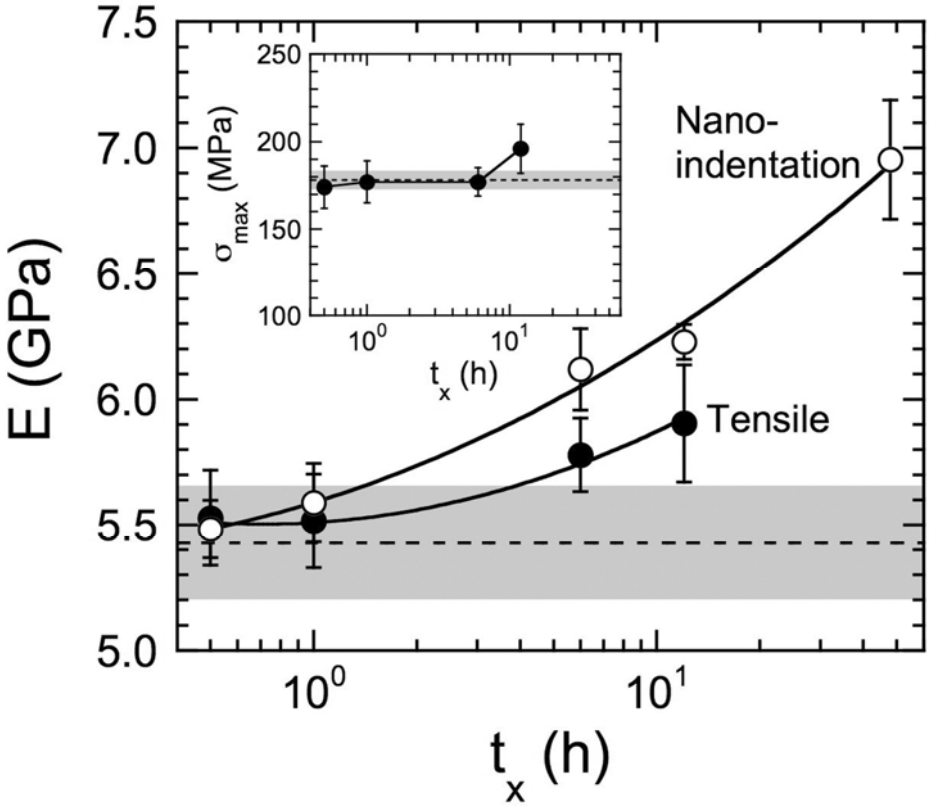

Figure 3-2. Tensile modulus and ultimate stress of cross-linked polyimide. Dependence of the modulus (E from tensile tests, ●; relative E from nanoindentation, ○) and ultimate stress (σ_{max}, inset) on t_x for PIm cross-linked by DAP. The solid lines serve as guides for the eye, and the error bars denote the standard error. Each dashed line and shaded region identifies the value and standard error, respectively, of unmodified PIm from tensile tests.

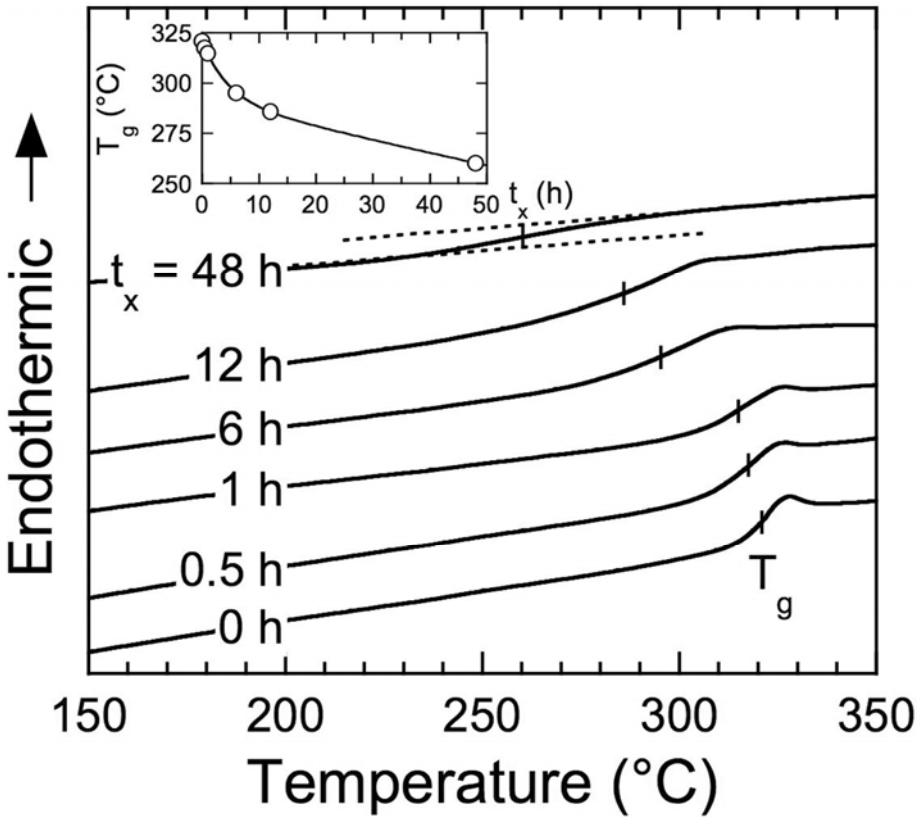

Figure 3-3. DSC thermograms collected from PIm before and after cross-linking with DAP (cross-link times are labeled). The position of T_g discerned from the inflection point on each thermogram is marked. In the inset, the variation of T_g with t_x is displayed, with the solid line serving as a guide for the eye.

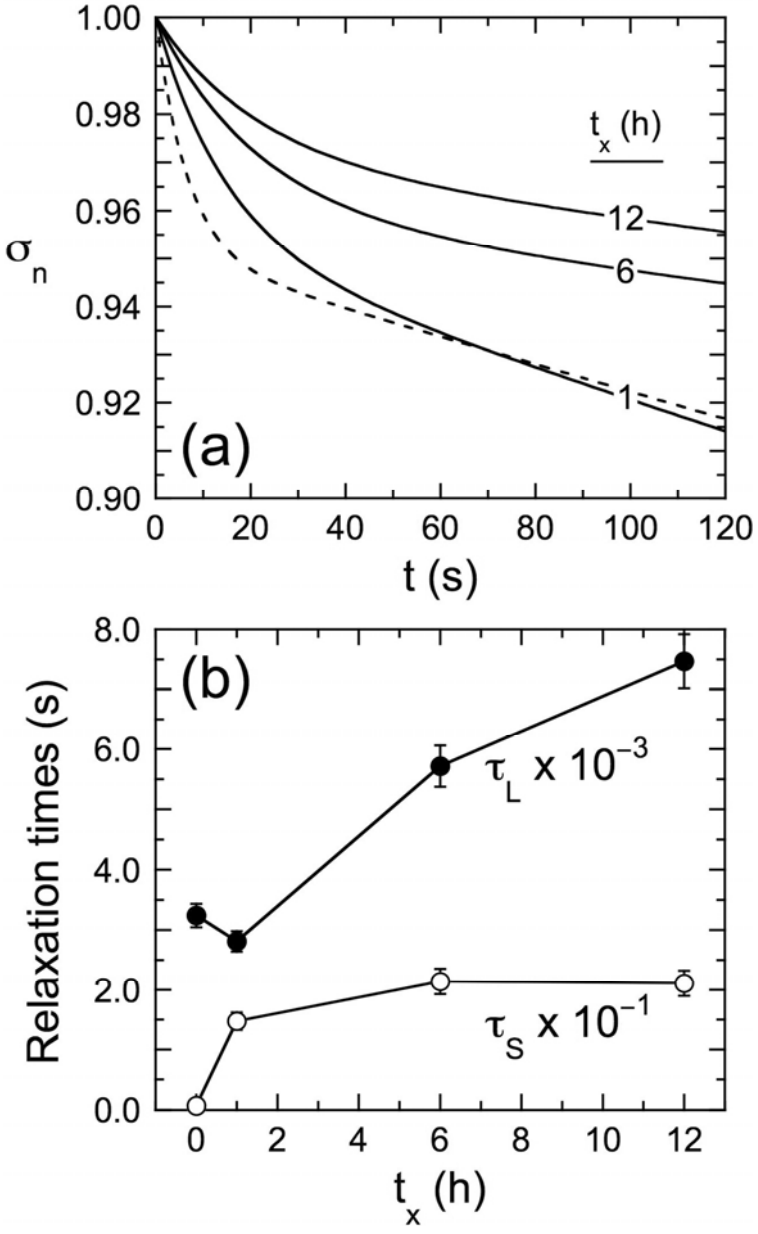

Figure 3-4. Stress relaxation curves and relaxation times. (a) Stress relaxation curves, in which σ_n is the measured stress normalized with respect to the initial stress, for unmodified PIm (dashed line) and cross-linked PIm (solid lines, labeled). (b) Short and long characteristic relaxation times (τ_S and τ_L, respectively) extracted from the stress relaxation curves in (a) with the biexponential expression provided in the text. The solid lines serve to connect the data, and the errors bars denote the standard error in the regressions.

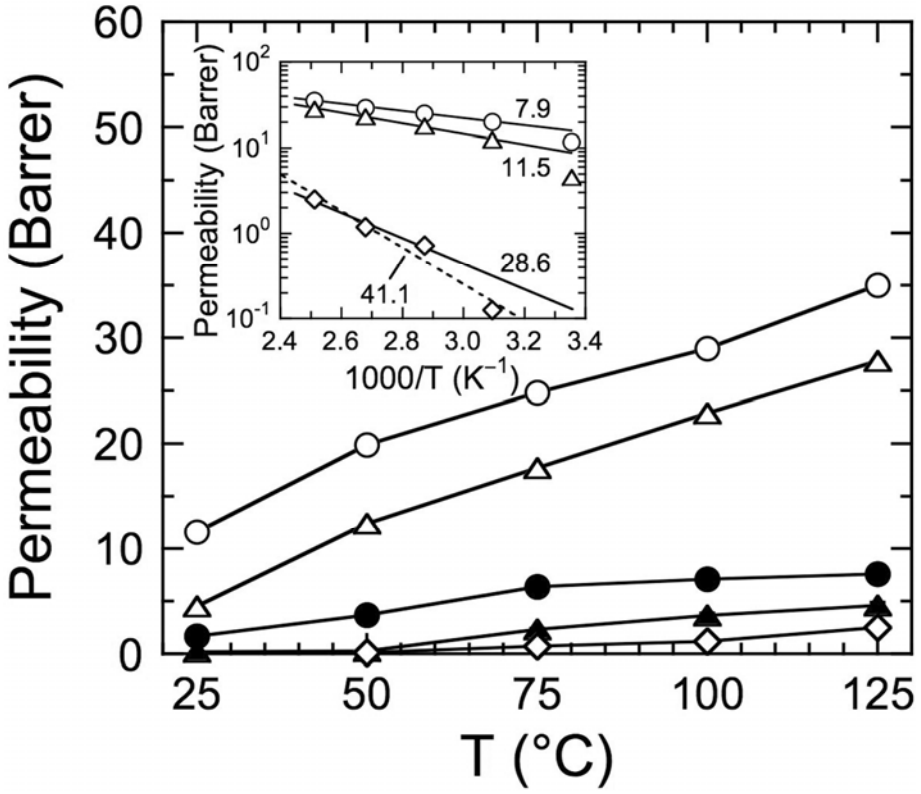

Figure 3-5. H_2 and CO_2 permeation data. Permeabilities of H_2 (open symbols) and CO_2 (filled symbols) shown as a function of temperature through PIm cross-linked for different times (in h): 0 (circles), 1 (triangles) and 48 (diamonds). The solid lines serve to connect the data. The inset is an Arrhenius representation of $P_{H_2}(1/T)$ wherein each solid line is a linear regression of the Arrhenius equation and its slope yields the activation energy for permeation (E_P, labeled in kJ/mol). While Arrhenius behavior tends to deviate at low temperatures, the dashed line for $t_x = 48$ h is a regression over all the data.

CHAPTER 4

In-Situ Growth of Pd-Containing Nanoparticles in Polymer Matrices

Christopher M. Aberg,[†] **Mohamed A. Seyam**,[†] **Scott A. Lassell**,[§]
Lyudmila M. Bronstein[%] and **Richard J. Spontak**[†‡]

[†]Department of Chemical & Biomolecular Engineering, North Carolina State University, Raleigh, NC 27695

[§]Department of Nuclear Engineering, North Carolina State University, Raleigh, NC 27695

[%]Department of Chemistry, Indiana University, Bloomington IN 47405

[‡]Department of Materials Science & Engineering, North Carolina State University, Raleigh, NC 27695

Abstract

Polymer nanocomposites continue to receive considerable attention as multifunctional hybrid materials, with most nanocomposites fabricated by physical dispersion of surface-functionalized nanoscale objects. In this study, we explore the viability of growing Pd-containing nanoparticles from Na_2PdCl_4 in two different polymers – hyper-cross-linked polystyrene (HPS) and an aromatic polyimide (PIm). In HPS, single Pd-containing nanoparticles possessing a relatively narrow size distribution (*ca*. 1-4 nm) are observed to form upon reduction of the divalent $PdCl_4^{-2}$ ions and cluster more readily if the reducing agent is introduced as a liquid. Single nanoparticles with a broad size distribution ranging from ~2 to 16 nm develop in PIm, which simultaneously undergoes chemical cross-linking during ion reduction. The conditions yielding Pd incorporation in PIm are explored through the use of instrumental neutron activation analysis. Such Pd-containing hybrid materials hold promise in molecular catalysis and gas separations.

Introduction

Polymer nanocomposites are of considerable contemporary interest since they combine the inexpensive cost, light weight, facile processability and robust properties of macromolecules with the specific chemical, optical or mechanical characteristics of inorganic nanoparticles to yield multifunctional hybrid materials.[1-4] Such nanocomposites are under development for a wide variety of (nano)technologies including, but not limited to, optical waveguides,[5,6] self-supported catalysts[7-10] and gas-separation membranes.[11-14] In many cases,

nanocomposites are fabricated by physically dispersing surface-functionalized nanoparticles into a polymer matrix. Although nanoparticle size and size distribution are long-recognized as important features governing the performance of nanocomposites,[15] surface functionalization is likewise a crucial consideration in this materials design strategy[16-19] since it is responsible for improving interfacial adhesion and reducing the natural tendency for the nanoparticles to aggregate, which consequently leads to an adverse decrease in available nanoparticle surface area. An alternative means by which to incorporate metal-containing nanoparticles into polymer matrices is through in-situ growth.[20-25] The approach underpinning this paradigm relies on the diffusion of a metal salt into a solvent-swollen polymer, followed by chemical reduction of the metal ion to the corresponding metal.

Previous studies have demonstrated that this procedure yields relatively monodisperse Pt and Co nanoparticles in nanoporous polymers such as hyper-cross-linked polystyrene (HPS),[9,22,24] which can be envisaged as a highly cross-linked polymer containing 2-3 nm nanoscale cavities. These cavities possess an inner surface area of *ca*. 10^3 m^2/g and effectively restrict the diffusion of neighboring nanoparticles and thus thwart aggregation. By doing so, catalytic reactions that exploit the high surface area of the nanoparticles can achieve high chemical conversion without compromising selectivity.[9,24,26] Since the nonpolar styrenic repeat units do not interact appreciably with Pt or Co, nanoparticles of these metals grown in HPS can be considered physically stabilized. Other examples of polymeric systems wherein confinement-stabilized nanoparticles can be grown with spatial specificity in an existing nanostructure include self-organizing block copolymers[27] and polymer

amphiphiles.[28,29] Even in these cases, however, modification of the polymer matrix to include polar functionalities can alter the spatial distribution of nanoparticles grown in-situ by promoting chemical stabilization.[30] With these two modes of nanoparticle stabilization in mind, we now turn our attention to specific nanoparticles of interest here.

Palladium is of tremendous commercial interest due to its catalytic properties, as well as its considerable affinity for hydrogen in gas-separation membranes and fuel cells,[31-33] with an average worldwide production rate of2.28×10^5 kg/yr in 2006 and 2007.[34] Due to its cost and limited abundance (~0.015 mg/kg by weight of the total Earth's lithosphere,[35] excluding commercial accessibility considerations), enlightened use of remaining Pd supplies may soon be required. The objective of this study is to investigate the viability of growing Pd-containing nanoparticles in two types of dense polymer matrices, one that stabilizes the nanoparticles by physical confinement and the other that relies on chemical interactions.

Experimental

The HPS employed in this study was produced according to the synthetic procedure described elsewhere,[36] and its physical characteristics were identical to those reported[9] earlier for Pt-containing nanocomposites, namely, an apparent inner surface area of 833 m^2/g and a pore size distribution maximum of ~2 nm. The other polymer examined here was a commercially available polyimide (PIm, Matrimid® 9725, a micropulverized form of Matrimid® 5218), provided in powder form by the MemFo group at the Norwegian University of Science and Technology (NTNU). The salt used here, sodium

tetrachloropalladate (Na_2PdCl_4), as well as diaminopropane (DAP), reagent-grade methanol (ML), dichloromethane (DCM) and sodium tetrahydridoborate ($NaBH_4$) were all purchased from Sigma-Aldrich and used as-received. Deionized water (DIW) was obtained from a Milli-Q water purification system.

Discrete HPS particles measuring 0.2 – 0.4 mm in diameter were impregnated with Na_2PdCl_4 in ML for 30 min at ambient temperature. Reduction of the $PdCl_4^{-2}$ anion was conducted with H_2 gas or a fresh 10% $NaBH_4$(aq) solution, with specimens subsequently dried under vacuum at 50°C. Dense PIm films were prepared by dissolving the polymer in DCM, followed by gravity filtration using glass fiber filter circles (Fisherbrand G6, 1.6 mm) to remove any insoluble solids, and solution casting onto a metal plate. After quiescent drying under ambient conditions for 24 h or more, the resultant film was dried under vacuum at 100°C and then cut into strips. Each strip was (*i*) immersed in a solution of Na_2PdCl_4 in either DIW or ML for a period of time (t_s) at a given temperature (refluxing with a water-jacketed condenser when necessary) to allow the salt to diffuse into the solvent-swollen film and (*ii*) introduced into ML containing 10% w/v DAP, a reported cross-linking agent for PIm. After a predetermined exposure time (t_x) at ambient temperature, each strip was removed and dried under ambient conditions for at least 5 days.

Transmission electron microscopy (TEM) was performed with a Zeiss EM902 electron spectroscopic microscope, equipped with an in-column energy filter, and a JEOL 2000FX electron microscope operated at 80 and 200 kV, respectively. Insoluble HPS-Pd powders were embedded in epoxy prior to sectioning at ambient temperature. Tough PIm

films with a high glass transition temperature (T_g > 200°C) were likewise cross-sectioned at ambient temperature. Images of the thin sections measuring *ca*. 50 nm thick, collected either on plate negatives and digitized at 1000 dpi or digitally on a CCD camera, were analyzed with the Adobe Photoshop software package and its Image Processing Toolkit. The Pd content in HPS-Pd was obtained by X-ray fluorescence (XRF) measurements performed with a Zeiss Jena VRA-30 spectrometer (Mo anode, LiF crystal analyzer and SZ detector). Analyses were based on the Co K_α line and a series of PS/Pd standards prepared by mixing 1 g of PS with 10–20 mg of standard Pd compounds. The time of data acquisition was constant at 10 s. The concentration of Pd in the PIm-Pd films was measured by instrumental neutron activation analysis (INAA) in conjunction with the 1 MW PULSTAR nuclear-fission reactor at North Carolina State University. Specimens were exposed to neutrons emanating from the thermal fission of U^{235}, which produces unstable isotopes in the sample that decay according to known pathways.[37] The isotope monitored in this study was ^{109m}Pd with a half-life of 4.696 min and the following decay sequence: (*i*) $^{108}Pd + n \rightarrow {}^{109m}Pd$; and (*ii*) $^{109m}Pd \rightarrow {}^{109}Pd + \gamma$ (via isomeric transition). The energy of the γ emission at 189 keV was monitored to discern the concentration of Pd in each specimen.

Results and Discussion

Representative TEM images acquired from HPS-Pd specimens subjected to H_2 and $NaHB_4$ reducing agents are presented in Figs. 1a and 1b, respectively. In each case, the concentration of Pd is 2.3 wt%. While the $NaHB_4$-reduced sample displays evidence of

irregularly shaped clusters measuring up to 20 nm in terms of an equivalent diameter, close examination of the two images reveals that the smallest discrete nanoparticles measure ~5 nm or less in diameter. A histogram of individual nanoparticle sizes generated from analyzing several different images of the H_2-reduced HPS-Pd is included in Fig. 1c and confirms that Pd nanoparticles approaching 1 nm across exist in this nanocomposite, which agrees well with our studies[9,24] of Pt nanoparticles in HPS of differing porosity. The difference in the extent of nanoparticle aggregation visible in Fig. 1 is attributed to the procedure employed to achieve Pd reduction. In the first case, H_2 gas is flowed through the HPS particles presumably increasing of mobility of metal species. Thus, the resultant nanoparticles are largely stabilized by the intrinsic nanoscale cavities within HPS. Reduction by aqueous $NaHB_4$, however, provides a liquid in a reaction area and slight HPS swelling, thus facilitating metal species migration and eventual aggregation. The observation that the Pd nanoparticles aggregate when nanoscale confinement is compromised affords evidence that nanoporous HPS does not promote chemical stabilization.

Introduction of chemical functionalities capable of interacting with metals into the host polymer is anticipated[30] to improve nanoparticle stability. In the second polymer examined here, carboxyl and ring-structured imide moieties may provide additional chemical stabilization. Incorporation of Pd nanoparticles into HPS has yielded a valuable nanocomposite platform in terms of molecular catalysis.[26] The motivation for growing Pd nanoparticles in PIm stems from the utility of both components in H_2 separation from mixed gas streams: (*i*) Pd possesses a unique chemical affinity for H_2, and (*ii*) PIm, a high-T_g glassy

thermoplastic, is inherently H_2-selective relative to conventional gases (especially CO_2) and organic vapors.[38] Selectivity in this context refers to the ratio of permeabilities between two penetrant gases/vapors, thereby providing a quantitative metric of the quality of gas separation across a membrane. Due to their relatively low free volume, glassy polymers tend to sieve penetrant molecules according to size so that H_2 exhibits high permeabilities and, hence, high selectivity, which is important in H_2 purification for an envisaged H_2 economy.[39,40] Recent studies have shown[41-44] that PIm chains can be chemically cross-linked with various diamines (e.g., DAP) to further limit the free volume available for molecular transport and increase the net H_2 selectivity of PIm. In this work, DAP is used for two concurrent purposes — to cross-link the PIm matrix and reduce the incorporated $PdCl_4^{-2}$ anions.

An illustrative example of a chemical spectrum obtained by non-destructive INAA is provided in Fig. 2 and clearly indicates the presence of a well-defined peak in the vicinity of 189 keV, which corresponds to the energy of the γ emission associated[37] with the radioactive decay of ^{109m}Pd to ^{109}Pd. In this figure, the solid line corresponds to a Gaussian fit to the data and confirms that the peak intensity is centered at 188.9 keV, in excellent agreement with prior literature reports, and that the full width of the peak at half-maximum (FWHM) is 1 keV. From the area under the curve relative to the other species present, the concentration of Pd can be quantitatively assessed with an experimental uncertainty of $\sim 3 \times 10^{-5}$ wt%. An interesting result in the INAA performed throughout this study is that the concentration of Cl associated with the $PdCl_4^{-2}$ ion precursor is typically about two orders of magnitude lower

than that of Pd (the corresponding uncertainty in the Cl measurements is ~1 x 10^{-8} wt%). Moreover, after exposure of the salt-containing PIm to the DAP/ML solution, heat generation and a color change from orange/brown to yellow are accompanied by the formation of macroscopic crystals that, according to energy dispersive spectroscopy, consist primarily of Na and Cl, with occasional and smaller concentrations of C, N and Pd. These observations are generally consistent with the chemical reduction of $PdCl_4^{-2}$ to Pd metal by DAP. We shall return to address this point later.

The dependence of Pd concentration in PIm-Pd on the time of DAP reduction/cross-linking (t_x) after 72 h of exposure to Na_2PdCl_4 is presented in Fig. 3 for two sets of experimental conditions. In the first, DIW is used to imbibe $PdCl_4^{-2}$ ions into the polymer at a salt concentration of 5 wt% under agitation at 100°C. Under these conditions, the Pd uptake initially increases with increasing t_x up to an apparent limit of about 0.31 wt%. In the second case, DIW is replaced by ML, and the salt solution concentration and temperature are both decreased (to 3 wt% and 45°C, respectively). Similar Pd uptake behavior is observed in Fig. 3 with the exception that the limit is noticeably higher (0.84 wt%), despite the lower starting salt concentration. These results indicate that the interior of PIm is more accessible to $PdCl_4^{-2}$ in the presence of ML, which agrees with expectation since PIm is a hydrophobic polymer. While it is nonetheless encouraging that limited Pd incorporation in PIm is achieved when $PdCl_4^{-2}$ ions are delivered to the polymer from an aqueous solution, we hereafter focus on PIm-Pd nanocomposites prepared only by salt incorporation from ML. The effect of solution concentration on Pd uptake after salt exposure for 72 h and a reduction/cross-linking time of

5 h is displayed in Fig. 4. These data, in conjunction with those shown in Fig. 3, imply that, at saturation conditions, temperature over the range explored has little influence on Pd uptake and that the time of exposure to DAP, during which divalent $PdCl_4^{-2}$ anions are chemically reduced, plays an important role. From Fig. 4, the variability in Pd uptake from specimen to specimen ranges from about 0.01 to 0.07 wt%.

A pair of TEM images collected from a PIm-Pd nanocomposite imbibed with $PdCl_4^{-2}$ ions from ML is provided in Fig. 5 and reveals that the Pd nanoparticles generated in PIm are non-uniformly dispersed (relative to Fig. 1a) and possess a broad size distribution. At the lower end of the distribution, the Pd nanoparticles measure about ~2 nm in diameter, whereas the largest ones observed are closer to 16 nm across. In addition to differences in dispersion and size distribution, several important features differentiate these nanoparticles from those grown in HPS. First, while the size distribution is larger, there is no evidence of nanoparticles aggregating to form fractal-like clusters, such as the ones observed in Fig. 1b. Instead, differences in the structure of PIm, which is not a nanoporous material as in the case of HPS, appear responsible for allowing coalescence of $PdCl_4^{-2}$ prior to chemical reduction. Second, the nanoparticles vary in optical density. If nanoparticle size and shape remain constant, such variation can only be explained in terms of mass density, with the darker nanoparticles being more dense than the lighter ones. Coexistence of nanoparticles varying in density suggests that the reduction reaction was incomplete under the experimental conditions employed to prepare this nanocomposite. Close examination of some of the lighter nanoparticles in Fig. 5b verifies that that they exhibit dark mottling, which would be consistent with partial

reduction to Pd metal. Lastly, some of the nanoparticles contain a bright center, which could be interpreted to mean that the nanoparticles exist as either three-dimensional toroids or hollow spheres. While it remains unclear at present why such nanoparticles would develop, we hasten to point out that metal-containing nanoparticles have been previously reported[45,46] as a result of a nanoscale Kirkendall-type mechanism. This observation is intriguing and certainly warrants further examination, but such morphological analysis is beyond the scope of this communication. Preliminary high-resolution lattice imaging and selected-area electron diffraction analyses do not indicate that these nanoparticles are crystalline. However, the sensitivity of these nanoparticles to a high-energy electron beam, accompanied by local specimen heating, has not been thoroughly discerned, and so the nature of these nanoparticles, but not their existence, remains in question.

Conclusions

Palladium nanoparticles measuring as small as ~1-2 nm have been grown in two different polymer matrices. In hyper-cross-linked polystyrene, relatively monodisperse Pd nanoparticles are physically stabilized via confinement in nanoscale cavities, whereas nanoparticles possessing a broad size distribution and variable morphologies develop in an aromatic polyimide. These materials show promise in molecular catalysis and gas separations, and the results presented here help to develop a more thorough fundamental understanding of how these nanoparticles (*i*) can be controllably grown and stabilized, and (*ii*) impart targeted functionality to nanocomposites.

Acknowledgments

This work was supported by NASA through the Environmental Systems Commercial Space Technology Center at the University of Florida and the Research Council of Norway under the NANOMAT Program. We thank Professor M.-B. Haag of NTNU for providing the PIm.

REFERENCES

[1] Krishnamoorti, R.; Vaia, R. A. (eds.) *Polymer Nanocomposites: Synthesis, Characterization and Modeling*; American Chemical Society: Washington, D. C., 2001.

[2] Bockstaller, M. R.; Mickiewicz R. A.; Thomas, E. L. *Adv. Mater.* **2005**, *17*, 1331.

[3] Podsiadlo, P.; Kaushik, A. K.; Arruda, E. M.; Waas, A. M.; Shim, B. S.; Xu, J. D.; Nandivada, H.; Pumplin, B. G.; Lahann, J.; Ramamoorthy, A.; Kotov, N. A. *Science* **2007**, *318*, 80.

[4] Kawazoe, M.; Ishida, H., *Macromolecules* **2008**, *41*, 2931.

[5] Beecroft, L. L.; Ober, C. K. *Chem. Mater.* **1997**, *9*, 1302.

[6] Fasolka, M. J.; Goldner, L. S.; Hwang, J.; Urbas, A. M.; DeRege, P.; Swager, T.; Thomas, E. L. *Phys. Rev. Lett.* **2003**, *90*, 016107.

[7] Schmid, G., Ed. *Nanoparticles: From Theory to Application.* Wiley-VCH: Weinheim, Germany, 2004.

[8] Claus, P.; Brueckner, A.; Mohr, C.; Hofmeister, H. *J. Am. Chem. Soc.* **2000**, *122*, 11430.

[9] Sidorov, S. N.; Volkov, I. V.; Davankov, V. A.; Tsyurupa, M. P.; Valetsky, P. M.; Bronstein, L. M.; Karlinsey, R.; Zwanziger, J. W.; Matveeva, V. G.; Sulman, E. M.; Lakina, N. V.; Wilder, E. A.; Spontak, R. J. *J. Am. Chem. Soc.* **2001**, *123*, 10502.

[10] Sarkar, A.; Mukherjee, T.; Kapoor, S. *J. Phys. Chem. C* **2008**, *112*, 3334.

[11] T. C. Merkel, B. D. Freeman, R. J. Spontak, Z. He, I. Pinnau, P. Meakin, A. J. Hill, *Science*, **2002**, *296*, 519.

[12] D. Q. Vu, W. J. Koros, S. J. Miller, *J. Membr. Sci.*, **2003**, *211*, 311.

[13] Hill, R. J. *Phys. Rev. Lett.* **2006**, *96*, 216001.

[14] W. Yave, K. V. Peinemann, S. Shishatskiy, V. Khotimskiy, M. Chirkova, S. Matson, E. Litvinova, N. Lecerf, *Macromolecules*, **2007**, *40*, 8991.

[15] Semagina, N.; Renken, A.; Kiwi-Minsker, L. *J. Phys. Chem. C* **2007**, *111*, 13933.

[16] Bockstaller, M. R.; Lapetnikov, Y.; Margel, S.; Thomas, E. L. *J. Am. Chem. Soc.* **2003**, *125*, 5276.

[17] Walls, H. J.; Riley, M. W.; Gupta, R. R.; Spontak, R. J.; Fedkiw, P. S.; Khan, S. A. *Adv. Funct. Mater*. **2003**, *13*, 710.

[18] Garcia, I.; Zafeiropoulos, N. E.; Janke, A.; Tercjak, A.; Eceiza, A.; Stamm, M.; Mondragon, I. *J. Polym. Sci. A: Polym. Chem.* **2007**, *45*, 925.

[19] Kim, B. J.; Fredrickson, G. H.; Hawker, C. J.; Kramer, E. J. *Langmuir* **2007**, *23*, 7804.

[20] Sidorov, S. N.; Bronstein, L. M.; Davankov, V. A.; Tsyurupa, M. P.; Solodovnikov, S. P.; Valetsky, P. M.; Wilder, E. A.; Spontak, R. J. *Chem. Mater.* **1999**, *11*, 3210.

[21] Hagio, H.; Sugiura, M.; Kobayashi, S. *Org. Lett.* **2006**, *8*, 375.

[22] Bronstein, L. M.; Goerigk, G.; Kostylev, M.; Pink, M.; Khotina, I. A.; Valetsky, P. M.; Matveeva, V. G.; Sulman, E. M.; Sulman, M. G.; Bykov, A. V.; Lakina, N. V.; Spontak, R. J. *J. Phys. Chem. B* **2004**, *108*, 18234.

[23] Schrinner, M.; Polzer, F.; Mei, Y.; Lu, Y.; Haupt, B.; Ballauff, M.; Goldel, A.; Drechsler, M.; Preussner, J.; Glatzel, U. *Macromol. Chem. Phys.* **2007**, *208*, 1542.

[24] Mei, Y.; Lu, Y.; Polzer, F.; Ballauff, M.; Drechsler, M. *Chem. Mater.* **2007**, *19*, 1062.

[25] Wen, F.; Zhang, W. Q.; Wei, G. W.; Wang, Y.; Zhang, J. Z.; Zhang, M. C.; Shi, L. Q. *Chem. Mater.* **2008**, *20*, 2144.

[26] Sulman, E.; Matveeva, V.; Doluda, V.; Nicoshvili, L.; Bronstein, L.; Valetsky, P.; Tsvetkova, I., *Top. Catal.* **2006**, *39*, 187.

[27] Kim, B. J.; Fredrickson, G. H.; Kramer, E. J. *Macromolecules* **2008**, *41*, 436.

[28] Bronstein, L. M.; Chernyshov, D. M.; Valetsky, P. M.; Wilder, E. A.; Spontak, R. J. *Langmuir* **2000**, *16*, 8221.

[29] Shtykova, E. V.; Svergun, D. I.; Chernyshov, D. M.; Khotina, I. A.; Valetsky, P. M.; Spontak, R. J.; Bronstein, L. M. *J. Phys. Chem. B* **2004**, *108*, 6175.

[30] Bronstein, L. M.; Linton, C.; Karlinsey, R.; Stein, B.; Svergun, D. I.; Zwanziger, J. W.; Spontak, R. J. *Nano Lett.* **2002**, *2*, 873.

[31] Paglieri, S. N.; Way, J. D. *Sep. Purif. Meth.* **2002**, *31*, 1.

[32] T. M. Nenoff, R. J. Spontak, C. M. Aberg, *MRS Bull.* **2006**, *31*, 735.

[33] N. W. Ockwig, T. M. Nenoff, *Chem. Rev.* **2007**, *107*, 4078.

[34] Kempthorne, D.; Myers, M. *Mineral Commodity Summaries 2008*; United States Government Printing Office: Washington, D. C., 2008; p.127.

[35] Patnaik, P. *Handbook of Inorganic Chemicals*; McGraw-Hill: New York, 2002; p. 686

[36] Davankov, V. A.; Tsyurupa, M. P. *React. Polym.* **1990**, *13*, 27.

[37] Schick, W. C., Jr.; Talbert, W. L., Jr. *Nucl. Phys. A* **1969**, *128*, 353.

[38] Hu, L., Xu, X., Ilconich, J.B., Ellis, S., Coleman, M. *J. Appl. Polym. Sci.* **2003**, *90*, 2011

[39] Ogden, J. M. *Phys. Today*, **2002**, *55*, 69.

[40] Turner, J. A. *Science*, **2004**, *305*, 972.

[41] Tin, P. S.; Chung, T. S.; Liu, Y.; Wang, R.; Liu, S. L.; Pramoda, K. P. *J. Membr. Sci.*, **2003**, *225*, 77.

[42] Shao, L.; Chung, T. S.; Goh, S. H.; Pramoda, K. P. *J. Membr. Sci.*, **2004**, *238*, 153; **2005**, *256*, 46; **2005**, *267*, 78.

[43] Chung, T. S.; Shao, L.; Tin, P. S. *Macromol. Rapid Commun.*, **2006**, *27*, 998.

[44] Aberg, C. M.; Ozcam, A. E.; Majikes, J. M.; Seyam, M. A.; Spontak, R. J. *Macromol. Rapid Commun.*, in press.

[45] Yin, Y.; Rioux, R. M.; Erdonmez, C. K.; Hughes, S.; Somorjai, G. A.; Alivisatos, A. P. *Science* **2004**, *304*, 711.

[46] Yin, Y.; Erdonmez, C. K.; Cabot, A.; Hughes, S.; Alivisatos, A. P. *Adv. Funct. Mater.* **2006**, *16*, 1389.

FIGURES AND TABLES

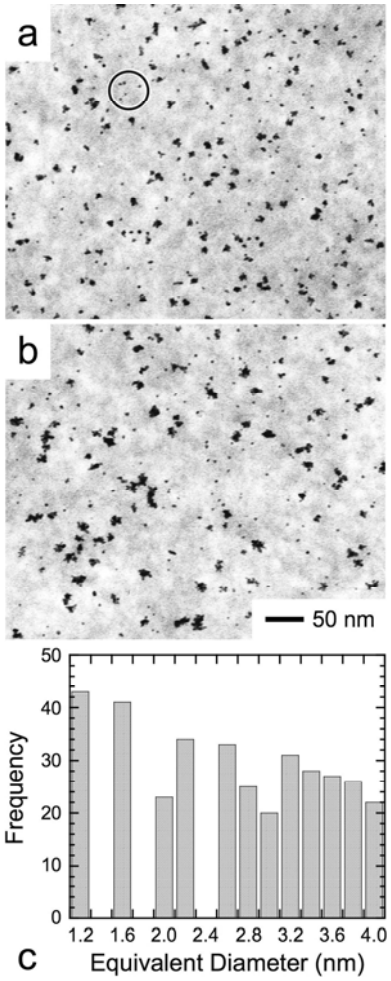

Figure 4-1. TEM images of HPS-Pd nanocomposites grown from conditions wherein ML is used to introduce $PdCl_4^{-2}$ ions into virgin HPS powder and either (a) H_2 or (b) $NaHB_4$(aq) is used to reduce $PdCl_4^{-2}$ anions to Pd metal (inferred from prior analogous studies of Pt). Note that the nanoparticle clusters in (b) are larger than those in (a), indicating that exposure of HPS to a liquid during reduction results in polymer swelling and promotes aggregation of individual nanoparticles (circle). The nanoparticle size distribution for the specimen in (a) is included in (c).

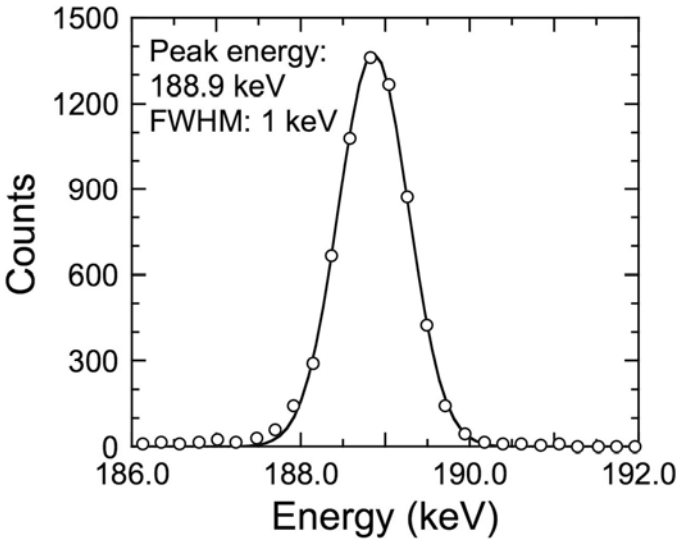

Figure 4-2. Illustrative chemical spectrum acquired from INAA of a PIm-Pd nano-composite. The peak at 188.9 keV corresponds to the energy of the γ emission that occurs as ^{109m}Pd decays to ^{109}Pd. The solid line denotes a Gaussian fit to the data, and the full width at half-maximum (FWHM) is found to be 1 keV.

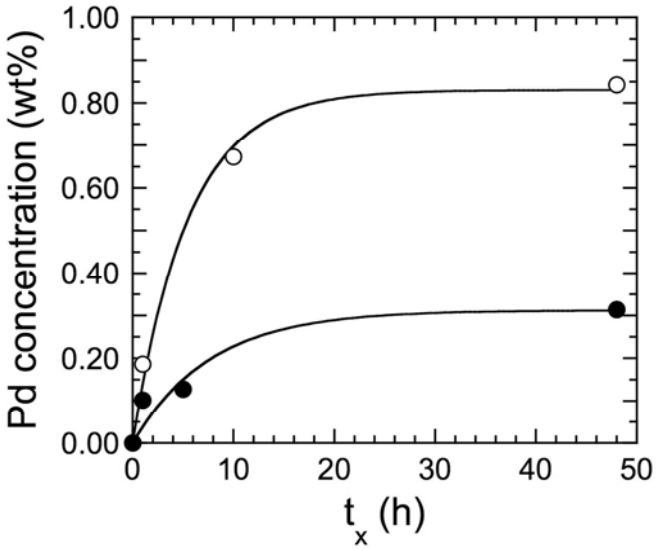

Figure 4-3. Pd uptake discerned from INAA as a function of DAP exposure time (t_x) for two sets of experimental conditions: DIW with 5 wt% Na_2PdCl_4 at 100°C (●) and ML with 3 wt% Na_2PdCl_4 at 45°C (○). In both cases, t_s = 72 h and the solid lines serve as guides for the eye.

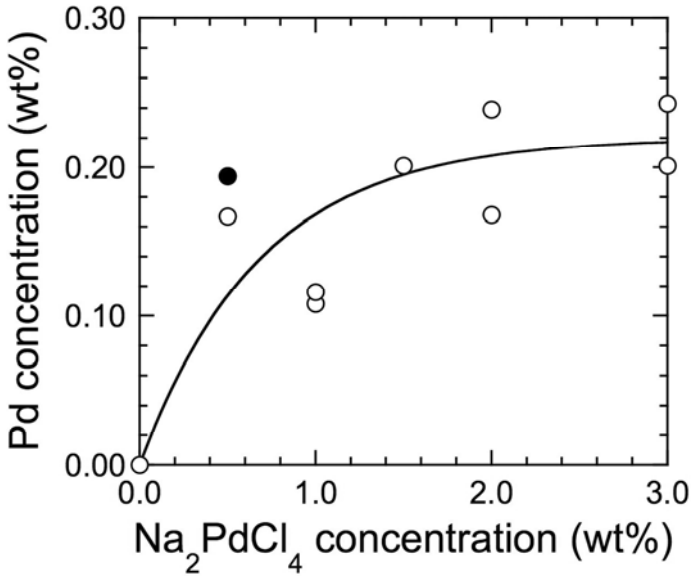

Figure 4-4. Dependence of Pd uptake on Na_2PdCl_4 solution concentration in ML at two temperatures (in °C): 25 (●) and 35 (○). In all cases, t_s = 72 h and t_x = 5 h. The solid line serves as a guide for the eye with respect to the data at 35°C.

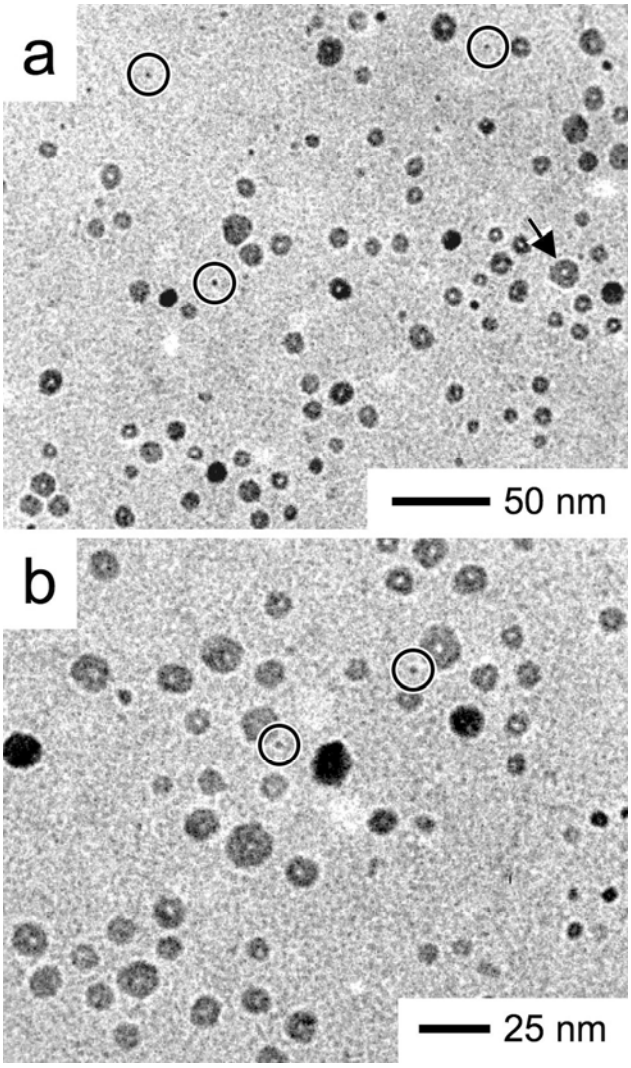

Figure 4-5. TEM images of PIm-Pd nanocomposites grown from conditions wherein ML is used to introduce $PdCl_4^{-2}$ ions and, subsequently, DAP into virgin PIm films. In (a), the non-uniformity of the Pd nanoparticles is apparent. Circled features in (a) and (b) identify the smallest nanoparticles, measuring ~2 nm in diameter. The arrow in (a) points to a single nanoparticle possessing a light center. Such nanoparticles are more clearly seen in (b). Note that some of the nanoparticles in both images appear more electron dense (darker) than others, suggesting that reduction of divalent $PdCl_4^{-2}$ anions to Pd metal may be incomplete.

CHAPTER 5

Conclusions and Future Research

Worldwide, as discussed in Chapter 1, a variety of membranes, organic and inorganic, have been and continue to be studied and optimized for the robust and economically efficient large-scale production of H_2. Each type of membrane possesses strengths and current weaknesses. With the current rise in oil prices, there is an ever-growing need to develop membranes capable of separating hydrogen cost-effectively to prove as a viable alternative to current fossil fuel demands. Considering the volume of H_2 that would be needed to support both the US and World energy demands, even small improvements in gas separation step could have a dramatic effect on the overall cost of operating a "hydrogen economy" or at least an economy where hydrogen plays a role in the alternative energy market. Polymeric membranes possess a great deal of potential, provided novel concepts are conceived to meet both short-term and long-term hydrogen separation goals.

While polymeric membranes have come a long way over the past decade, it is clear that more work is required in order to create competitive technologies that will help to reduce production costs for a sustainable hydrogen economy. As presented in this current work with the polyimide (PIm), Matrimid®, and evidenced by previous poly-ether work from Patel et al., the genre of cross-linked non-traditional polymers is emerging as one that shows promise for use in the separation of hydrogen and carbon dioxide through either H_2- or CO_2-selective applications. The versatility of the cross-linking methodology provides the ability to not only tailor diffusion by the altering the degree of cross-linking, but also allows for functionality to be added to the network structure based upon the choice of cross-linker.

As demonstrated by the discussion in Chapter 2 and the results presented in Chapter 3, cross-linking provides a relatively simple, yet effective route by which one can manipulate the gas transport properties of a polymer membrane intended for the separation of H_2 and CO_2. Extensive chemical cross-linking of PIm results in significant changes in mechanical, thermal and transport properties, showing tremendous promise for the material. Long-time PIm cross-linking generates a material that differs considerably from virgin PIm in terms of macroscopic and microscopic property development. The membrane essentially acts as a barrier for the passage of CO_2 these long cross-link time periods. It is inherently simple to change the degree of cross-linking, by varying the exposure time, thereby altering the transport characteristics of the PIm. Controllable, selective transport of hydrogen, carbon dioxide, and other gases can be achieved as researchers gain further knowledge on how to manipulate the free volume or chemical groups of a polymer such that the diffusive or solubility characteristics can be controlled. A more broad cross-linking investigation of diamines varying in length and size would enable us to correlate property development with the various diamine chemistries at different cross-linking times.

Currently a great deal of effort is going into incorporating palladium into membranes, born out of the availability of the metal both in natural quantity and type (i.e. salts). Because of the limited availability, the greatest amount of surface area from the least amount of material is ideal. We have demonstrated that Pd nanoparticles measuring as small as ~1-2 nm can be grown from Pd salts in two different polymer matrices, their growth and dispersity largely dictated by type and size of the network in which they are grown. In hyper-cross-

linked polystyrene, relatively monodisperse Pd nanoparticles are physically stabilized via confinement in nanoscale cavities, whereas nanoparticles possessing a broad size distribution and variable morphologies develop in an aromatic polyimide. These materials show promise in molecular catalysis and gas separations, and the results presented here help to develop a more thorough fundamental understanding of how these nanoparticles (*i*) can be controllably grown and stabilized, and (*ii*) impart targeted functionality to nanocomposites. A more thorough investigation is warranted however, one in which we explore the timing of Pd salt addition. Perhaps more control over the particle size could be had if the salt were added after cross-linking the PIm.

Combination of the two technologies explored in this work could potentially lead to hybrid materials in which the strengths of organic and inorganic membranes could work synergistically to provide superior hydrogen separation capability. Further study of the transport properties of the separate and combined materials will be necessary to determine the various interactions of each modification. One way in which the solubility element of the permeability can be determined is through gravimetric sorption. By measuring the uptake of hydrogen and carbon dioxide on a gravimetric sorption balance, we can determine the extent of contributing effect that the cross-linking and the addition of palladium-containing nano-particles have on the transport properties.